Theory of projectile-electron excitation and loss in relativistic collisions with atoms

A.B. Voitkiv
Max-Planck-Institut für Kernphysik
Saupfercheckweg 1, 69117 Heidelberg, Germany
e-mail: Alexander.Voitkiv@mpi-hd.mpg.de
phone: 6221 516 609 fax: 6221 516 604

October 21, 2003

Abstract

We review the recent progress in the theory of relativistic ion-atom collisions where the projectile-ion initially carries active electrons. We present a detailed discussion of quantum and semiclassical first order theories for the projectile-electron excitation and loss in relativistic collisions with neutral atomic targets. The influence of the higher order terms in the projectile-target interaction on the projectile-electron excitation and loss in ultrarelativistic collisions is considered by using the 'light-cone' approximation.

The theories discussed are applied to study (i) excitation and loss probabilities as functions of the collision impact parameter and (ii) excitation and loss cross sections. Calculations for cross sections are compared with experimental data.

PACS: 34.10.+x, 34.50.Fa
Keywords: relativistic ion-atom collisions

Contents

1 Introduction

Two basic processes, which are of great interest for atomic collision physics, can occur in nonrelativistic collisions between a bare nucleus (projectile) and an atom (target). (i) The atom can be excited or ionized by the interaction with the projectile (target excitation or ionization). (ii) One or more atomic electrons can be picked up by the nucleus and form bound or low-lying continuum states of the corresponding projectile-ion. The pick-up process can proceed with or without emission of radiation and is called radiative or nonradiative electron capture, respectively. A combination of (i) and (ii) is also possible.

If initially a projectile is not a fully stripped ion but carries one or more electrons, then in collisions with atomic targets these electrons can be excited and/or lost. In the rest frame of the

ion this can be viewed as excitation or 'ionization' of the ion by the impact of the incident atom. The atom has electrons which may influence the motion of the electrons of the ion in different ways. Therefore, the physics of the ion excitation and 'ionization' by the neutral atom impact will in general strongly differ from that for excitation and ionization in collisions with a bare atomic nucleus. Thus, in collisions of partially stripped ions with neutral atoms a qualitatively new process, (iii) the projectile-electron excitation and/or loss, may become possible.

The advent of accelerators of heavy ions, where the ions can reach velocities approaching the speed of light, has stimulated a great interest in the study of relativistic atomic collisions. Besides the processes (i)-(iii), in such collisions lepton pair production can occur. In ultrarelativistic electromagnetic collisions the pair creation is possible, in principle, for any leptons but the highest production rates are reached for the process (iv) of electron-positron pair production. [1]

The investigations of the processes (i)-(iv) in the relativistic domain of collision velocities have attracted much attention during the last two decades. Detailed discussions of the processes (i), (ii) and (iv) and broad reviews on these topics can be found in papers [1]- [3] and in a recent book [4]. In the present article we will focus our attention on the projectile-electron excitation and loss in relativistic collisions.

Projectile-electron excitation and loss in nonrelativistic ion-atom collisions have been extensively explored experimentally and theoretically. First order and more sophisticated treatments have been developed and applied for considering the different aspects of these processes and a large amount of experimental data has been obtained (for reviews see [5]- [7]). The situation is quite different, both in experiment and in theory, for the relativistic domain of collision energies. There has been obtained a substantial amount of experimental data on cross sections for the projectile-electron loss at collision energies starting with $\sim$ 100 MeV/u and higher, which usually are regarded already as relativistic. However, up to now just a few experiments (see [8]- [10]) were performed at such collision parameters (projectile and target atomic numbers, collision energy) where the action of the target electrons can actually be modified in a pronounced way by the relativistic effects arising due to collision velocities approaching the speed of light. Further, even relativistic generalizations of nonrelativistic first order theories, which allow to extend the descriptions of collisions of two atomic particles both carrying active electrons for the domain of relativistic collision velocities, have been formulated only very recently [11]- [12].

In the present article the main emphasis will be laid on considerations of theoretical approaches. From the theoretical point of view the study of relativistic atomic collisions, compared to that of nonrelativistic ones, is to some extent simpler, since in many cases, because of very high collision velocities, first order theories may serve as a sound basis. However, one should keep in mind that even first order relativistic theories may become substantially more complicated compared to their nonrelativistic counterparts.

[1] Electron-positron pair production could also occur in collisions with relatively low velocities, where a quasimolecular state of the system 'the nuclei + electron' is formed, provided the colliding nuclei have so high charges that at certain inter-nuclear distances this state 'dives' into the negative-energy continuum.

The present article is first of all a review, however, some new theoretical results are also reported. The main goals of this article are two-fold. First, we want to present a detailed discussion of the recent developments in the study of projectile-electron excitation and loss processes in relativistic collisions with neutral atoms. Second, we hope that this article will not only be an attempt to summarize our present understanding of physics of these processes but could also stimulate further experimental and theoretical activities in this field.

This article is organized as follows.

In the next section a brief overview of the theory of projectile-electron excitation and loss in fast nonrelativistic collisions is given. This section is auxiliary and aims at the introduction of basic ideas and some methods for considerations of nonrelativistic projectile-target collisions and it does not contain any extensive review and discussion. The reader interested in obtaining more information about the projectile-electron excitation and loss in nonrelativistic collisions can be referred to [5]- [7].

In section 3 we give detailed discussions of quantum and semiclassical first order theories for descriptions of relativistic collisions of two atomic particles which both initially carry active electrons. Besides formulating these theories, in this section we consider such points as equivalence of the semiclassical and quantum treatments, the nonrelativistic limit of these theories, gauge independence of obtained results e.t.c.. The Lorentz gauge, which is manifestly covariant, will be used throughout the section as a basic gauge. In addition, formulas for transition amplitudes and cross sections, derived in the Coulomb gauge, will also be given and the interrelation between results, obtained by using the Lorentz and Coulomb gauges, will be analyzed in detail.

Section 4 is devoted to considering some methods for treating projectile-electron excitation and loss in ultrarelativistic collisions which go beyond first order approximations in the interaction between the electron of the projectile and the atomic target.

Sections 5 and 6 contain mainly applications of the theoretical approaches, considered in the previous sections, to concrete collision processes. In section 5 we discuss impact parameter dependencies for probabilities of projectile-electron excitation and loss in relativistic collisions. Cross sections are considered in section 6, where results of calculations are compared with available experimental data. In particular, in this section we present detailed discussions of the various aspects of the behaviour of the total and differential cross sections for the electron loss from hydrogen-like heavy ions colliding with atoms at collision energies covering a broad range of ~ 0.1 - 1000 GeV/u. In section 6 we also consider simultaneous excitation-loss and double loss in relativistic collisions of heavy helium-like ions with neutral many-electron atoms. Besides, section 6 includes brief discussions of free and bound-free electron-positron pair production in collisions between a bare nucleus and a neutral atom and of excitation and break-up of pionium colliding with atoms at relativistic velocities. All these processes have much in common with the projectile-electron excitation and loss. For example, in the Dirac sea picture the bound-free pair production is very closely related to the projectile-electron loss process. On the other hand, although the strong interaction is of crucial importance for physics of the pions π^+ and π^- constituting pionium, the interaction between pionium and atoms occurs predominantly via

the electromagnetic interaction and in this sense pionium just represents some exotic atomic object.

Atomic units are used throughout except where otherwise stated.

2 Theory of projectile-electron excitation and loss in fast nonrelativistic collisions with atoms: a brief overview

2.1 Quantum consideration. Plane-wave Born approximation

In quantum considerations of atomic collisions all atomic particles, electrons and nuclei, are treated quantum mechanically. The simplest quantum mechanical approach for considering nonrelativistic collisions of two structured atomic particles - first order plane-wave (or plane-wave Born) approximation - was formulated long ago by Bates and Griffing [13]- [15]. Later on this approximation was used in many papers devoted to the different aspects of the projectile-electron excitation and loss in collisions with neutral atoms and simplest molecules (for a broad review on this topic see [5] and [6] where also references to many original papers can be found).

The formulation of the plane-wave Born approximation for nonrelativistic collisions is elementary and represents no difficulty. Here we sketch very briefly how one can derive first order cross sections using an approach, which is slightly more complicated compared to the standard derivation of cross sections (see e.g. [13], [5]- [7]) and, to our knowledge, has not been used in the literature. However, for the purpose of the present review article this approach has a valuable merit since it permits a natural generalization for the case of relativistic collisions.

Let us consider a collision between a projectile-ion and a target-atom. The charges of the nuclei of the colliding particles are Z_I and Z_A, respectively, and v is the collision velocity. For simplicity we will assume for the moment that each of the colliding atomic particles has initially only one electron. The S-matrix element describing transitions in the colliding system can be quite generally written as

$$\mathcal{S}_{fi} = -i \int_{-\infty}^{+\infty} dt \int d^3\mathbf{x} \varrho_I(\mathbf{x},t)\, \varphi_A(\mathbf{x},t). \tag{1}$$

Here $\varrho_I(\mathbf{x},t)$ is the transition charge density created by the projectile at time t and space point $\mathbf{x}$ and $\varphi_A(\mathbf{x},t)$ is the transition scalar potential generated by the target atom at the same t and $\mathbf{x}$. [2] Throughout the article the indices A and I stand for the atom and ion, respectively. The scalar potential, created by the target in the collision, is a solution of Poisson's equation

$$\Delta\varphi_A(\mathbf{x},t) = -4\pi\varrho_A(\mathbf{x},t)\ , \tag{2}$$

where $\varrho_A(\mathbf{x},t)$ is the transition charge density of the target.

[2] Of course, one can take the S-matrix element in a fully equivalent form where the target charge density is coupled with the projectile scalar potential.

The charge densities are given by

$$\begin{aligned}\varrho_I(\mathbf{x},t) &= \int d^3\mathbf{R}_I\, d^3\mathbf{r}\Psi^\star_{I,f}(\mathbf{R}_I,\mathbf{r},t)\left[Z_I\delta(\mathbf{x}-\mathbf{R}_I)-\delta(\mathbf{x}-\mathbf{r})\right]\Psi_{I,i}(\mathbf{R}_I,\mathbf{r},t),\\ \varrho_A(\mathbf{x},t) &= \int d^3\mathbf{R}_A\, d^3\boldsymbol{\rho}\Psi^\star_{A,f}(\mathbf{R}_A,\boldsymbol{\rho},t)\left[Z_A\delta(\mathbf{x}-\mathbf{R}_A)-\delta(\mathbf{x}-\mathbf{r})\right]\Psi_{A,i}(\mathbf{R}_A,\boldsymbol{\rho},t). \qquad (3)\end{aligned}$$

Within the first-order treatment, $\Psi_{I,i}$ ($\Psi_{A,i}$) and $\Psi_{I,f}$ ($\Psi_{A,f}$) are approximated by unperturbed initial and final states of the projectile (target), respectively. The form of these states is well known: they are a product of a plane-wave, representing the motion of the center of mass of the projectile-ion (target-atom), and a function which describes the internal motion of the electron in the projectile (target). Further, in (3) $\mathbf{R}_I$ is the coordinate of the projectile nucleus, $\mathbf{r}$ is the coordinate of the projectile electron with respect to the projectile nucleus, $\mathbf{R}_A$ the coordinate of the target nucleus and $\boldsymbol{\rho}$ the coordinate of the target electron with respect to the target nucleus.

The target scalar potential and the integrals in Eq.(1) are conveniently evaluated by using Fourier transforms for the charge densities ϱ_I, ϱ_A and the scalar potential φ_A, e.g. $\varrho_A(\mathbf{x},t) = \frac{1}{4\pi^2}\int d\omega d^3\mathbf{q}\exp(i\mathbf{q}\cdot\mathbf{x}-i\omega t)\lambda_A(\mathbf{q},\omega)$, where λ_A is the Fourier transform of ϱ_A. Using the standard procedure of obtaining a cross section from a known S-matrix transition element, one can show that the cross section for a collision, in which the electron of the projectile makes a transition from an initial internal state ψ_0 into a final internal state ψ_n and the electron of the target makes a transition from its internal initial state u_0 to a final state u_m, is given by

$$\sigma^{0\to m}_{0\to n} = \frac{4}{v^2}\int d^2\mathbf{q}_\perp \frac{\mid F^I_{0n}(\mathbf{q})\; F^A_{0m}(-\mathbf{q})\mid^2}{q^4}. \qquad (4)$$

Here $\mathbf{q}=(\mathbf{q}_\perp, q_{min})$ is the momentum transfer to the projectile where $\mathbf{q}_\perp$ is the two-dimensional part of the momentum, which is perpendicular to the collision velocity $\mathbf{v}$, and q_{min} is the minimum momentum transfer to the projectile given by

$$q_{min} = \frac{\varepsilon_n-\varepsilon_0+\epsilon_m-\epsilon_0}{v}, \qquad (5)$$

where $\varepsilon_{0(n)}$ and $\epsilon_{0(m)}$ are the initial (final) electron energies in the internal states of the projectile and target, respectively. Further, in Eq.(4)

$$\begin{aligned}F^I_{0n}(\mathbf{q}) &= Z_I\delta_{n0}-\int d^3\mathbf{r}\psi^*_n(\mathbf{r})\exp(i\mathbf{q}\cdot\mathbf{r})\psi_0(\mathbf{r}) = Z_I\delta_{n0}-\langle\psi_n\left|\exp(i\mathbf{q}\cdot\mathbf{r})\right|\psi_0\rangle\\ F^A_{0m}(\mathbf{q}) &= Z_A\delta_{m0}-\int d^3\boldsymbol{\rho}u^*_m(\boldsymbol{\rho})\exp(i\mathbf{q}\cdot\boldsymbol{\rho})u_0(\boldsymbol{\rho}) = Z_A\delta_{m0}-\langle u_m\left|\exp(i\mathbf{q}\cdot\boldsymbol{\rho})\right|u_0\rangle. \qquad (6)\end{aligned}$$

When considering collisions of a projectile carrying initially an electron with a target we will be interested in the study of those collisions where the projectile electron makes a transition, i.e. when it gets excited or lost and $n\neq 0$. In what follows we will not consider collisions where $n=0$, i.e. collisions which are elastic for the projectile. While final states of the projectile are observed in experiment, there is often no experimental information about the final state of the

target. Therefore, in order to describe theoretically such a situation, one has to calculate the cross section

$$\sigma_{0\to n} = \sum_m \sigma_{0\to n}^{0\to m}, \tag{7}$$

where the summation has to be performed over all possible final states of the target including the continuum. It is convenient to split the first order cross section (7) into two parts and discuss them separately.

2.1.1 Screening mode

One part represents the contribution to the cross section (7) from collisions in which the target electron remains in the initial state, i.e. from collisions where this electron can be considered as 'passive'. This part reads

$$\sigma_{0\to n}^{s} = \frac{4}{v^2}\int d^2\mathbf{q}_\perp Z_{A,eff}^2(\mathbf{q}_0)\frac{|\,\langle\psi_n\mid \exp(i\mathbf{q}_0\cdot\mathbf{r})\mid\psi_0\rangle\,|^2}{q^4}. \tag{8}$$

Here $\mathbf{q}_0 = \left(\mathbf{q}_\perp, \frac{\varepsilon_n-\varepsilon_0}{v}\right)$ and $Z_{A,eff} = Z_A - \langle u_0\,|\exp(-i\mathbf{q}_0\cdot\boldsymbol{\rho})|\,u_0\rangle$ is the effective charge of the target which is 'seen' by the electron of the projectile in collisions where the target does not change its internal state. Considering this effective charge as a function of the momentum transfer one can note the following important points (see [7], [16] and references therein). The value of the effective charge $Z_{A,eff}$ varies in the limits $Z_A - 1 < Z_{A,eff} < Z_A$. [3] The charge $Z_{A,eff}$ approaches its lower and upper limits in collisions where the momentum transfer q_0 is much lower and much larger, respectively, than a typical electron momentum in the initial target state.

It is seen that the effect of the target electron(s) in collisions, where the target remains in its initial internal state, is to weaken the effect of the target nucleus on the projectile electron, i.e. to partially or completely screen the nucleus. Therefore, the collision mode, in which the target does not change its internal state, is often called the *screening mode* or simply *screening*. This mode is also termed *elastic*, meaning that it is elastic for the target. In the present article we will use both these notations.

2.1.2 Antiscreening mode

The second part of the cross section (7) describes collisions in which the target electron makes transitions. It reads

$$\begin{aligned}\sigma_{0\to n}^{a} &= \sum_{m\neq 0}\sigma_{0\to n}^{0\to m}\\ &= \frac{4}{v^2}\sum_{m\neq 0}\int d^2\mathbf{q}_\perp\frac{|\,\langle u_m\mid\exp(-i\mathbf{q}\cdot\boldsymbol{\rho})\mid u_0\rangle\langle\psi_n\mid\exp(i\mathbf{q}\cdot\mathbf{r})\mid\psi_0\rangle\,|^2}{q^4}.\end{aligned} \tag{9}$$

[3] If the target contains N_A electrons then $Z_A - N_A < Z_{A,eff} < Z_A$.

Eq.(9) deals with the collision mode where not only the electron of the projectile but also that of the target are 'active' in the collision. In this mode the electron of the projectile makes a transition solely due to the interaction with the target electron whereas the interaction of the projectile electron with the target nucleus does not influence this transition. Contributions from collisions, in which the target changes its initial internal state, increase the total cross section (7). This action of the target electron is opposite to that in the screening mode where the electron screens the target nucleus and decreases the cross section compared to collisions with the bare nucleus. Therefore, the collision mode, in which the target changes its internal state, is often called *antiscreening*. This mode is also termed *doubly inelastic* or simply *inelastic*. In what follows we will use the terms 'inelastic' or 'antiscreening' to denote collisions where the initial internal state of the target is changed.

2.1.3 Collisions with large momentum transfer. Free collision model

Let us consider collisions in which the minimum momentum transfer q_{min}, given by Eq.(5), and, thus, the total momentum transfer q are much larger than a typical momentum of the target electron in the initial target state. Such a situation can occur if the atomic number Z_I of the projectile substantially exceeds that of the target Z_A and the collision velocity is not too high.

Elastic mode. For the elastic mode the effective charge $Z_{A,eff} = Z_A - \langle u_0 \,|\exp(-i\mathbf{q}_0 \cdot \boldsymbol{\rho})|\, u_0\rangle$, because of the rapid oscillations of the integrand due to the factor $\exp(-i\mathbf{q}_0 \cdot \boldsymbol{\rho})$, becomes approximately equal to the charge Z_A of the bare target nucleus. Therefore, in collisions with the large momentum transfer the screening effect of the target electron is very weak.

Inelastic mode. In collisions with large momentum transfers the rapid oscillations of the term $\exp(-i\mathbf{q} \cdot \boldsymbol{\rho})$ in the integrands of the transition matrix elements $\langle u_m \mid \exp(-i\mathbf{q} \cdot \boldsymbol{\rho}) \mid u_0\rangle$ can make them negligible. These oscillations, however, can be compensated in the case when final states of the target electron are continuum states where the electron momentum $\mathbf{k}$ with respect to the target nucleus is close to $-\mathbf{q}$, i.e. where $\mathbf{k} \approx -\mathbf{q}$ or, by separating the transverse and longitudinal parts, $\mathbf{k}_\perp \approx -\mathbf{q}_\perp$ and $k_z \approx -q_{min}$.

The condition $\mathbf{k}_\perp \approx -\mathbf{q}_\perp$ simply implies that nearly the whole transverse momentum transfer to the target has to be taken by the target electron alone.

More insight into the collision physics can be obtained by considering the condition $k_z \approx -q_{min}$. Taking into account the explicit form of q_{min}, this condition can be rewritten as a quadratic equation for k_z which has solutions

$$k_z^{\pm} \approx -v \pm \sqrt{v^2 - k_\perp^2 - 2(\varepsilon_n - \varepsilon_0 - \epsilon_0)}. \tag{10}$$

If $\frac{v^2}{2} < (\varepsilon_n - \varepsilon_0 - \epsilon_0) \approx (\varepsilon_n - \varepsilon_0)$ then both roots in Eq.(10) are complex. Physically it means that in such a case, due to the restrictions imposed by the energy-momentum conservation in the collision, there are no target states where the rapidly oscillating factor $\exp(-i\mathbf{q} \cdot \boldsymbol{\rho})$ can be compensated by a similar term arising from the final motion of the target electron. As a result, the inelastic contribution (9) to the cross section (7) is negligible in this case.

The roots $k_z^{\pm}$, given by Eq.(10), become real if $\frac{v^2}{2} > (\varepsilon_n - \varepsilon_0 + k_\perp^2/2 - \epsilon_0)$. If, in addition, we assume that $\frac{v^2}{2} \gg (\varepsilon_n - \varepsilon_0 + k_\perp^2/2 - \epsilon_0)$, then these roots are given by $k_z^+ \approx -(0.5k_\perp^2 + \varepsilon_n - \varepsilon_0 - \epsilon_0)/v$ and $k_z^- \approx -2v$. In the rest frame of the projectile these roots correspond to an electron having the z-komponent of the momentum approximately equal to v and $-v$, respectively, where $v > 0$ is the velocity of the incident target. Analysis shows that the contribution of the electrons with $k_z \approx k_z^-$ to the inelastic cross section is much smaller than that of the electrons with $k_z \approx k_z^+$ and can be neglected. A rough estimate for the contribution to the inelastic cross section (9) from collisions in which $k_z \approx -(0.5k_\perp^2 + \varepsilon_n - \varepsilon_0)/v$ can be easily obtained if one neglects the dependence of q_{min} on the final energy of the target electron. In such a case the integration over the final continuum states of the target electron in (9) is elementary performed by assuming that, because of large k, these states can be approximated by plane waves. The result is

$$\sigma_{0\to n}^a \simeq \frac{4}{v^2}\int d^2\mathbf{q}_\perp \frac{\mid \langle\psi_n \mid \exp(i\mathbf{q}_0\cdot\mathbf{r}) \mid \psi_0\rangle \mid^2}{q_0^4}, \tag{11}$$

where $\mathbf{q}_0 = \left(\mathbf{q}_\perp, \frac{\varepsilon_n - \varepsilon_0}{v}\right)$. This cross section can be interpreted as describing transitions of the electron in the projectile under the action of a fast free electron which has initially velocity v with respect to the projectile. Combining Eqs.(11) and (8) and taking into account that $Z_{A,eff} \approx Z_A$ we see that the cross section (7) in collisions with large momentum transfers can be approximated by

$$\sigma_{0\to n} \approx (Z_A^2 + 1)\sigma_{0\to n}^{pr}, \tag{12}$$

where $\sigma_{0\to n}^{pr}$ is the cross section for collisions in which the projectile electron makes a transition $0 \to n$ due to the interaction with a point-like unit charge moving with velocity v in the projectile frame. According to Eq.(12) the target nucleus and the target electron act incoherently in the collision. If the atom has initially Z_A electrons the factor $Z_A^2 + 1$ in Eq.(12) should be replaced by $Z_A^2 + Z_A$. Eq.(12) is the essence of the free collision model introduced long ago by N.Bohr. This model, in particular, suggests that the relative importance of the elastic mode in the projectile-target collisions should rapidly increase with increasing atomic number of the neutral target.

The free collision model is quite simple and physically appealing but not very accurate. Better results for the cross sections can be obtained by applying the so called impulse approximation which is closely related to the free collision model. The application of the impulse approximation to the projectile electron excitation and loss was discussed in a review article [5] where also references to original articles were given. The impulse approximation takes into account the inner motion of the electrons in the target atom by averaging the projectile cross sections over the momentum distribution of these electrons in their initial bound state. An useful discussion of the relationship between the plane-wave Born and impulse approximations was presented in [17].

2.2 Semiclassical considerations

In the theory of fast ion-atom collisions quite often only electrons are treated quantum mechanically whereas the nuclei of the colliding partners are regarded as classical particles and their relative motion is described in terms of a classical trajectory with a certain impact parameter **b** and a collision velocity **v**. Such an approach is called *semiclassical*. Although according to quantum mechanics the impact parameter in general does not represent a measurable quantity, the semiclassical approach has important merits. First, by considering transition probabilities as a function of the impact parameter one can get an additional insight into the collision physics. Second, the impact parameter consideration is usually more convenient for treatments which go beyond the first order approximation in the projectile-target interaction. Third, formulating a theory in terms of impact parameter allows one to apply the independent electron approximation for evaluating cross sections of multielectron transitions.

Let us consider a collision between a projectile-ion with a nuclear charge Z_I, which initially has one electron, and a neutral target atom with atomic number Z_A by using the semiclassical approximation. In this approximation the electronic system of the colliding particles containing $Z_A + 1$ electrons is described by the time-dependent Schrödinger equation

$$\left(i\frac{\partial}{\partial t} - H_i^{el} - H_a^{el} - V \right) \Psi^{el}(\mathbf{r}, \{\boldsymbol{\rho}\}, t) = 0. \tag{13}$$

Here, $\Psi^{el}(\mathbf{r}, \{\boldsymbol{\rho}\}, t)$ is the time-dependent wavefunction describing the electronic degrees of freedom, $\mathbf{r}$ is the coordinate of the electron of the ion with respect to the ion nucleus and $\{\boldsymbol{\rho}\} = \{\boldsymbol{\rho_1}, \boldsymbol{\rho_1}, ...\}$ is the set of the coordinates of the electrons of the atom with respect to the atomic nucleus. In Eq.(13) H_i^{el} and H_a^{el} are the electronic Hamiltonians of the ion and atom, respectively, and

$$V = \frac{Z_I Z_A}{R(t)} - \frac{Z_A}{\mid \mathbf{R}(t) + \mathbf{r} \mid} - \sum_{j=1}^{Z_A} \frac{Z_I}{\mid \mathbf{R}(t) - \boldsymbol{\rho_j} \mid} + \sum_{j=1}^{Z_A} \frac{1}{\mid \mathbf{R}(t) - \boldsymbol{\rho_j} + \mathbf{r} \mid} \tag{14}$$

is the interaction between the ion and the atom. The term $\frac{Z_I Z_A}{R(t)}$ represents the Coulomb nucleus-nucleus interaction. In fast collisions this interaction does not influence electron transitions and, therefore, this term can be omitted. Starting with collision energies of a few thousand electron volts the projectile-ion motion is well described by a straight line $\mathbf{R}(t) = \mathbf{b} + \mathbf{v}t$, where **b** and **v** are the impact parameter and the collision velocity, respectively.

One way to solve Eq.(13) is to expand the wavefunction in a complete set, $\{\varphi_\alpha(\mathbf{r}, \{\boldsymbol{\rho}\})\}$, of internal wavefunctions of the non-interacting ion-atom system

$$\Psi^{el} = \sum_\alpha a_\alpha(t)\, \exp(-iE_\alpha t)\, \varphi_\alpha, \tag{15}$$

where E_α is the sum of internal electronic energies of the ion and atom. We assume that so called electron translational factors as well as kinetic energies of the relative motion of the electrons are included in the wavefunctions φ_α. It is implied that the summation in (15) runs

also over continuum states of the electron in the ion and those of the electrons in the atom. Inserting Eq.(15) into Eq.(13) one obtains for the unknown time-dependent coefficients a_α the following infinite system of differential equations

$$i\frac{da_\alpha}{dt} = \sum_{\alpha'} V_{\alpha\alpha'}(t)\exp(i(E_\alpha - E_{\alpha'})t)a_{\alpha'}. \tag{16}$$

At large collision velocities transitions of the electrons between different centers (charge exchange channels) are suppressed because of the electron translational factors and can be neglected. For electron transitions at the same centers the translational factors for initial and final states as well as kinetic energies of the relative motion of the electrons in the corresponding exponents mutually cancel. Therefore, the term $V_{\alpha\alpha'} = \langle\varphi_\alpha \mid V(t) \mid \varphi_{\alpha'}\rangle$ can be rewritten as $V_{\alpha\alpha'} = \langle\chi_\alpha \mid V(t) \mid \chi_{\alpha'}\rangle$, where the functions χ_α describe the internal motion of the electrons within the colliding particles.

2.2.1 First-order approximation

The first order transition amplitude is obtained from (16) if we set $a_{\alpha'} = \delta_{\alpha' 0}$ on the right hand side of this equation. Then the first-order solution is given by

$$a_\alpha(\mathbf{b}) = -i\int_{-\infty}^{+\infty} dt V_{\alpha 0}(t)\exp(i(E_\alpha - E_0)t). \tag{17}$$

Neglecting the antisymmetrization of the electron of the ion and the electrons of the atom, the electronic states χ_α are written as

$$\begin{aligned}\chi_0(\mathbf{r},\{\boldsymbol{\rho}\}) &= \psi_0(\mathbf{r})\,u_0(\{\boldsymbol{\rho}\})\\ \chi_\alpha(\mathbf{r},\{\boldsymbol{\rho}\}) &= \psi_n(\mathbf{r})\,u_m(\{\boldsymbol{\rho}\}),\end{aligned} \tag{18}$$

where ψ_0 and ψ_n are the initial and final electronic states of the projectile and u_0 and u_m are those for the atom. Since we consider only collisions where $n \neq 0$ then the third interaction term in Eq.(14) does not contribute to the transition amplitude (17) and the latter reads

$$\begin{aligned}a_{0\to n}^{0\to m}(\mathbf{b}) = \quad & i\int_{-\infty}^{+\infty} dt\exp(i(\varepsilon_n + \epsilon_m - \varepsilon_0 - \epsilon_0)t)\\ & \times\left\langle \psi_n u_m \left| \frac{Z_A}{|\mathbf{R}(t)+\mathbf{r}|} - \sum_{j=1}^{Z_A}\frac{1}{|\,\mathbf{R}(t)-\boldsymbol{\rho_j}+\mathbf{r}\,|}\right| \psi_0 u_0\right\rangle.\end{aligned} \tag{19}$$

By applying the integral representation $1/|\mathbf{x}| = (1/2\pi^2)\int d^3\mathbf{q}\exp(i\mathbf{q}\cdot\mathbf{x})/q^2$ to the Coulomb potentials $1/|\mathbf{R}(t)+\mathbf{r}|$ and $1/|\,\mathbf{R}(t)-\boldsymbol{\rho_j}+\mathbf{r}|$ the amplitude (19) is transformed into

$$\begin{aligned}a_{0\to n}^{0\to m}(\mathbf{b}) = \frac{i}{\pi v}\int d^2\mathbf{q}_\perp \quad & \exp(-i\mathbf{q}_\perp\cdot\mathbf{b})\left\langle u_m\left| Z_A - \sum_j^{Z_A}\exp(-i\mathbf{q}\cdot\boldsymbol{\rho_j})\right| u_0\right\rangle\\ & \times\frac{\langle\psi_n\,|\exp(i\mathbf{q}\cdot\mathbf{r})|\,\psi_0\rangle}{q^2},\end{aligned} \tag{20}$$

where $\mathbf{q} = (\mathbf{q}_\perp, q_{min})$ with q_{min} given by Eq.(5). It is easy to show [18] that the semiclassical first-order cross section

$$\sigma_{0\to n}^{0\to m} = \int d^2\mathbf{b} \left| a_{0\to n}^{0\to m}(\mathbf{b}) \right|^2 \tag{21}$$

coincides with that following from the plane-wave Born approximation.

Theoretical considerations based on the first-order perturbation theory in the projectile-target interaction are expected to represent a reasonable approximation for treating the projectile electron excitation and loss in fast collisions with neutral atoms provided $Z_A \ll v$ (or at least $Z_A < v$).

When, for a given collision velocity, the target atomic number substantially increases, the interaction between the electron of the projectile and the target becomes too strong, making first-order theories irrelevant. In reality each transition from the initial electron state of the projectile would lead to a reduction of the population of this state making further transitions from this state less probable. Such a reduction is not taken into account in first-order theories. The latter ones do not preserve unitarity and, therefore, often result in strongly overestimated cross sections in the case of large perturbations. This may be especially true for the screening mode where the screened field of the target nucleus can become so strong in collisions with small impact parameters that first order calculations yield elastic cross sections which are an order of magnitude larger than the experimental total cross sections (see [19]- [20]). Clearly, in such a case better approaches are necessary in order to describe the projectile electron excitation and loss processes.

2.2.2 Coupled channel approaches

The system of the differential equations (16) is equivalent to the Schrödinger equation (13) and, in this sense, is exact. However, it includes an infinite number of channels and cannot be solved without making approximations. One way to solve approximately the system (16) would be to keep all the channels and to develop a perturbation series by using an iteration procedure. Coupled channel approaches represent an alternative. They consist of (i) a restriction of the number of channels considered and (ii) an exact (numerical) solution of the resulting finite set of the coupled equations. Coupled channel approaches preserve unitarity and, compared to first order treatments, are much better suited for considering strong perturbations.

In [20] a coupled channel approach was applied to calculate cross sections for the electron loss from $He^+(1s)$ in collisions with Ne, Ar and Kr atoms at collision energies $0.25 - 1$ MeV/u. Because of technical difficulties coupled channel calculations were performed by assuming that the target atom is 'frozen' in its ground state, i.e. only the screeening cross section was calculated. Substantial improvements in the results for the loss cross section, compared to first order calculations, were reported in [20].

Coupled channel approaches have been proved to be very useful also for treating projectile-target collisions at relatively low velocities where the electron capture plays an important role [21].

2.2.3 Sudden approximation

Equations (16) can be solved analytically if we assume that the exponents of the oscillating factors on the right hand side of (16) are small and can be neglected. This is the case if the effective collision time $T(b)$, when the interaction $V(t)$ reaches considerable magnitudes, is short compared to typical electron transition times $\tau_{\alpha\alpha'} \simeq |E_\alpha - E_{\alpha'}|^{-1}$, i.e. if $|E_\alpha - E_{\alpha'}|\, T \ll 1$. If we neglect these oscillating factors then the solution of the infinite set of equations (16) reads [22]

$$\begin{aligned} a^{SA}_{0\to n,0\to m}(t) &= < \chi_\alpha \mid \exp\left(-i\int_{-\infty}^{t} dt\, V(t)\right) \mid \chi_0 > \\ &= \left\langle u_m\, \psi_n \left| \exp\left(-i\int_{-\infty}^{t} dt'\, V(t')\right) \right| \psi_0\, u_0 \right\rangle, \end{aligned} \tag{22}$$

where the interaction V includes the last three terms of (14). The above amplitude has the familiar form of the transition amplitude obtained within the first order of the Magnus (or sudden) approximation [23] (see also [24]). The valuable merit of the sudden approximation is that it preserves unitarity. For the total probability to find the electronic system of the colliding particles in any of its possible state one has

$$P^{SA}_{tot}(\mathbf{b}) = \sum_{n,m} \left| a^{SA}_{0\to n,0\to m}(t) \right|^2 \equiv 1. \tag{23}$$

Within the sudden approximation the cross section reads

$$\sigma^{SA}_{0\to n,0\to m} = \int d^2\mathbf{b} \left| \left\langle u_m\, \psi_n \left| \exp\left(-i\int_{-\infty}^{+\infty} dt\, V(t)\right) \right| \psi_0\, u_0 \right\rangle \right|^2. \tag{24}$$

Eq.(24) was used in [25] as a starting point for calculations of the electron loss from $He^+(1s)$ in collisions with many-electron atoms in the range of collision velocities where the application of the first order treatment may overestimate the loss cross section by an order of magnitude. A reasonable agreement with experiment was reported in [25].

3 Projectile-electron excitation and loss in relativistic collisions with atoms: first order considerations

3.1 Preliminary remarks

To our knowledge, the first attempt to formulate a theory for the projectile-electron loss in relativistic collisions with neutral atomic targets was made in [26]. The approach of [26] to this problem was based on the first order perturbative treatment of ionization in relativistic collisions with structureless point-like charges [27], [28]. In order to take into account the fundamental difference between the actions of a point-like charge and a neutral atom in the collision, results for the projectile-electron loss in nonrelativistic collisions with neutral atoms were employed and

some intuitive assumptions were introduced to adapt the nonrelativistic results to relativistic collisions. The most complete set of results for the loss process in relativistic collisions, obtained in this way, was presented in a paper of Anholt and Becker [29]. In that paper the electron loss in ultrarelativistic collisions was considered for a variety of projectile-target pairs for collision energies up to those corresponding to $\gamma \leq 1000$, where γ is the collisional Lorentz factor. The key finding of [29] was that the loss cross section for any projectile-target pair can be well approximated for the range $5 \div 10 \lesssim \gamma \lesssim 1000$ by the following simple formula: $\sigma_{loss} = A + B \ln \gamma$, where the parameters A and B depend on the projectile-target pair but are γ-independent.

One should note that the structure of the above expression closely resembles that of the cross section for single ionization of atoms (e.g. K-shell ionization) by point-like charged particles moving at relativistic velocities. In particular, the above loss cross section includes the term $\ln \gamma$ which is well known to appear in the cross section for atomic ionization by relativistic charged particles. In the loss cross section such a term would arise if collisions with large impact parameters $b_{max} \sim v\gamma/\omega_{fi}$, where v is the collision velocity and ω_{fi} is the energy transfer to the atomic electron, would substantially contribute to the loss process.

Elementary estimates show, however, that even in the case when one considers the electron loss from the heaviest hydrogen-like projectiles, for which the energy transfers ω_{fi} reach the largest values (and, therefore, b_{max} are smaller than those for lighter projectiles), the impact parameters $b_{max} \sim v\gamma/\omega_{fi}$ can substantially exceed the size of a neutral atom already in collisions where the Lorentz factor is still far below 1000. Therefore, it is rather obvious that the simple expression for the loss cross section, suggested in [29], in general cannot be valid for ultrarelativistic collisions. In particular, as the same estimates suggest, this expression should not be applied to evaluate cross sections for the electron loss from very heavy ions at $\gamma \sim 50$ and higher and its applicability may become even more questionable in cases of the electron loss from lighter ions (for illustrations see figures 1 and 2).

The main reason for this is that the formula of Anholt and Becker does not account for important peculiarities in the screening effect of the atomic electrons in collisions with large γ. However, this shortcoming has not been revealed for more than 10 years until a recent experiment [8] on electron loss from ultrarelativistic hydrogen-like Pb ions unveiled the considerable difference between the predictions of the theory of [29] and the experimental observations.

It was Sørensen, who first pointed out in [30], that the loss cross section, obtained in [29], does not correctly describe screening effects in ultrarelativistic collisions. As an alternative, Sørensen suggested in [30], within the framework of first order perturbation theory, a simple model to describe the elastic part of the electron loss cross section. Within this model the elastic part is separated into contributions from 'close' and 'distant' collisions. The dividing distance between the 'close' and 'distant' collisions was chosen in [30] to be essentially the radius of the electron bound state in the projectile. The close-collision contribution was evaluated (i) by regarding the projectile electron as free and (ii) by assuming that the action of the neutral atom on the projectile electron is equivalent to that of the atomic nucleus whereas the atomic electrons play no role. The distant-collision contribution was estimated by using the method of

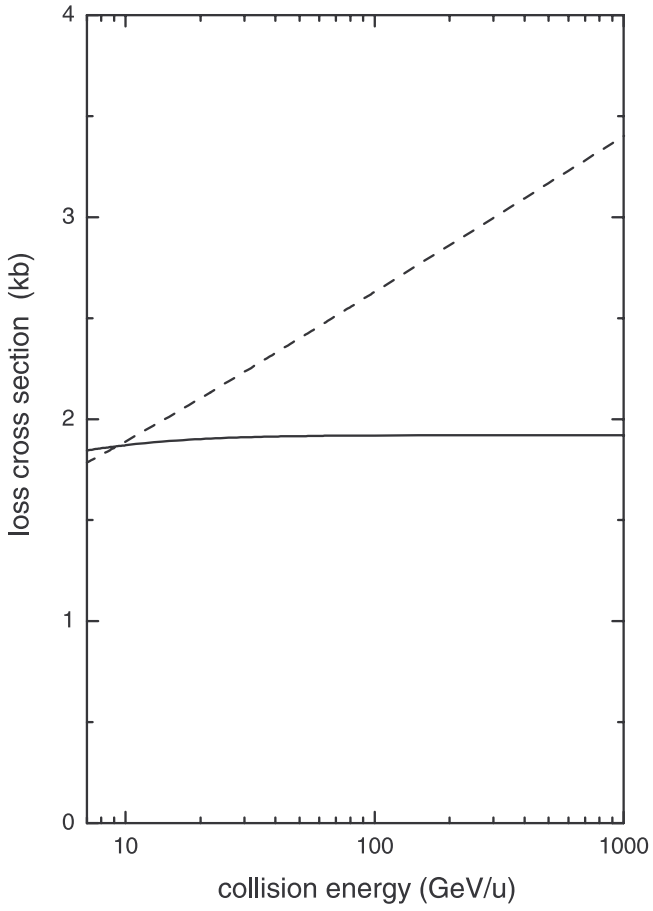

Figure 1: Total cross section for the electron loss from $7 - 1000$ GeV/u Sn^{49+} ions ($Z_I = 50$) colliding with Ne atoms ($Z_A = 10$). The dash line was obtained by using the formula of Anholt and Becker [29]. The solid line shows results calculated with Eqs.(133) and (134) of the present paper.

equivalent photons. The inelastic part of the loss cross section cannot be treated within such an approach. Therefore, the total loss cross section σ_t was estimated as $\sigma_t = (1 + 1/Z_A)\sigma_{scr}$ where σ_{scr} is the elastic part and the rest accounts for the incoherent action of Z_A 'active' atomic electrons.

The model, briefly described above, is not very rigorous. For example, although the result for the total loss cross section in the model is dependent on the impact parameter, which separates 'close' and 'distant' collisions, the latter is not strictly defined. Further, the projectile electron can be treated as (quasi-) free only in collisions where the momentum transfer to the electron is much larger than its typical momentum in the initial bound state of the projectile (all the momenta are considered in the projectile frame). However, even for 'close' impact parameters this is not the case for the overwhelming majority of the collisions. In addition, there is also a substanial arbitrariness in estimating the contribution arising from the 'distant'

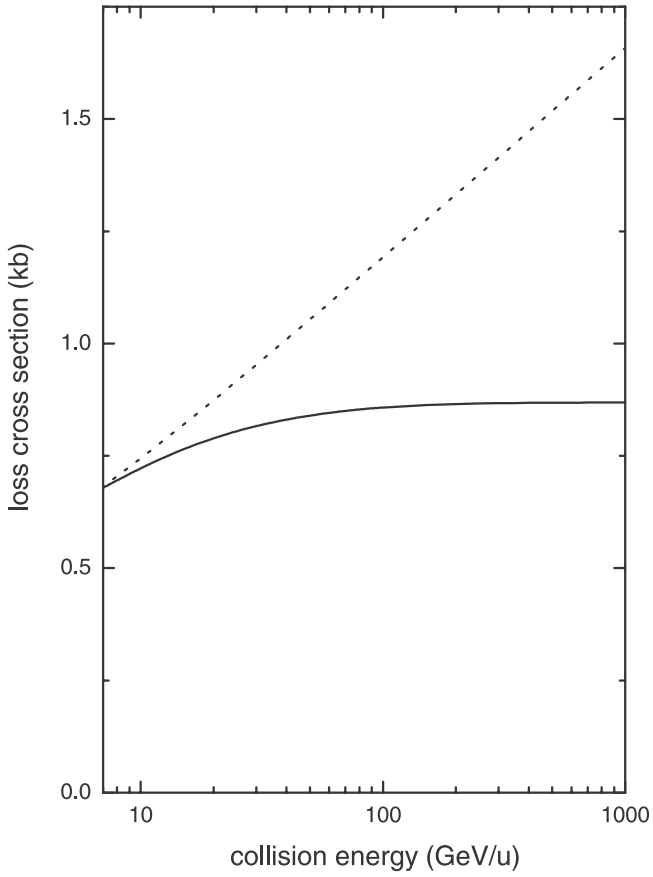

Figure 2: Same as in figure 1 but for the electron loss from Hg^{79+} ($Z_I = 80$).

collisions. Nevertheless, despite these shortcomings, the model of [30] is physically appealing and cross section values reported in [30] are in surprisingly good agreement with experiment and results of more rigorous treatments.

The detailed discussion of the recent progress achieved in the developments of such treatments is the very topic of this and next sections.

3.2 Simplified semiclassical consideration

We start with a simplified semiclassical first-order consideration for the screening part of the projectile-electron excitation or loss in relativistic collisions with an atomic target [31]. It is convenient to consider the collision in the projectile-ion frame. The nucleus of the ion with charge Z_I is assumed to be at rest and taken as the origin. The relative motion of the neutral atom is treated classically. The nucleus of the incident neutral atom with atomic number Z_A moves on a straight-line trajectory $\mathbf{R}(t) = \mathbf{b} + \mathbf{v}t$, where $\mathbf{b}$ is the impact parameter and $\mathbf{v} = (0, 0, v)$ the collision velocity. This nucleus is 'dressed' by the electrons, the positions of which are assumed to be 'frozen' with respect to the nucleus. The coordinates of the electrons

with respect to the origin are $\mathbf{r}_j = \mathbf{R}(t) + \boldsymbol{\eta}_j$, where $\boldsymbol{\eta}_j$ are the coordinates of the electrons with respect to the nucleus of the atom.

The fields created by the incident atom are described by the scalar potential $\Phi(\mathbf{r}, t)$ and the vector potential $\mathbf{A}(\mathbf{r}, t)$ obeying the Maxwell equations which in the Lorentz gauge read

$$\begin{aligned} \Delta\Phi(\mathbf{r}, t) - \frac{1}{c^2}\frac{\partial^2\Phi(\mathbf{r}, t)}{\partial t^2} &= -4\pi\rho(\mathbf{r}, t) \\ \Delta\mathbf{A}(\mathbf{r}, t) - \frac{1}{c^2}\frac{\partial^2\mathbf{A}(\mathbf{r}, t)}{\partial t^2} &= -\frac{4\pi}{c}\mathbf{J}(\mathbf{r}, t), \end{aligned} \tag{25}$$

where $c \simeq 137$ a.u. is the speed of light. Considering for the moment that the incident atom is represented by a beam of point-like classical charges, which all have the same velocity $\mathbf{v}$, the charge and current densities of the incident atom are simply given by

$$\begin{aligned} \rho(\mathbf{r}, t) &= Z_A\delta(\mathbf{r} - \mathbf{R}(t)) - \sum_j^{N_A}\delta(\mathbf{r} - \mathbf{R}(t) - \boldsymbol{\eta}_j) \\ \mathbf{J}(\mathbf{r}, t) &= \rho(\mathbf{r}, t)\mathbf{v}, \end{aligned} \tag{26}$$

where the sum runs over all atomic electrons ($N_A = Z_A$ for the neutral atom). Equations (25) can be solved by using Fourier transformations:

$$\begin{aligned} \Phi(\mathbf{r}, t) &= \frac{1}{4\pi^2}\int d^3\mathbf{q}\int_{-\infty}^{+\infty} d\omega F(\mathbf{q}, \omega)\exp(i(\mathbf{q}\cdot\mathbf{r} - \omega t)) \\ \rho(\mathbf{r}, t) &= \frac{1}{8\pi^3}\int d^3\mathbf{q}\int_{-\infty}^{+\infty} d\omega\delta(\omega - \mathbf{q}\cdot\mathbf{v})\,\exp(i(\mathbf{q}\cdot(\mathbf{r} - \mathbf{b}) - \omega t)) \\ &\quad \left(Z_A - \sum_j \exp(-i\mathbf{q}\cdot\boldsymbol{\eta}_j)\right). \end{aligned} \tag{27}$$

Inserting (27) into (25) we get for the Fourier transform $F(\mathbf{q}, \omega)$

$$F(\mathbf{q}, \omega) = \frac{2\,\delta(\omega - \mathbf{q}\cdot\mathbf{v})\exp(-i\mathbf{q}\cdot\mathbf{b})}{q^2 - \frac{\omega^2}{c^2}}\left(Z_A - \sum_j \exp(-i\mathbf{q}\cdot\boldsymbol{\eta}_j)\right) \tag{28}$$

and obtain the integral representation for the scalar potential:

$$\Phi(\mathbf{r}, t) = \frac{1}{2\pi^2}\int d^3\mathbf{q}\,\frac{\exp(i\mathbf{q}\cdot(\mathbf{r} - \mathbf{b} - \mathbf{v}t))}{q^2 - \frac{(\mathbf{q}\mathbf{v})^2}{c^2}}\left(Z_A - \sum_j \exp(-i\mathbf{q}\cdot\boldsymbol{\eta}_j)\right). \tag{29}$$

In the Lorentz gauge the vector potential is very simply related to the scalar one by

$$\mathbf{A}(\mathbf{r}, t) = \frac{\mathbf{v}}{c}\Phi(\mathbf{r}, t). \tag{30}$$

The quantum nature of the 'frozen' electrons of the incident atom can be explicitly taken into account by using the following replacement:

$$\sum_j \exp(-i\mathbf{q}\cdot\boldsymbol{\eta}_j) \to \langle\varphi_0(\boldsymbol{\zeta}_{\boldsymbol{N}})\left|\sum_j \exp(-i\mathbf{q}\cdot\boldsymbol{\eta}_j)\right|\varphi_0(\boldsymbol{\zeta}_{\boldsymbol{N}})\rangle. \tag{31}$$

In (31) $\varphi_0(\boldsymbol{\zeta_N})$ is the electronic wavefunction of the ground state of the incident atom, transformed into the rest frame of the ion, $\boldsymbol{\zeta_N} = \{\boldsymbol{\eta_1},\boldsymbol{\eta_2},...,\boldsymbol{\eta_N}\}$ is the 3-N dimensional vector representing the coordinates of the N electrons of the incident atom with respect to the nucleus of the atom ($\boldsymbol{\zeta_N}$ is given in the ion frame).

We will assume that the ion has a single electron. In the ion frame the interaction of this electron with the incident atom reads

$$V_{int}(\mathbf{r},t) = -\Phi(\mathbf{r},t)\left(1 - \frac{1}{c}\mathbf{v}\cdot\boldsymbol{\alpha}\right) \tag{32}$$

where $\mathbf{r}$ and $\boldsymbol{\alpha}$ are the coordinates and the Dirac matrixes, respectively, for the electron of the ion and Φ is given by Eq.(29) with the replacement (31).

Within the first order perturbation theory the electron transition amplitude $a_{0\to n}$ is given by

$$\begin{aligned} a_{0\to n} &= \frac{i}{2\pi^2}\int_{-\infty}^{+\infty} dt\exp(i\omega_{n0}t)\int d^3\mathbf{q}\,\frac{<\psi_n(\mathbf{r})\mid \exp(i\mathbf{q}\cdot\mathbf{r})\left(1-\frac{1}{c}\mathbf{v}\cdot\boldsymbol{\alpha}\right)\mid\psi_0(\mathbf{r})>}{q^2-\frac{\omega_{n0}^2}{c^2}} \\ &\quad\times Z_{A,eff}(\mathbf{q})\exp(-i\mathbf{q}\cdot(\mathbf{b}+\mathbf{v}t)), \end{aligned} \tag{33}$$

where $\psi_0(\mathbf{r})e^{-i\varepsilon_0 t}$ is the electron ground state, $\psi_n(\mathbf{r})e^{-i\varepsilon_n t}$ the final electron state and $\omega_{n0} = \varepsilon_n - \varepsilon_0$ is the transition frequency of the electron of the ion. The indices 0 and n denote all quantum numbers of the corresponding states including spin. [4] Further, in Eq.(33) the quantity

$$Z_{A,eff}(\mathbf{q}) = Z_A - \langle\varphi_0(\boldsymbol{\zeta_N})\left|\sum_j \exp(-i\mathbf{q}\cdot\boldsymbol{\eta}_j)\right|\varphi_0(\boldsymbol{\zeta_N})\rangle \tag{34}$$

represents an 'effective charge' of the projectile-atom which depends on the momentum transfer $\mathbf{q}$ in the collision.

Integration over time in (33) gives the factor $2\pi\delta(\mathbf{qv}+\varepsilon_0-\varepsilon_n)$ which allows one to integrate easily over the longitudinal component, $q_z = \mathbf{qv}/v$, of the momentum transfer $\mathbf{q}$. The result of these two integrations is

$$\begin{aligned} a_{0\to n} &= \frac{i}{\pi v}\int d^2\mathbf{q}_\perp\,\frac{<\psi_n(\mathbf{r})\mid \exp(i\mathbf{q}\cdot\mathbf{r})\left(1-\frac{1}{c}\mathbf{v}\cdot\boldsymbol{\alpha}\right)\mid\psi_0(\mathbf{r})>}{q_\perp^2+\frac{\omega_{n0}^2}{v^2\gamma^2}} \\ &\quad\times Z_{A,eff}(\mathbf{q})\exp(-i\mathbf{q}_\perp\cdot\mathbf{b}). \end{aligned} \tag{35}$$

Here, $\gamma = \frac{1}{\sqrt{1-v^2/c^2}}$ and now $\mathbf{q} = (\mathbf{q}_\perp, q_z)$ has a fixed z-component, $q_z = \frac{\varepsilon_n-\varepsilon_0}{v}$, which represents the minimum momentum transfer to the ion in the ion frame. In Eq.(35) the integration runs over the transverse momentum transfer $\mathbf{q}_\perp$, $0 \le q_\perp < \infty$, $\mathbf{q}_\perp\cdot\mathbf{v} = 0$.

[4] The state $\psi_n(\mathbf{r})$ may also be a continuum state, properly normalized. In that case the electron loss occurs and $\mid a_{0\to n}\mid^2$ is the transition density. In order to obtain the total cross section for electron loss one has to integrate over the final continuum states of the ion.

The corresponding cross section, $\sigma_{0\to n}$, is given by

$$\sigma_{0\to n} = \int d^2\mathbf{b} \mid a_{0\to n} \mid^2 . \tag{36}$$

Inserting the transition amplitude (35) into (36) and performing the integration over the impact parameter in (36) with the help of the relation

$$\int d^2\mathbf{b} \exp(i(\mathbf{q}_\perp - \mathbf{q'}_\perp)\cdot\mathbf{b}) = (2\pi)^2\delta(\mathbf{q}_\perp - \mathbf{q'}_\perp) \tag{37}$$

we obtain

$$\sigma_{0\to n} = \frac{4}{v^2}\int d^2\mathbf{q}_\perp Z^2_{A,eff}(\mathbf{q}) \frac{|< \psi_n(\mathbf{r}) \mid \exp(i\mathbf{q}\cdot\mathbf{r})\left(1 - \frac{1}{c}\mathbf{v}\cdot\boldsymbol{\alpha}\right) \mid \psi_0(\mathbf{r}) >|^2}{(q_\perp^2 + \frac{\omega_{n0}^2}{v^2\gamma^2})^2}. \tag{38}$$

Since the second term on the right hand side of Eq.(34) is simply the elastic form-factor of the atom, the effective charge (34) is given by (see e.g. [32])

$$Z_{A,eff}(\mathbf{q}) = Z_A - \int d\boldsymbol{\eta}\, \rho_{el}(\boldsymbol{\eta})\, \exp(-i\mathbf{q}\cdot\boldsymbol{\eta}), \tag{39}$$

where $\rho_{el}(\boldsymbol{\eta})$ is the charge density of the electrons in the incident atom given in the rest frame of the ion. Using the results of the paper by Salvat et al [33], where the analytical screening functions for all neutral atoms are presented, one can show that the density is given by

$$\rho_{el}(\boldsymbol{\eta}) = \frac{\gamma\, Z_A}{4\pi\sqrt{\eta_x^2 + \eta_y^2 + \gamma^2\eta_z^2}} \sum_{i=1}^{3} A_i\, \kappa_i^2\, \exp\left(-\kappa_i\sqrt{\eta_x^2 + \eta_y^2 + \gamma^2\eta_z^2}\right). \tag{40}$$

Here A_i ($\sum_i A_i = 1$) and κ_i are constants for a given atom which are tabulated for all atomic elements in [33]. Using (39), (40) and the condition $\sum_i A_i = 1$ the effective atomic charge $Z_{A,eff}(\mathbf{q})$ can be written as

$$Z_{A,eff}(\mathbf{q}) = Z_A \times \left(q^2 - (\mathbf{q}\cdot\mathbf{v})^2/c^2\right) \sum_{i=1}^{3} \frac{A_i}{\kappa_i^2 + q^2 - (\mathbf{q}\cdot\mathbf{v})^2/c^2}. \tag{41}$$

Inserting (41) into (38) we get [31]:

$$\sigma_{0\to n} = \frac{4Z_A^2}{v^2}\sum_{i,j} A_i\, A_j \int d^2\mathbf{q}_\perp \frac{|< \psi_n(\mathbf{r}) \mid \exp(i\mathbf{q}\cdot\mathbf{r})\left(1 - \frac{1}{c}\mathbf{v}\cdot\boldsymbol{\alpha}\right) \mid \psi_0(\mathbf{r}) >|^2}{(q_\perp^2 + \frac{\omega_{n0}^2}{v^2\gamma^2} + \kappa_i^2)(q_\perp^2 + \frac{\omega_{n0}^2}{v^2\gamma^2} + \kappa_j^2)}. \tag{42}$$

Let us briefly discuss the behaviour of the cross section (42) in two important limiting cases: (i) in relativistic collisions with a point-like charge and (ii) in nonrelativistic collisions with a neutral atom.

(i) If we neglect the screening in (42) by setting all κ_i to be equal to zero, we recover the well known form for the first order cross sections for collisions with a bare nucleus having a charge Z_A:

$$\sigma_{0\to n} = \frac{4Z_A^2}{v^2}\int d^2\mathbf{q}_\perp \frac{|< \psi_n(\mathbf{r}) \mid \exp(i\mathbf{q}\cdot\mathbf{r})\left(1 - \frac{1}{c}\mathbf{v}\cdot\boldsymbol{\alpha}\right) \mid \psi_0(\mathbf{r}) >|^2}{(q_\perp^2 + \frac{\omega_{n0}^2}{v^2\gamma^2})^2}. \tag{43}$$

(ii) In the limit $c = \infty$ the screening cross section (42) reduces to its nonrelativistic form

$$\sigma_{0\to n} = \frac{4Z_A^2}{v^2} \sum_{i,j} A_i\, A_j \int d^2\mathbf{q}_\perp \frac{|< \psi_n(\mathbf{r}) \mid \exp(i\mathbf{q}\cdot\mathbf{r}) \mid \psi_0(\mathbf{r}) >|^2}{(q_\perp^2 + \frac{\omega_{n0}^2}{v^2} + \kappa_i^2)(q_\perp^2 + \frac{\omega_{n0}^2}{v^2} + \kappa_j^2)}, \tag{44}$$

which can be obtained from the nonrelativistic cross section (8) by using the representation (41) for the effective atomic charge where one has to set $c = \infty$.

An important general feature of the screening in relativistic collisions immediately follows from the comparison of Eqs.(42) and (44). In nonrelativistic collisions, if the ion is a heavy ion and the atom is a light atom with all screening constants κ_i not exceeding substantially unity, the screening is not important because the term $\frac{\omega_{n0}^2}{v^2} \sim \frac{Z_I^4}{v^2}$ dominates over all κ_i^2 in the denominators of the integrand in (44). However, the situation changes drastically for ultrarelativistic collisions. It is evident that for any projectile-target pair the terms κ_i^2 will be larger than $\frac{\omega_{n0}^2}{v^2\gamma^2} \sim \frac{Z_I^4}{v^2\gamma^2}$ provided γ is high enough. Thus, in a sharp contrast to nonrelativistic collisions, in ultrarelativistic collisions the screening of the atomic nucleus by atomic electrons is in general of great importance even for heavy-ion-light-atom collision partners and, in particular, may substantially reduce the excitation and loss cross sections compared to collisions with the unscreened nuclei.

The above discussed semiclassical approach for the projectile-electron excitation and loss in relativistic collisions is rather simple. It, however, is not appropriate to treat the antiscreening mode of the collisions. Besides, it is not yet clear how the assumption that the atomic electrons are 'frozen' and do not represent a source of the (space) charge current in the target frame, could influence the result obtained for the screening mode. Keeping these two points in mind, we now proceed to discuss more general first order theories.

3.3 Plane-wave Born approximation

In this subsection we consider the first order quantum treatment for relativistic collisions of two atomic particles, which both carry (active) electrons. The general form of the transition S-matrix element which describes collisions of atomic particles, interacting via the electromagnetic field, is given by (see e.g. [34])

$$S_{fi} = \left(-\frac{i}{c} \int d^4x\, J_\mu^I(x)\, A_A^\mu(x) \right)_{fi}. \tag{45}$$

This formula represents the natural generalization of the nonrelativistic expression (1) for the relativistic case. Here, $J_\mu^I(x)$ ($\mu = 0, 1, 2, 3$) is the electromagnetic 4-current of the projectile-ion at a space-time point x, $A_A^\mu(x)$ is the 4-potential of the electromagnetic field created by the target-atom at the same point x, and c is the speed of light. The contravariant a^μ and covariant a_μ 4-vectors are given by $a^\mu = (a^0, \mathbf{a})$ and $a_\mu = (a^0, -\mathbf{a})$. The metric tensor $g_{\mu\nu}$ of the four-dimensional space is defined by $g_{00} = -g_{11} = -g_{22} = -g_{33} = 1$ and $g_{\mu\nu} = 0$ for $\mu \neq \nu$. In (45) and below the summation over repeated greek indices is implied.

The 4-potential obeys the Maxwell equation which, in the Lorentz gauge, reads

$$\Box A_A^\mu(x) = -\frac{4\pi}{c} J_A^\mu(x), \tag{46}$$

where $J_A^\mu(x)$ is the 4-current of the target-atom and

$$\Box = \mathbf{\Delta} - \frac{\partial^2}{c^2 \partial t^2}$$

is the D'Alembert operator.

Since the nuclear and atomic energy scales are very different, Coulomb collisions between the ion and the atom, resulting in excitation of nuclear degrees of freedom, are usually of negligible importance for cross sections of electron transitions. Therefore, the nuclei of the atom and the ion can be regarded as point-like unstructured charges.

Simple estimates show that in a reference frame, where the atom or the ion is initially at rest, its typical recoil velocity after the collision is not only nonrelativistic but is also orders of magnitude less than the Bohr velocity $v_0 = 1$ a.u..

Taking into account the two points mentioned above, the transition matrix element (45) can be calculated as follows. First, the ion current $J_\mu^I(x)$ is evaluated in the reference frame K_I, where the ion is initially at rest. Second, the atom current $J'^\mu_A(x_A)$ is calculated in the reference frame K_A, where the atom is initially at rest, and then the atom potential $A'^\mu_A(x_A)$ is evaluated in this frame. Finally, this potential is transformed to the frame K_I in order to calculate the transition matrix elements and corresponding cross sections in K_I.

Assuming that the ion carries only one electron the transition 4-current J_μ^I of the ion in the frame K_I is written as

$$\begin{aligned} J_0^I(x) &= c \int d^3\mathbf{R}_I \int d^3\mathbf{r} \Psi_f^\dagger(\mathbf{R}_I, \mathbf{r}, t) \left(Z_I \delta^{(3)}(\mathbf{x} - \mathbf{R}_I) - \delta^{(3)}(\mathbf{x} - \mathbf{R}_I - \mathbf{r}) \right) \Psi_i(\mathbf{R}_I, \mathbf{r}, t) \\ J_l^I(x) &= c \int d^3\mathbf{R}_I \int d^3\mathbf{r} \Psi_f^\dagger(\mathbf{R}_I, \mathbf{r}, t)\, \alpha_l\, \delta^{(3)}(\mathbf{x} - \mathbf{R}_I - \mathbf{r}) \Psi_i(\mathbf{R}_I, \mathbf{r}, t);\ l = 1, 2, 3. \end{aligned} \tag{47}$$

In Eq.(47) Z_I is the atomic number of the ion, $\mathbf{R}_I$ is the coordinate of the ion nucleus, $\mathbf{r}$ is the coordinate of the electron of the ion with respect to the ion nucleus, α_l are the Dirac matrixes for the electron of the ion, and $\delta^{(3)}$ is the 3-dimensional delta-function. The mass of the nucleus is much larger than that of the electron. Therefore, in the frame K_I the 3-velocity of the ion nucleus is negligible compared to that of the electron and we have neglected in the second line in (47) the contribution to the ion current due to the motion of the nucleus. The large mass of the nucleus also permitted us to omit that part of the ion current, which is connected with the spin degrees of the nucleus of the ion. Further, in a first order treatment the initial and final states in Eq.(47) are just unperturbed states of the ion and are given by

$$\Psi_j(\mathbf{R}_I, \mathbf{r}, t) = \frac{1}{\sqrt{V_I}} \exp(i\mathbf{P}_j^I \cdot \mathbf{R}_I - iE_j^I t) \psi_{0,n}(\mathbf{r}). \tag{48}$$

Here the symbol j stands for both i and f, which refer to the initial and final states of the ion, respectively, $\mathbf{P}_i^I$ and $\mathbf{P}_f^I$ are the total 3-momenta ($\mathbf{P}_i^I = 0$), E_i^I and E_f^I the total energies (including the rest energies) of the ion, ψ_0 and ψ_n are the initial and final internal states of the ion, V_I is a normalization volume for the plane wave describing a free motion of the ion before and after the collision. The ansatz (48) represents a common form of a wavefunction for a free atomic system moving with a nonrelativistic velocity, where we have neglected the spin of the nucleus and the difference between the coordinate of the nucleus of the ion and the coordinate of the center of mass of the ion. The justification of both approximations lies in the extremely large difference between the masses of nuclei and of electrons.

We will not be interested in discussing collisions where the ion remains in its initial internal state. Therefore, in what follows only $n \neq 0$ will be considered. Inserting (48) into (47) and integrating over $\mathbf{R}_I$ we obtain

$$J_\mu^I(x) = c\,\frac{F_\mu^I(n0;\mathbf{P}_f^I - \mathbf{P}_i^I)}{V_I}\exp(i(\mathbf{P}_i^I - \mathbf{P}_f^I)\cdot\mathbf{x} - i(E_i^I - E_f^I)t). \tag{49}$$

We will refer to the 4-component quantity $F_\mu^I(n0;\mathbf{P}_f^I - \mathbf{P}_i^I)$ with components

$$\begin{aligned} F_0^I(n0;\mathbf{P}_f^I - \mathbf{P}_i^I) &= -\int d^3\mathbf{r}\,\psi_n^\dagger(\mathbf{r})\,\exp(i(\mathbf{P}_f^I - \mathbf{P}_i^I)\cdot\mathbf{r})\,\psi_0(\mathbf{r}) \\ F_l^I(n0;\mathbf{P}_f^I - \mathbf{P}_i^I) &= \int d^3\mathbf{r}\,\psi_n^\dagger(\mathbf{r})\,\exp(i(\mathbf{P}_f^I - \mathbf{P}_i^I)\cdot\mathbf{r})\,\alpha_l\psi_0(\mathbf{r}) \end{aligned} \tag{50}$$

as to the inelastic form-factor of the ion.

Now we turn to evaluating the potential $A'^\mu_A(x_A)$, created by the atom in the frame K_A where the atom is initially at rest. Here, $x_A = (ct_A, \mathbf{x}_A)$ is the space-time 4-vector in K_A. In a way similar to that used to get the ion current (49), one can show that, within the first-order consideration, the 4-current of the atom in the frame K_A reads

$$J'^\mu_A(x_A) = c\,\frac{F_A^\mu(m0;\mathbf{P}'^A_f - \mathbf{P}'^A_i)}{V'_A}\exp(i(\mathbf{P}'^A_i - \mathbf{P}'^A_f)\cdot\mathbf{x}_A - i(E'^A_i - E'^A_f)t_A). \tag{51}$$

In Eq.(51) $\mathbf{P}'^A_{i,f}$ ($\mathbf{P}'^A_i = 0$) are the 3-momenta and $E'^A_{i,f}$ the total energies (including the rest energies) of the atom in the initial and final states, respectively, and V'_A is a normalization volume for the atom in the frame K_A. The components of the form-factor of the atom F_μ^A are defined by

$$\begin{aligned} F_0^A(m0;\mathbf{P}'^A_f - \mathbf{P}'^A_i) &= Z_A\delta_{m0} - \int\prod_{i=1}^{N_A} d^3\boldsymbol{\xi}_i\,u_m^\dagger(\boldsymbol{\tau}_{N_A})\sum_{j=1}^{N_A}\exp(i(\mathbf{P}'^A_f - \mathbf{P}'^A_i)\cdot\boldsymbol{\xi}_j)\,u_0(\boldsymbol{\tau}_{N_A}) \\ F_l^A(m0;\mathbf{P}'^A_f - \mathbf{P}'^A_i) &= \int\prod_{i=1}^{N_A} d^3\boldsymbol{\xi}_i\,u_m^\dagger(\boldsymbol{\tau}_{N_A})\sum_{j=1}^{N_A}\alpha_{l(j)}\,\exp(i(\mathbf{P}'^A_f - \mathbf{P}'^A_i)\cdot\boldsymbol{\xi}_j)\,u_0(\boldsymbol{\tau}_{N_A}), \end{aligned} \tag{52}$$

where Z_A is the atomic number, N_A is the number of electrons of the atom, $\alpha_{l(j)}$ are the Dirac matrices for the j-th electron, $u_{0,m}$ are the initial and final internal states of the atom,

$\boldsymbol{\tau}_{N_A} = \{\boldsymbol{\xi}_1, \boldsymbol{\xi}_2, ..., \boldsymbol{\xi}_{N_A}\}$ represents the coordinates of the N_A atomic electrons with respect to the atomic nucleus.

The zeroth components of the form-factor of the ion (50) and of the atom (52) are similar to the form-factors which appear in the nonrelativistic theory of projectile excitation and loss (see Eq.(6)). However, the other three components in (50) and (52) are absent in the nonrelativistic theory.

The Maxwell equation $\Box' A'^{\mu}_{A}(x_A) = -\frac{4\pi}{c} J'_A{}^{\mu}(x_A)$ can be solved by using a 4-dimensional Fourier transformation

$$\begin{aligned} A'^{\mu}_{A}(x_A) &= \frac{1}{(2\pi)^2}\int d^4k\, B^{\mu}_{A}(k)\, \exp(ikx_A) \\ J'_A{}^{\mu}(x_A) &= \frac{c}{V'_A}\int d^4k\, \exp(ikx_A)\, \delta^{(4)}(k + P'^{A}_{f} - P'^{A}_{i}) F^{\mu}_{A}(m0; -\mathbf{k}), \end{aligned} \tag{53}$$

where $P'^{A}_{i,f}$ are the 4-momenta of the atom in the frame K_A, $\mathbf{k}$ is the 'spatial' part of k and $k\,x_A = k_\mu x^{\mu}_{A}$. Inserting (53) into the Maxwell equation, the Fourier transform $B^{\mu}_{A}(k)$ is found to be

$$B^{\mu}_{A}(k) = 4\pi\, \frac{(2\pi)^2\, \delta^{(4)}(k + P'^{A}_{f} - P'^{A}_{i})}{k^2 - i\varsigma}\, \frac{F^{\mu}_{A}(m0; -\mathbf{k})}{V'_A}. \tag{54}$$

Correspondingly, the 4-potential is given by

$$A'^{\mu}_{A}(x_A) = 4\pi\, \frac{\exp(i(P'^{A}_{i} - P'^{A}_{f})x_A)}{(P'^{A}_{i} - P'^{A}_{f})^2 - i\varsigma}\, \frac{F^{\mu}_{A}(m0; \mathbf{P}'^{A}_{f} - \mathbf{P}'^{A}_{i})}{V'_A}. \tag{55}$$

In Eqs.(54) and (55) the term $-i\varsigma$ with $\varsigma \to +0$ gives a prescription to handle the singularity.

If we denote by $\Lambda_{\mu\nu}$ the matrix for the Lorentz transformation from the frame K_A to the frame K_I, then the potential of the atom in the frame K_I is given by

$$\begin{aligned} A^{\mu}_{A}(x) &= \Lambda^{\mu}_{\nu}\, A'^{\nu}_{A}(\Lambda^{-1}\, x) \\ &= 4\pi\, \frac{\exp(i(P^{A}_{i} - P^{A}_{f})x)}{(P^{A}_{i} - P^{A}_{f})^2 - i\varsigma}\, \Lambda^{\mu}_{\nu}\, \frac{F^{\nu}_{A}(m0; \mathbf{P}'^{A}_{f} - \mathbf{P}'^{A}_{i})}{\gamma\, V_A}. \end{aligned} \tag{56}$$

In Eq.(56) P^{A}_{i} and P^{A}_{f} are the initial and final 4-momentum of the atom in the frame K_I, $V_A = V'_A/\gamma$ is the normalization volume for the atom in K_I, $\gamma = 1/\sqrt{1 - \frac{v^2}{c^2}}$ is the Lorentz factor and $\mathbf{v} = (0, 0, v)$ the velocity of the incident atom in K_I.

The 3-momentum transfer to the atom $\mathbf{Q} = \mathbf{P}'^{A}_{f} - \mathbf{P}'^{A}_{i}$ in the frame K_A can be rewritten in terms of the atom momentum in the frame K_I and the atomic initial and final internal energies, given in the frame K_A,

$$\begin{aligned} \mathbf{Q} &= \left(\mathbf{P}^{A}_{f\perp} - \mathbf{P}^{A}_{i\perp}, \frac{1}{\gamma}(P^{A}_{f\parallel} - P^{A}_{i\parallel}) + \frac{v}{c^2}(E'^{A}_{i} - E'^{A}_{f})\right) \\ &= \left(\mathbf{P}^{A}_{f\perp} - \mathbf{P}^{A}_{i\perp}, \frac{1}{\gamma}(P^{A}_{f\parallel} - P^{A}_{i\parallel}) - \frac{v}{c^2}(\epsilon_m - \epsilon_0)\right). \end{aligned} \tag{57}$$

Here $\mathbf{P}^A_\perp$ and $P^A_\parallel$ are the parts of the 3-momentum $\mathbf{P}^A$ of the atom in the frame K_I, which are perpendicular and parallel to the velocity $\mathbf{v}$. Further, ϵ_0 and ϵ_m are the initial and final electron energies of the atom given in the atomic frame. In the second line of Eq.(57) the recoil energy of the atom in the frame K_A has been neglected because it is negligible due to very large atomic mass.

By inserting the right hand sides of Eqs.(49) and (56) into Eq.(45) and performing there the integration over d^4x we obtain

$$S_{fi} = -i\frac{4\pi}{V_I V_A}(2\pi)^4\,\delta^{(4)}(P^I_i + P^A_i - P^I_f - P^A_f)\,G_{fi}, \tag{58}$$

where

$$G_{fi} = \frac{F^I_\mu(n0;\mathbf{q})\,\gamma^{-1}\,\Lambda^\mu_\nu\,F^\nu_A(m0;\mathbf{Q})}{(P^A_i - P^A_f)^2 - i\varsigma} \tag{59}$$

and $\mathbf{q} = \mathbf{P}^I_f - \mathbf{P}^I_i = \mathbf{P}^A_i - \mathbf{P}^A_f$ is the 3-dimensional momentum transfer to the ion in the frame K_I. Having derived the transition S-matrix, one can now obtain the cross section of a process where the electron of the ion and those of the atom make a transition $\psi_0 \to \psi_n$ and $u_0 \to u_m$, respectively. This cross section reads [11]

$$\begin{aligned}\sigma^{0\to m}_{0\to n} &= \frac{4}{v^2}\frac{E^A_f}{E^A_i}\int d^2\mathbf{q}_\perp \mid G_{fi}\mid^2 = \frac{4}{v^2}\frac{E^A_f}{E^A_i}\\ &\times\int d^2\mathbf{q}_\perp \frac{\mid F^I_\mu(n0;\mathbf{q}_\perp,q_{min})\,\gamma^{-1}\,\Lambda^\mu_\nu\,F^\nu_A(m0;-\mathbf{q}_\perp,-q_{min}/\gamma - \frac{v}{c^2}(\epsilon_m-\epsilon_0))\mid^2}{\left(q^2_\perp + q^2_{min} - (E^I_f - E^I_i)^2/c^2\right)^2 + \varsigma^2}.\end{aligned} \tag{60}$$

Here E^A_i and $E^A_f = E^A_i + E^I_i - E^I_f$ are the initial and final total energies of the atom given in the ion frame. Further, the integration over the absolute value of the transverse part $\mathbf{q}_\perp$ of the momentum transfer $\mathbf{q}$, which is perpendicular to the initial momentum $\mathbf{P}^A_i$ of the incident atom, runs from 0 to some maximal value $q^{max}_\perp$ which can be safely set equal to infinity. With the same accuracy the factor E^A_f/E^A_i in (60) can be equated to unity. Neglecting the recoil energy of the ion in the frame K_I, the difference between the total ion energies in that frame, $E^I_f - E^I_i$, is replaced by $\varepsilon_n - \varepsilon_0$, where ε_0 and ε_n are the energies of the electron of the ion in the initial and final internal states, ψ_0 and ψ_n, respectively. The component q_{min} of the momentum transfer $\mathbf{q}$, which is parallel to the initial momentum of the incident atom and represents the minimum momentum transfer to the ion in the frame K_I, is determined from the energy conservation in the collision and is given by [11]

$$q_{min} = \frac{\varepsilon_n - \varepsilon_0}{v} + \frac{\epsilon_m - \epsilon_0}{v\gamma}. \tag{61}$$

By introducing the quantity

$$\begin{aligned}Q_{min} &= \frac{q_{min}}{\gamma} + \frac{v}{c^2}(\epsilon_m - \epsilon_0)\\ &= \frac{\epsilon_m - \epsilon_0}{v} + \frac{\varepsilon_n - \varepsilon_0}{v\gamma},\end{aligned} \tag{62}$$

where $-Q_{min}$ represents the minimum momentum transfer to the atom in the frame K_A, the cross section (60) can be rewritten in a more symmetric form:

$$\begin{aligned}\sigma_{0\to n}^{0\to m} = & \frac{4}{v^2}\int d^2\mathbf{q}_\perp \frac{\mid F_\mu^I\left(n0;\mathbf{q}_\perp,q_{min}\right)\,\gamma^{-1}\,\Lambda_\nu^\mu\,F_A^\nu\left(m0;-\mathbf{q}_\perp,-Q_{min}\right)\mid^2}{\left(\mathbf{q}^2-\frac{(\varepsilon_n-\varepsilon_0)^2}{c^2}\right)^2+\varsigma^2} \\ = & \frac{4}{v^2}\int d^2\mathbf{q}_\perp \\ & \frac{\mid F_\mu^I\left(n0;\mathbf{q}_\perp,\frac{\varepsilon_n-\varepsilon_0}{v}+\frac{\epsilon_m-\epsilon_0}{v\gamma}\right)\,\gamma^{-1}\,\Lambda_\nu^\mu\,F_A^\nu\left(m0;-\mathbf{q}_\perp,-\frac{\epsilon_m-\epsilon_0}{v}-\frac{\varepsilon_n-\varepsilon_0}{v\gamma}\right)\mid^2}{\left(q_\perp^2+\frac{(\varepsilon_n-\varepsilon_0+\epsilon_m-\epsilon_0)^2}{v^2\gamma^2}+2(\gamma-1)\frac{(\varepsilon_n-\varepsilon_0)(\epsilon_m-\epsilon_0)}{v^2\gamma^2}\right)^2+\varsigma^2}. \end{aligned} \quad (63)$$

If the condition $(\varepsilon_n-\varepsilon_0)(\epsilon_m-\epsilon_0)\geq 0$ is fulfilled in the collision, the integrand in Eqs.(60) and (63) becomes free of singularities. From the physical point of view it means that for such a case the restrictions, imposed by the energy-momentum conservation in the collision, do not permit the electromagnetic interaction between the systems to be transmitted by a photon with the energy-momentum relation $k^2=0$. In what follows we consider only collisions in which $(\varepsilon_n-\varepsilon_0)(\epsilon_m-\epsilon_0)\geq 0$, where the term ς^2 may be omitted. Before turning to the consideration of such collisions, however, we shall briefly comment on the situation where the singularity does appear in the cross section.

3.3.1 On the possibility to exchange a photon with $k^2=0$

The singularity in the integrand of (63) appears when $(\varepsilon_n-\varepsilon_0)(\epsilon_m-\epsilon_0)<0$, i.e. when the collision leads to the excitation of one of the colliding particles and the de-excitation of the other one. The analysis of the denominator in (63) shows that the electromagnetic interaction between the colliding composite systems can now occur via an exchange of a photon with the energy-momentum relation $k^2=0$ which is inherent to a real photon. In order to get some insight why the denominator in the integrand of Eq.(63) becomes singular, let us consider this denominator in more detail. It can be equal to zero if

$$\frac{(\varepsilon_n-\varepsilon_0+\epsilon_m-\epsilon_0)^2}{v^2\gamma^2}+2(\gamma-1)\frac{(\varepsilon_n-\varepsilon_0)(\epsilon_m-\epsilon_0)}{v^2\gamma^2}\leq 0. \quad (64)$$

To be definite, let us assume that the ion gets excited $(\varepsilon_n-\varepsilon_0>0)$ and the atom is deexcited $(\epsilon_m-\epsilon_0<0)$ in the collision. Then we obtain that the inequality (64) holds if

$$\mid\epsilon_m-\epsilon_0\mid\sqrt{\frac{c-v}{c+v}}\leq\varepsilon_n-\varepsilon_0\leq\mid\epsilon_m-\epsilon_0\mid\sqrt{\frac{c+v}{c-v}}. \quad (65)$$

It is well known in the theory of relativistic Doppler effect (see e.g. [35]) that the emission of radiation in the atomic frame K_A (in all directions) with a fixed frequency ω_0 would result in the ion frame K_I in the radiation spectrum with frequencies ω

$$\omega_0\sqrt{\frac{c-v}{c+v}}\leq\omega\leq\omega_0\sqrt{\frac{c+v}{c-v}}. \quad (66)$$

Comparing Eqs.(65) and (66) we see that the interaction between the atom and the ion in the collision process occurs via the emission of a photon with the energy $\omega_0 =\mid \epsilon_m - \epsilon_0 \mid$ by the atom in the frame K_A and the absorption of the same photon, but now having the energy $\omega = \varepsilon_n - \varepsilon_0$, by the ion in the frame K_I. Thus, it is the occurrence of such a 'resonant' coupling between the transitions of the electron of the ion and those of the atom, which results in the singularity. Due to the resonant coupling the corresponding first-order transition probability decreases much slower with increasing the collision impact parameter, compared to the case when such a singularity is absent [12] [5], and the cross section diverges. That calls the validity of the first order treatment for the 'resonant' collisions into question.

In the case of nonrelativistic collisions ($\gamma = 1$) the problem with the singularity does not appear.

3.4 Semiclassical approximation

Additional important information about physics of the ion-atom collisions can be obtained by considering impact parameter dependencies of the projectile-electron excitation and loss. Such dependencies can be studied within the semiclassical approximation where both the nuclei are regarded as classical particles. In section (3.2.1) we have discussed the simplified version of the semiclassical approximation. That treatment, however, is not appropriate for considering the antiscreening mode. In addition, even for the screening mode $m = 0$ the first order cross section (63) contains the more complicated coupling between the form-factors of the ion and atom and in general does not coincide with the cross section (38) obtained within the simplified semiclassical approximation. Therefore, now we will consider the general version of the first order semiclassical approximation for the projectile-electron excitation and loss in relativistic collision.

The starting expression for the semiclassical transition amplitude is formally the same as that used to develop the first order plane-wave approximation in the previous subsection

$$a_{fi} = -\frac{i}{c} \int d^4x \, J^I_\mu(x) \, A^\mu_A(x). \tag{67}$$

As before, $J^I_\mu(x)$ denotes the electromagnetic transition 4-current of the ion at a space-time point x and $A^\mu_A(x)$ is the 4-potential of the electromagnetic field created by the atom at the same point x. Now, however, these quantities and the transition amplitude (67) have to be evaluated within the first order perturbation theory where only the electrons are treated quantum mechanically whereas the nuclei are regarded as classical particles and their relative motion is assumed to be straight-line.

[5] Note that this increase in the effective range of the interaction resembles the situation with the resonant interaction of two identical atoms at rest, where initially one of the atoms is in the ground state and the second is excited. In such a case the atom-atom interaction is proportional to the inverse cube of the inter-atomic distance. This dependence is to be compared with the inverse sixth power of the distance for van der Waals forces (see e.g. [36], pp. 522-524).

The evaluation of the semi-classical matrix element (67) can be split in steps exactly similar to those used to obtain the first order results in the previous subsection. Namely, the ion current $J^I_\mu(x)$ is evaluated in the reference frame K_I, where the ion nucleus is at rest. The current $J'^\mu_A(x_A)$ and potential $A'^A_\mu(x_A)$ of the atom are calculated in the reference frame K_A, where the atomic nucleus is at rest. Then the atom potential is transformed to the frame K_I, where the transition matrix elements and corresponding probabilities are evaluated.

Assuming that the nucleus of the ion in the frame K_I rests at the origin, the transition 4-current J^I_μ of the ion reads

$$\begin{aligned} J^I_0(x) &= c\int d^3\mathbf{r}\Psi^\dagger_n(\mathbf{r},t)\,\left(Z_I\delta^{(3)}(\mathbf{x})-\delta^{(3)}(\mathbf{x}-\mathbf{r})\right)\Psi_0(\mathbf{r},t),\\ J^I_l(x) &= c\int d^3\mathbf{r}\Psi^\dagger_n(\mathbf{r},t)\,\alpha_l\,\delta^{(3)}(\mathbf{x}-\mathbf{r})\Psi_0(\mathbf{r},t);\; l=1,2,3. \end{aligned} \tag{68}$$

In Eq.(68) Z_I is the atomic number of the ion, $\mathbf{r}$ is the coordinate of the electron of the ion with respect to the ion nucleus, α_l are the Dirac matrices for the electron of the ion and $\delta^{(3)}$ is the three-dimensional delta-function. Further, $\Psi_{0,n}(\mathbf{r},t)=\psi_{0,n}(\mathbf{r})\exp(-i\varepsilon_{0,n}t)$ are the initial and final electronic states of the ion with the energies $\varepsilon_{0,n}$. As in the previous sections we will be interested only in collisions where the internal state of the ion is changed: $n\neq 0$.

It is convenient to rewrite the 4-current (68) using the integral representation

$$\delta^{(3)}(\mathbf{x})=\frac{1}{(2\pi)^3}\int d^3\mathbf{k}\exp(-i\mathbf{k}\cdot\mathbf{x}) \tag{69}$$

for the δ-functions in (68). This yields

$$J^I_\mu(x)=\frac{c}{(2\pi)^3}\int d^3\mathbf{k}\exp\left(i(\varepsilon_n-\varepsilon_0)t-i\mathbf{k}\cdot\mathbf{x}\right)F^I_\mu(n0;\mathbf{k}). \tag{70}$$

In Eq.(70) the four components $F^I_\mu(n0;\mathbf{k})$ of the inelastic form-factor of the ion are given by

$$\begin{aligned} F^I_0(n0;\mathbf{k}) &= -\int d^3\mathbf{r}\,\psi^\dagger_n(\mathbf{r})\,\exp(i\mathbf{k}\cdot\mathbf{r})\,\psi_0(\mathbf{r})\\ F^I_l(n0;\mathbf{k}) &= \int d^3\mathbf{r}\,\psi^\dagger_n(\mathbf{r})\,\exp(i\mathbf{k}\cdot\mathbf{r})\,\alpha_l\psi_0(\mathbf{r}). \end{aligned} \tag{71}$$

Similarly, for the transition 4-current of the atom in the atom rest frame K_A one obtains

$$\begin{aligned} J'^A_\mu(x_A) &= \frac{c}{(2\pi)^3}\int d^3\mathbf{k}\exp\left(i(\epsilon_m-\epsilon_0)t_A-i\mathbf{k}\cdot\mathbf{x}_A\right)F^A_\mu(m0;\mathbf{k})\\ &= \frac{c}{(2\pi)^3}\int d^4k\exp(ikx_A)F^A_\mu(m0;\mathbf{k})\delta\left(\frac{\omega+\epsilon_0-\epsilon_m}{c}\right). \end{aligned} \tag{72}$$

In Eq.(72) $x_A=(ct_A,\mathbf{x}_A)$, $k=\left(\frac{\omega}{c},\mathbf{k}\right)$ and $kx_A=\omega t_A-\mathbf{k}\cdot\mathbf{x}_A$. The components of the atomic

form-factor F_μ^A are given by

$$\begin{aligned} F_0^A(m0;\mathbf{k}) &= Z_A\delta_{m0} - \int \prod_{i=1}^{N_A} d^3\boldsymbol{\xi}_i\, u_m^\dagger(\boldsymbol{\xi}_1,...,\boldsymbol{\xi}_{N_A}) \sum_{i=1}^{N_A} \exp(i\mathbf{k}\cdot\boldsymbol{\xi}_i)\, u_0(\boldsymbol{\xi}_1,...,\boldsymbol{\xi}_{N_A}); \\ F_l^A(m0;\mathbf{k}) &= \int \prod_{i=1}^{N_A} d^3\boldsymbol{\xi}_i\, u_m^\dagger(\boldsymbol{\xi}_1,...,\boldsymbol{\xi}_{N_A}) \sum_{i=1}^{N_A} \alpha_{l(i)}\, \exp(i\mathbf{k}\cdot\boldsymbol{\xi}_i)\, u_0(\boldsymbol{\xi}_1,...,\boldsymbol{\xi}_{N_A}). \end{aligned} \tag{73}$$

As before, Z_A is the atomic number, N_A is the number of the electrons of the atom, $\alpha_{l(i)}$ are the Dirac matrices for the i-th electron, $u_{0,m}$ are the wavefunctions describing initial and final electronic states of the atom, $\epsilon_{0,m}$ are the energies of these states and $\boldsymbol{\xi}_i$ is the coordinate of the i-th atomic electron with respect to the atomic nucleus.

The potential $A'^A_\mu(x_A)$, which is created by the atom in its rest frame, is to be calculated from the Maxwell equation

$$\left(\boldsymbol{\Delta}_A - \frac{\partial^2}{c^2\partial t_A^2}\right) A'^A_\mu(x_A) = -\frac{4\pi}{c} J'^A_\mu(x_A), \tag{74}$$

where $J'^A_\mu(x_A)$ is the transition 4-current of the atom determined by Eqs.(72) and (73). Eq.(74) can be easily solved with the help of a four-dimensional Fourier transformation. The result is

$$A'^A_\mu(x_A) = \frac{\exp(i(\epsilon_m-\epsilon_0)t_A)}{2\pi^2} \int d^3\mathbf{k} \exp(-i\mathbf{k}\cdot\mathbf{x}_A) \frac{F_\mu^A(m0;\mathbf{k})}{\mathbf{k}^2 - \frac{(\epsilon_m-\epsilon_0)^2}{c^2}}. \tag{75}$$

Let the atom move in the frame K_I along a straight-line trajectory with velocity $\mathbf{v} = (0,0,v)$ and impact parameter $\mathbf{b} = (b_1, b_2, 0)$. Let $\Lambda_{\mu\nu}$ be the Lorentz transformation matrix from the frame K_A to the frame K_I. Then, taking into account that $t_A = \gamma(t - \frac{v}{c^2}x_3)$, $x_{A1} = x_1 - b_1$, $x_{A2} = x_2 - b_2$ and $x_{A3} = \gamma(x_3 - vt)$, the atomic 4-potential in the frame K_I is given by

$$\begin{aligned} A_A^\mu(x_1,x_2,x_3,t) &= \frac{1}{2\pi^2} \exp\left(i(E_m - E_0)t + i(p_i - p_f)x_3\right) \\ &\quad \times \int d^3\mathbf{k} \exp\left(-i\mathbf{k}_\perp\cdot(\mathbf{x}_\perp - \mathbf{b}) - ik_3\gamma(x_3 - vt)\right) \frac{\Lambda^\mu_\nu F_A^\nu(m0;\mathbf{k})}{\mathbf{k}^2 - \frac{(\epsilon_m-\epsilon_0)^2}{c^2}}. \end{aligned} \tag{76}$$

Here, $\mathbf{x}_\perp = (x_1, x_2, 0)$, $E_0 = \gamma\epsilon_0$ and $E_m = \gamma\epsilon_m$ are the total energies of the atomic electrons in the initial and final states, respectively, given in the frame K_I. Further, $p_i = \frac{v}{c^2}E_0$ and $p_f = \frac{v}{c^2}E_m$. In Eq.(76) the component k_3 is parallel and $\mathbf{k}_\perp$ is perpendicular to the collision velocity. Introducing the vector $\mathbf{q} = (\mathbf{q}_\perp, q_3) = (\mathbf{k}_\perp, \gamma k_3)$ Eq.(76) is rewritten as

$$\begin{aligned} A_A^\mu(x) = \quad & \frac{1}{2\pi^2} \int d^3\mathbf{q} \frac{\Lambda^\mu_\nu \gamma^{-1} F_A^\nu(m0;\mathbf{q}_\perp, \gamma^{-1}q_3)}{\mathbf{q}_\perp^2 + \frac{q_3^2}{\gamma^2} - \frac{(\epsilon_m-\epsilon_0)^2}{c^2}} \\ & \times \exp\left(-i\mathbf{q}_\perp(\mathbf{x}_\perp - \mathbf{b}) - i(q_3 - p_i + p_f)x_3\right) \exp\left(i(E_m - E_0 + q_3 v)t\right). \end{aligned} \tag{77}$$

Inserting Eqs.(70) and (77) into Eq.(67), we obtain for the transition amplitude

$$\begin{aligned} a_{fi}(\mathbf{b}) = \quad & a_{0\to n}^{0\to m}(\mathbf{b}) = \\ & -\frac{i}{2\pi^2(2\pi)^3}\int d^4x \int d^3\mathbf{k} \int d^3\mathbf{q} \frac{F_\mu^I(n0;\mathbf{k}_\perp,k_3)\Lambda^\mu_\nu \gamma^{-1} F_A^\nu(m0;\mathbf{q}_\perp,\gamma^{-1}q_3)}{\mathbf{q}_\perp^2+\frac{q_3^2}{\gamma^2}-\frac{(\epsilon_m-\epsilon_0)^2}{c^2}} \\ & \times \exp\left(-i(\mathbf{k}_\perp+\mathbf{q}_\perp)\cdot(\mathbf{x}_\perp-\mathbf{b})-i(q_3+k_3-p_i+p_f)x_3\right) \\ & \times \exp\left(i(E_m+\varepsilon_n-E_0-\varepsilon_0+q_3 v)t\right). \end{aligned} \tag{78}$$

This transition amplitude describes the collision process where the electron of the ion makes a transition $0\to n$ and the electrons of the atom make a transition $0\to m$. After performing an 8-fold integration in (78) and redenoting $\mathbf{q}_\perp$ by $-\mathbf{q}_\perp$ one arrives at the following expression for the transition amplitude [12]

$$\begin{aligned} a_{0\to n}^{0\to m}(\mathbf{b}) = \quad & -\frac{i}{\pi v}\int d^2\mathbf{q}_\perp \exp(-i\mathbf{q}_\perp\cdot\mathbf{b})\times \\ & \frac{F_\mu^I\left(n0;\mathbf{q}_\perp,q_{min}\right)\,\gamma^{-1}\,\Lambda^\mu_\nu\,F_A^\nu\left(m0;-\mathbf{q}_\perp,-Q_{min}\right)}{q_\perp^2+\frac{(\varepsilon_n-\varepsilon_0+\epsilon_m-\epsilon_0)^2}{v^2\gamma^2}+2(\gamma-1)\frac{(\varepsilon_n-\varepsilon_0)(\epsilon_m-\epsilon_0)}{v^2\gamma^2}}. \end{aligned} \tag{79}$$

In (79) the integration runs over the two-dimensional vector $\mathbf{q}_\perp$ ($0\le q_\perp<\infty$), which is perpendicular to the collision velocity, and the minimum momentum transfers q_{min} and Q_{min} are defined by Eqs.(61) and (62), respectively.

By comparing the semiclassical transition amplitudes, given by Eqs.(79) and (35), one can draw two main conclusions. First, in contrast to the simplified semiclassical treatment the general version of the semiclassical approximation allows one to consider also collisions in which both projectile and target electrons make transitions. Second, even for the screening mode the transition amplitude Eq.(35) is, in general, not equivalent to that given by Eq. (79) since the latter includes more complicated coupling between the form-factors of the ion and atom.

3.5 Equivalence of the semiclassical and the plane-wave Born treatments

In the semiclassical approximation the cross section of a process, where the electron of the ion makes a transition $\psi_0\to\psi_n$ and those of the atom make a transition $u_0\to u_m$, reads

$$\sigma_{0\to n}^{0\to m} = \int d^2\mathbf{b}\ \mid a_{0\to n}^{0\to m}(\mathbf{b})\mid^2 . \tag{80}$$

After inserting the amplitude from Eq.(79) into (80) we first perform the two-dimensional integration over the impact parameter, which gives the δ-function

$$\int d^2\mathbf{b}\,\exp(i(\mathbf{q}_\perp-\mathbf{q}'_\perp)\mathbf{b}) = (2\pi)^2\,\delta^2(\mathbf{q}_\perp-\mathbf{q}'_\perp). \tag{81}$$

This allows one to easily evaluate a further two-dimensional integration over one of the transverse momenta $\mathbf{q}_\perp$, $\mathbf{q}'_\perp$ and to obtain for the cross section

$$\sigma_{0\to n}^{0\to m} = \frac{4}{v^2}\int d^2\mathbf{q}_\perp \times \frac{\mid F_\mu^I\left(n0;\mathbf{q}_\perp,\frac{\varepsilon_n-\varepsilon_0}{v}+\frac{\epsilon_m-\epsilon_0}{v\gamma}\right)\,\gamma^{-1}\,\Lambda_\nu^\mu\,F_A^\nu\left(m0;-\mathbf{q}_\perp,-\frac{\epsilon_m-\epsilon_0}{v}-\frac{\varepsilon_n-\varepsilon_0}{v\gamma}\right)\mid^2}{\left(q_\perp^2+\frac{(\varepsilon_n-\varepsilon_0+\epsilon_m-\epsilon_0)^2}{v^2\gamma^2}+2(\gamma-1)\frac{(\varepsilon_n-\varepsilon_0)(\epsilon_m-\epsilon_0)}{v^2\gamma^2}\right)^2}. \quad (82)$$

The cross section (82) is identical to that given by (63). The latter was obtained within the plane-wave Born treatment under the usual assumptions that the recoils of the nuclei can be neglected in the rest frames of these nuclei and that the maximum momentum transfer in the collision can be set to infinity.

3.6 Relativistic features and the nonrelativistic limit

Using the explicit form of the Lorentz transformation matrix Λ_ν^μ (see e.g. [4]) the relativistic coupling of the form-factors in Eq.(82) can be written as:

$$F_\mu^I\,\gamma^{-1}\,\Lambda_\nu^\mu\,F_A^\nu = \left(F_0^I+\frac{v}{c}F_3^I\right)\left(F_A^0+\frac{v}{c}F_A^3\right)+\frac{F_3^IF_A^3}{\gamma^2}+\frac{F_1^IF_A^1+F_2^IF_A^2}{\gamma}. \quad (83)$$

Compared to the nonrelativistic cross section, given by Eqs.(4) and (6), Eqs.(82) and (83) contain two types of relativistic effects. The first type depends on the collision velocity v and disappears when $v/c \ll 1$. In detail it includes the following:

i. The retardation effect which leads to the appearance of the Lorentz factor in the denominator in the integrand of (82) and decreases its value, thus, tending to increase the cross section.

ii. In contrast to collisions with nonrelativistic velocities the minimum momenta q_{min} and Q_{min}, transferred to the ion and to the atom in the corresponding reference frames, are no longer equal (see (61) and (62)). In addition, each of these momenta depends differently on the transition energies $\varepsilon_n-\varepsilon_0$ and $\epsilon_m-\epsilon_0$. Correspondingly the form-factors of the ion and of the atom depend differently on the energies. That has important consequences for the shielding effects in relativistic collisions.

iii. The coupling between the zeroth and third components of the form-factors in Eq.(83).

The second type is due to relativistic effects in the inner motions of the electron of the ion and those of the atom and it does not disappear when $v/c \ll 1$. It includes the coupling between the space components of the corresponding form-factors in (83) [6].

In the full nonrelativistic limit $c\to\infty$ both types of relativistic effects vanish and the cross section (82) goes over into the corresponding nonrelativistic result (4).

[6] One should note that this coupling was never considered for nonrelativistic collisions.

3.7 Gauge invariance. Coulomb gauge

As is well known, the electromagnetic 4-potentials A_μ are not uniquely defined and depend on the choice of gauge. Namely, any transformation of the form $A^\mu \to A'^\mu = A^\mu - \partial^\mu f$, where f is an arbitrary scalar function of x, leaves the electromagnetic field unchanged.

Formally the gauge independence of the transition matrix elements (45) and (67) can be proven by noting that one has

$$\begin{aligned}
&\int d^4x\, J^I_\mu(x)\ (A^\mu_A(x) - \partial^\mu f(x)) \\
&= \int d^4x\, J^I_\mu(x)\, A^\mu_A(x) - \int d^4x\, \partial^\mu \left(J^I_\mu(x) f(x)\right) + \int d^4x\, f(x) \partial^\mu J^I_\mu(x) \\
&= \int d^4x\, J^I_\mu(x)\, A^\mu_A(x), \qquad (84)
\end{aligned}$$

where we used the charge conservation condition, expressed by the continuity equation,

$$\partial^\mu J^I_\mu(x) = 0 \qquad (85)$$

and the usual assumption that the terms $J^I_\mu(x) f(x)$ vanish on the 4-dimensional hyper-sphere of infinite radius surrounding the charges. Using (49)-(52), (70)-(73) and the Dirac equations for the electron of the ion and those of the atom one can show that the first-order transition currents of the ion and atom obey (85) provided exact electronic states of the ion and atom are used. One can also show that in the momentum space the continuity equation for the current reads

$$k_\mu F^\mu = \frac{\omega_{fi}}{c} F^0(fi;\mathbf{k}) - k_x F^1(fi;\mathbf{k}) - k_y F^2(fi;\mathbf{k}) - k_z F^3(fi;\mathbf{k}) = 0. \qquad (86)$$

Here, $k^\mu = \left(\frac{\omega_{fi}}{c}, k_x, k_y, k_z\right)$ is the 4-momentum transfer to the particle (ion or atom) in the collision where the particle makes a transition $i \to f$ between its internal states and $F^\mu(fi;\mathbf{k})$ are the form-factors of the particle. Both k^μ and $F^\mu(fi;\mathbf{k})$ are given in the rest frame of the particle. Eq.(86) represents a very useful relationship between the components of the form-factors.

In actual calculations one is often forced to use some approximations, e.g. for electronic initial and final states of the colliding particles. In such a case the charge current in general will not be conserved and calculated results will not be gauge-independent. Since the Lorentz gauge is manifestly covariant, it is especially suited for a general consideration. However, in actual calculations this gauge may not always represent the best possible choice. For example, as we learn from the theory of ionization of atoms (or electron removal from ions) by collisions with point-like charges (see [28], [37], [38]), a special care must be taken when treating ultra-relativistic collisions in the Lorentz gauge in the case when approximate electronic states of the atom are used [7]. At the same time calculations in the Coulomb gauge are not so crucially

[7] The origin of the difficulties with the application of the Lorentz gauge is the near cancellation occurring in this gauge at $\gamma \gg 1$ between the contributions from the scalar and vector potentials to the z-component of the electric field [38].

sensitive to the accuracy of the electronic states (see [28], [37], [38]). Therefore, we present also results for the semiclassical transition amplitude and the cross section which were obtained by using the Coulomb gauge for the description of the field of the incident atom in *the ion rest frame* K_I [8].

In the Coulomb gauge the transition amplitude is given by

$$a_{0\to n}^{0\to m}(\mathbf{b}) = -\frac{i}{\pi v}\int d^2\mathbf{q}_\perp \exp(-i\mathbf{q}_\perp\cdot\mathbf{b})\left\{\frac{F_0^I\,(n0;\mathbf{q})\,L_0}{\mathbf{q}^2} + \frac{1}{\mathbf{q}^2-\frac{\omega_{n0}^2}{c^2}}\sum_{s=1}^{3}F_s^I\,(n0;\mathbf{q})\,L_s\right\}, \quad (87)$$

where $\omega_{n0}=\varepsilon_n-\varepsilon_0$ and $\mathbf{q}=(\mathbf{q}_\perp,q_{min})$ are the energy and momentum transfer to the ion in the ion frame. Further,

$$\begin{aligned}
L_0 &= F_0^A\,(m0;\mathbf{Q}) - \frac{v}{c}F_3^A\,(m0;\mathbf{Q})\\
L_{1(2)} &= -\frac{1}{\gamma}F_{1(2)}^A\,(m0;\mathbf{Q}) - \frac{\omega_{n0}}{c}\frac{q_{1(2)}}{\mathbf{q}^2}\left(F_0^A\,(m0;\mathbf{Q}) - \frac{v}{c}F_3^A\,(m0;\mathbf{Q})\right)\\
L_3 &= -F_3^A\,(m0;\mathbf{Q})\left(1-\frac{v\omega_{n0}}{c^2}\frac{q_{min}}{\mathbf{q}^2}\right) + F_0^A\,(m0;\mathbf{Q})\left(\frac{v}{c}-\frac{\omega_{n0}}{c}\frac{q_{min}}{\mathbf{q}^2}\right),
\end{aligned} \quad (88)$$

where $\mathbf{Q}=(-\mathbf{q}_\perp,-Q_{min})$ is the momentum transfer to the atom in its rest frame. The minimum momentum transfers q_{min} and Q_{min} are given by Eqs.(61) and (62). The transition amplitudes (79) and (87) are identical provided exact states for the electron of the ion are used.

Using the analogy with ionization-excitation processes in collisions with point-like charges, the first and second terms on the right-hand side of Eq.(87) can be termed as *longitudinal* and *transverse*, respectively. The first term represents the contribution to the transition amplitude which is due to the interaction of the electron of the ion with the scalar potential of the incident atom. In the Coulomb gauge the latter is the instantaneous (nonrelativistic) Coulomb potential that is reflected in (87) by the absence of the retardation correction $-\omega_{n0}^2/c^2$ in the photon propagator $\mathbf{q}^{-2}$. The transverse contribution arises due to the interaction with the vector potential of the incident atom. In the Coulomb gauge this interaction can be regarded as transmitted by a virtual photon with polarization vector perpendicular to the photon momentum $\mathbf{q}$, i.e. by a photon with transverse polarization. Indeed, one can show that the following condition holds

$$\mathbf{q}\cdot\mathbf{L}=0, \quad (89)$$

where $\mathbf{L}=(L_1,L_2,L_3)$. Such a condition is inherent to a transverse photon with polarization vector $\sim\mathbf{L}$. Note that the equation (89) is just the consequence of the continuity equation for the charge and current densities of the atom. Therefore, the condition given by (89) may be not fulfilled if any approximation for these densities are used (for example, if these densities are calculated with approximate electronic states).

The cross section, which corresponds to the transition amplitude (87), reads

$$\sigma_{0\to n}^{0\to m} = \frac{4}{v^2}\int d^2\mathbf{q}_\perp\left|\frac{\langle\psi_n(\mathbf{r})\,|L_0\exp(i\mathbf{q}\cdot\mathbf{r})|\,\psi_0(\mathbf{r})\rangle}{\mathbf{q}^2} - \frac{\langle\psi_n(\mathbf{r})\,|\mathbf{L}\cdot\boldsymbol{\alpha}\,\exp(i\mathbf{q}\cdot\mathbf{r})|\,\psi_0(\mathbf{r})\rangle}{\mathbf{q}^2-\frac{\omega_{n0}^2}{c^2}}\right|^2, \quad (90)$$

[8] We remind that the Coulomb gauge is not covariant.

where the ion form-factors $F_0^I(n0;\mathbf{q})$ and $F_s^I(n0;\mathbf{q})$ have been expressed according to Eqs.(71).

In some cases the terms in the integrand of (90), which are proportional to $1/\mathbf{q}^2$ and $1/(\mathbf{q}^2-\omega_{n0}^2/c^2)$, can be squared separately. This is possible, for example, when calculating the total cross section for the electron loss from an unpolarized initial state ψ_0. In this case one can choose the quantization axis for the initial and final electron states of the ion to be along the total momentum transfer $\mathbf{q}$. In the case of a transverse photon with linear momentum $\mathbf{q}$ the projection of its angular momentum on the direction of $\mathbf{q}$ may take values ± 1. However, for the case of a longitudinal photon such a projection is zero. Therefore, for electron states ψ_0 and ψ_n, which are quantized along $\mathbf{q}$ and characterized by definite values of the magnetic quantum number, the matrix elements $\langle\psi_n|\exp(i\mathbf{q}\cdot\mathbf{r})|\psi_0\rangle$ and $\langle\psi_n|\mathbf{L}\cdot\boldsymbol{\alpha}\exp(i\mathbf{q}\cdot\mathbf{r})|\psi_0\rangle$ will satisfy different selection rules and the corresponding terms in the integrand of (90) can be squared separately. This will result in splitting the total loss cross section into two parts. These parts, where the corresponding integrands contain the terms proportional to $1/\mathbf{q}^4$ and $1/(\mathbf{q}^2-\omega_{n0}^2/c^2)^2$, can be called *longitudinal* and *transverse* [9] contributions, respectively, to the loss cross section.

3.8 Simplification of the atomic transition 4-current: the 'nonrelativistic atom' approximation

In general, the full relativistic coupling (see Eqs.(83) and (87)-(88)) of the form-factors of the ion and atom is rather complicated. It is not only much more involved than its nonrelativistic limit but is also substantially more complicated even compared to the corresponding coupling obtained in the simplified version of the semiclassical approximation for the screening mode in relativistic collisions.

In order to get simpler equations for the projectile-electron excitation and loss cross sections it was suggested in [11] to neglect the space components of the atomic form-factor, i.e. to disregard the 3-current of the atom in the atom rest frame. [10] This step would break the symmetry between the descriptions of the ion and the atom in our consideration because the space components of the current of the ion in the ion frame are kept. However, one could immediately argue that, since we are interested in the study of the electron excitation (loss) processes mainly in (from) heavy and very heavy ions colliding with neutral atoms, this symmetry breaking in most cases should not be important because the electron of a highly charged ion and those of a neutral atom are not expected to behave similarly in the collision.

Let us first make some rough estimates for the atomic form-factors in (52) (or in (73)). The component $F_A^0(m0;\mathbf{Q})$ of the atomic form-factor is connected with the charge distribution

[9] In theory of K-shell ionization by point-like charges the spin-flip part of the transverse contribution is sometimes separated and the ionization cross section is regarded as a sum of the longitudinal, transverse and spin-flip terms [28]. We, however, find it more consistent to speak about just the longitudinal and transverse terms of the cross section since the spin-flip term is a natural part of the coupling of the electron with the transverse photon.

[10] It is not very surprising that for the screening mode this would reduce the transition amplitudes and the corresponding cross sections exactly to the results following from the simplified semiclassical consideration of the subsection 3.2.

inside the atom. The components $F_A^l(m0;\mathbf{Q})$ are connected with the current, created by the motion of the electrons inside the atom in the rest frame of the atom. One can estimate roughly the magnitude of $F_A^l(m0;\mathbf{Q})$ as $F_A^l(m0;\mathbf{Q}) \sim \frac{v_e}{c} F_A^0(m0;\mathbf{Q})$ where v_e is a characteristic velocity of the atomic electrons. For light and not too heavy atoms one has $v_e \ll c$ for all atomic electrons and the absolute value of all three components $F_A^l(m0;\mathbf{Q})$ are much smaller compared to that of $F_A^0(m0;\mathbf{Q})$. In heavy atoms the very inner electrons can have relativistic velocities. However, because the number of these electrons is relatively small compared to the total number of atomic electrons they are not expected to increase considerably the absolute value of $F_A^l(m0;\mathbf{Q})$. Therefore, the neglect of $F_A^l(m0;\mathbf{Q})$ seems to be approximately justified also for heavy atoms. In [11] the neglect of the space components of the atomic form-factor was termed 'the nonrelativistic atom (NRA) approximation'.

In the screening mode the electron of the ion makes a transition whereas the atomic electrons do not, and the symmetry between the highly charged ion and the neutral atom in the consideration becomes even more formal. Therefore, it seems to be obvious that the NRA approximation should be better suited for the elastic mode. Indeed, analysis of the elastic atomic form-factors (see Appendix A) and test calculations for the elastic mode suggest that in some cases the space components of the elastic atomic form-factor vanish *per se* and, thus, the NRA 'approximation' may actually even become exact.

In general, more care should be taken when using the NRA approximation for the inelastic mode. In the very rough estimates given above typical electron velocities in the free atom were chosen to draw conclusions about the relative importance of the form-factor components of the atom. However, in collisions with heavy projectile-ions the minimum momentum transfer $Q_{min} = \frac{\varepsilon_n - \varepsilon_0}{v\gamma} + \frac{\epsilon_m - \epsilon_0}{v}$ can be large compared to the typical electron momenta in the atom. Because of this, the atomic electrons can acquire velocities $\sim Q = \sqrt{\mathbf{q}_\perp^2 + Q_{min}^2}$, which are considerably higher than the typical electron velocities in the atomic ground state. Since it has been assumed, that the atomic electrons are nonrelativistic in the collisions, it means that the condition $Q \ll c$ has to be fulfilled. The contributions of the atomic currents J'^1_A and J'^2_A to the transition matrix elements are suppressed by a factor of γ (see Eq.(83)) and the range of relatively large perpendicular momentum transfers $q_\perp \sim Z_I$ is not of great importance for the collision process. Therefore, the condition $Q \ll c$ can be replaced by $Q_{min} \ll c$. Further, if we estimate the energy difference $\varepsilon_n - \varepsilon_0$ as $\sim Z_I^2$ then the following condition

$$\gamma \gg \frac{Z_I^2}{vc}$$

is obtained for the use of the NRA approximation in relativistic collisions. It is certainly fulfilled for collisions with, say, $\gamma > 4$ for any heavy ion.

Another limitation for the application of the NRA approximation for the inelastic mode is also expected. As was already mentioned, it is well known in the theory of atomic ionization by a point-like charged particle that an important near cancellation may occur in the Lorentz gauge between the contributions of the scalar and vector potentials of the charged particle. A similar situation we may encounter here because of the presence of the term $\left(F_A^0 + \frac{v}{c} F_A^3\right)$. Using

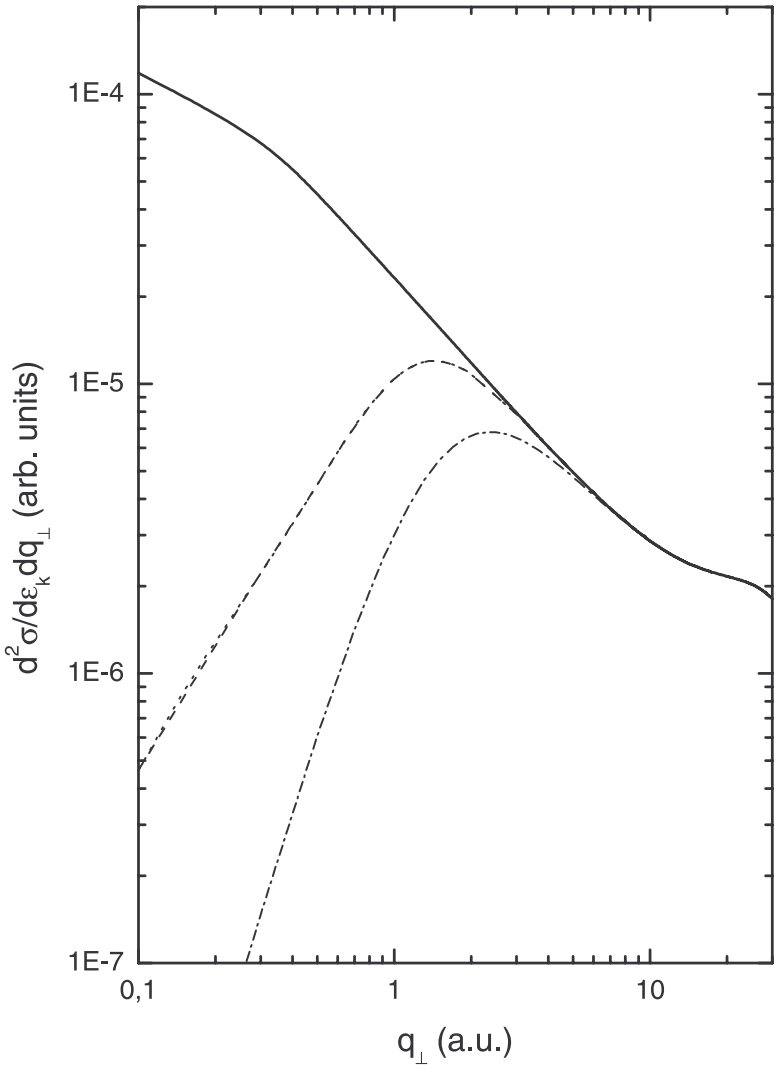

Figure 3: Doubly differential cross section $d^2\sigma/dq_\perp d\varepsilon_k$ for the electron loss from a projectile-ion in 100 GeV/u As^{32+} +H(1s) collisions. The cross section is given in the projectile frame as a function of the perpendicular part of the momentum transfer for a fixed energy of $\varepsilon_k = 10.8$ keV for the electron emitted from the ion. Dash and dot curves: the cross section for collisions, where hydrogen is ionized, calculated by using the full form-factor coupling (83) and the NRA approximation, respectively. In the latter two calculations the integration over all hydrogen continuum states has been performed. Dash-dot curve: the cross section for the elastic mode. For a comparison, the cross section in collisions with bare hydrogen nuclei is shown by a solid curve.

Eq.(86) one can show that

$$\begin{aligned} F_A^0(\mathbf{Q}) + \frac{v}{c} F_A^3(\mathbf{Q}) &= \langle u_m \left| \exp(i\mathbf{Q}\cdot\boldsymbol{\xi}) \right| u_0 \rangle + \frac{v}{c} \langle u_m \left| \alpha_z \exp(i\mathbf{Q}\cdot\boldsymbol{\xi}) \right| u_0 \rangle \\ &= \langle u_m \left| \exp(i\mathbf{Q}\cdot\boldsymbol{\xi}) \right| u_0 \rangle \left(1 + \frac{v}{c^2} \frac{\epsilon_m - \epsilon_0}{Q_{min}} \right) \\ &\quad - \frac{v}{cQ_{min}} \langle u_m \left| (\alpha_x Q_x + \alpha_y Q_y) \exp(i\mathbf{Q}\cdot\boldsymbol{\xi}) \right| u_0 \rangle , \end{aligned} \tag{91}$$

where for simplicity we assumed that the atom has just one electron. The right-hand side of Eq.(91) will be close to $F_A^0(\mathbf{Q})$ if one has simultaneously that (i) $v(\epsilon_m-\epsilon_0)/(c^2\,|Q_{min}|)\ll 1$ and (ii) $|F_A^0(\mathbf{Q})|\gg \frac{v}{c|Q_{min}|}\,|\langle u_m\,|(\alpha_x Q_x+\alpha_y Q_y)\exp(i\mathbf{Q}\cdot\boldsymbol{\xi})|\,u_0\rangle|$. The inequality (i) means that the condition $\gamma\ll\frac{c^2}{v^2}\frac{\varepsilon_n-\varepsilon_0}{\epsilon_m-\epsilon_0}$ must be fulfilled. Estimating the transition energies $\varepsilon_n-\varepsilon$ and $\epsilon_m-\epsilon_0$ as roughly given by $\sim Z_I^2$ and $\sim Z_A^2$, respectively, the above condition reads $\gamma\ll\frac{c^2}{v^2}\frac{Z_I^2}{Z_A^2}$. Taking into account that $c\boldsymbol{\alpha}$ represents the velocity operator, assuming that a typical 'transition' velocity of the electron in the atom can be approximated as $\sim Z_A$ and keeping in mind the restriction set by the inequality (i), one can show that the inequality (ii) reduces to $\gamma\ll\frac{c^2}{v^2}\frac{Z_I^2}{Z_A^2}$ which is just the same condition as that obtained from the inequality (i). Thus, $F_A^0(\mathbf{Q})+\frac{v}{c}F_A^3(\mathbf{Q})$ can be approximated by $F_A^0(\mathbf{Q})$ provided one has

$$\gamma\ll\frac{c^2}{v^2}\frac{Z_I^2}{Z_A^2}.$$

By combining results of the previous two paragraphs, we obtain the following estimate for the range of the validity of the NRA approximation for the inelastic mode

$$\frac{Z_I^2}{vc}\ll\gamma\ll\frac{Z_I^2}{vc}\frac{c^3}{vZ_A^2}, \tag{92}$$

where for collisions with many-electron atoms the atomic number Z_A should be replaced by some 'averaged' nuclear charge $\langle Z_A\rangle$ of the atom which is 'seen' by the majority of the atomic electrons. For light atoms, where $\langle Z_A\rangle$ does not substantially exceed 1, the condition (92) is not very restrictive. For collisions with heavy atoms the limitations imposed by Eq.(92) become rather formal since the antiscreening mode is of minor importance for such collisions.

In figure 3 we illustrate the validity of the NRA approximation for the inelastic mode of 100 GeV/u As^{32+} + H(1s) collisions.

3.9 Change of gauge. Calculations with approximate states for the projectile electron

In the nonrelativistic atom approximation the cross section (63), (82), which was obtained in the Lorentz gauge, reduces to

$$\begin{aligned}\sigma_{0\to n}^{0\to m} &= \frac{4}{v^2}\int d^2\mathbf{q}_\perp\left|Z_A\delta_{m0}-\langle u_m(\boldsymbol{\tau})\left|\sum_{j=1}^{Z_A}\exp(i\mathbf{Q}\cdot\boldsymbol{\xi}_j)\right|u_0(\boldsymbol{\tau})\rangle\right|^2\\ &\times\frac{\left|\left\langle\psi_n(\mathbf{r})\left|\left(1-\frac{v}{c}\alpha_z\right)\exp(i\mathbf{q}\cdot\mathbf{r})\right|\psi_0(\mathbf{r})\right\rangle\right|^2}{\left(\mathbf{q}^2-\frac{\omega_{n0}^2}{c^2}\right)^2},\end{aligned} \tag{93}$$

where $\omega_{n0}=\varepsilon_n-\varepsilon_0$. Let us consider the term

$$\frac{\left\langle\psi_n(\mathbf{r})\left|\left(1-\frac{v}{c}\alpha_z\right)\exp(i\mathbf{q}\cdot\mathbf{r})\right|\psi_0(\mathbf{r})\right\rangle}{\mathbf{q}^2-\frac{\omega_{n0}^2}{c^2}}, \tag{94}$$

which is a very important ingredient of the integrand in the cross section (93). This term can be cast into different forms which may be more convenient for further calculations. Here we will briefly discuss two of them.

1. The first form is obtained as follows. By applying the continuity equation (86) to the ion, that yields

$$\langle\psi_n(\mathbf{r})\,|\boldsymbol{\alpha}\cdot\mathbf{q}\,\exp(i\mathbf{q}\cdot\mathbf{r})|\,\psi_0(\mathbf{r})\rangle = \frac{\omega_{n0}}{c}\,\langle\psi_n(\mathbf{r})\,|\exp(i\mathbf{q}\cdot\mathbf{r})|\,\psi_0(\mathbf{r})\rangle\,, \tag{95}$$

and rewriting the term in (94), which contains the Dirac matrix α_z, according to

$$v\alpha_z = \mathbf{v}\cdot\boldsymbol{\alpha} = \left(\mathbf{v} - \frac{\omega_{n0}}{q^2}\mathbf{q}\right)\cdot\boldsymbol{\alpha} + \frac{\omega_{n0}}{q^2}\mathbf{q}\cdot\boldsymbol{\alpha}, \tag{96}$$

it is not difficult to show that the following identity holds

$$\begin{aligned}&\frac{\langle\psi_n(\mathbf{r})\,|\left(1-\frac{v}{c}\alpha_z\right)\,\exp(i\mathbf{q}\cdot\mathbf{r})|\,\psi_0(\mathbf{r})\rangle}{\mathbf{q}^2-\frac{\omega_{n0}^2}{c^2}} = \\ &\frac{\langle\psi_n(\mathbf{r})\,|\exp(i\mathbf{q}\cdot\mathbf{r})|\,\psi_0(\mathbf{r})\rangle}{\mathbf{q}^2} - \frac{1}{c}\frac{\langle\psi_n(\mathbf{r})\,|\boldsymbol{\lambda}\cdot\boldsymbol{\alpha}\,\exp(i\mathbf{q}\cdot\mathbf{r})|\,\psi_0(\mathbf{r})\rangle}{\mathbf{q}^2-\frac{\omega_{n0}^2}{c^2}}.\end{aligned} \tag{97}$$

Here the 'polarization' vector $\boldsymbol{\lambda}$ is given by $\boldsymbol{\lambda} = \mathbf{v} - \frac{\omega_{n0}}{q^2}\mathbf{q}$. Inserting the right-hand side of (97) into Eq.(93) we obtain

$$\begin{aligned}\sigma_{0\to n}^{0\to m} &= \frac{4}{v^2}\int d^2\mathbf{q}_\perp \left|Z_A\delta_{m0} - \langle u_m(\boldsymbol{\tau})\left|\sum_{j=1}^{Z_A}\exp(i\mathbf{Q}\cdot\boldsymbol{\xi}_j)\right|u_0(\boldsymbol{\tau})\rangle\right|^2 \\ &\times\left|\frac{\langle\psi_n(\mathbf{r})\,|\exp(i\mathbf{q}\cdot\mathbf{r})|\,\psi_0(\mathbf{r})\rangle}{\mathbf{q}^2} - \frac{1}{c}\frac{\langle\psi_n(\mathbf{r})\,|\boldsymbol{\lambda}\cdot\boldsymbol{\alpha}\,\exp(i\mathbf{q}\cdot\mathbf{r})|\,\psi_0(\mathbf{r})\rangle}{\mathbf{q}^2-\frac{\omega_{n0}^2}{c^2}}\right|^2.\end{aligned} \tag{98}$$

It is important to note that the above form of the cross section directly follows from the consideration in the Coulomb gauge. Indeed, by using the nonrelativistic atom approximation for the Coulomb gauge cross section (90), the latter reduces to exactly the same cross section (98). Thus, simple manipulations (95)-(96) with the transition matrix elements for the electron of the ion turn out to be effectively equivalent to the transformation of the 4-potentials of the incident atom from the Lorentz gauge to the Coulomb one.

Since within the nonrelativistic atom approximation only the zero component of the atomic current is kept, the condition (89) will in general not be fulfilled. Instead, we obtain that $\boldsymbol{\lambda}\cdot\mathbf{q} = (\epsilon_m - \epsilon_0)/\gamma$. Thus, in collisions in the inelastic mode the 'polarization' vector $\boldsymbol{\lambda}$ of the 'transverse' virtual photon is not strictly perpendicular to the photon momentum $\mathbf{q}$. However, for high-energy ion-atom collisions involving highly charged ions the angle ϑ characterizing the deviation of the polarization vector $\boldsymbol{\lambda}$ from the transverse direction is estimated to be given by $\vartheta \sim \frac{\epsilon_n-\epsilon_0}{\gamma(\varepsilon_n-\varepsilon_0)}$. Since this angle is very small, the deviation can be neglected and we may assume that $\boldsymbol{\lambda}\cdot\mathbf{q} = 0$ also for the inelastic transitions.

2. The second form can be obtained by using for the ion a transformation similar to that given by (91) for the atom

$$\left\langle \psi_n(\mathbf{r}) \left| \left(1 - \frac{v}{c}\alpha_z\right) \exp(i\mathbf{q}\cdot\mathbf{r}) \right| \psi_0(\mathbf{r}) \right\rangle = \langle \psi_n(\mathbf{r}) \left| \exp(i\mathbf{q}\cdot\mathbf{r}) \right| \psi_0(\mathbf{r}) \rangle \left(1 - \frac{v\omega_{n0}}{c^2 q_{min}}\right) + \frac{v}{c q_{min}} \langle \psi_n(\mathbf{r}) \left| (q_x\alpha_x + q_x\alpha_y) \exp(i\mathbf{q}\cdot\mathbf{r}) \right| \psi_0(\mathbf{r}) \rangle . \quad (99)$$

For the elastic mode the factor $(1 - v\omega_{n0}/(c^2 q_{min}))$ is exactly equal to γ^{-2}. Taking into account the condition (92), one can show that for the inelastic mode this factor is approximately equal to γ^{-2}. Therefore, for both modes the cross section (93) can be rewritten as

$$\sigma_{0\to n}^{0\to m} = \frac{4}{v^2}\int d^2\mathbf{q}_\perp \left| Z_A\delta_{m0} - \langle u_m(\boldsymbol{\tau}) \left| \sum_{j=1}^{Z_A} \exp(i\mathbf{Q}\cdot\boldsymbol{\xi}_j) \right| u_0(\boldsymbol{\tau}) \rangle \right|^2 \frac{1}{\left(\mathbf{q}^2 - \frac{\omega_{n0}^2}{c^2}\right)^2} \times \left| \frac{\langle \psi_n(\mathbf{r}) \left| \exp(i\mathbf{q}\cdot\mathbf{r}) \right| \psi_0(\mathbf{r}) \rangle}{\gamma^2} + \frac{\langle \psi_n(\mathbf{r}) \left| (q_x\alpha_x + q_x\alpha_y) \exp(i\mathbf{q}\cdot\mathbf{r}) \right| \psi_0(\mathbf{r}) \rangle}{c q_{min}/v} \right|^2 . \quad (100)$$

As we have seen, the application of the continuity equation for the ion current in the form given by Eq.(97) is effectively equivalent to the transformation of the 4-potentials of the incident atom from the Lorentz gauge to the Coulomb gauge. One can show that the use of the continuity equation for the ion current in the form given by Eq.(99) actually corresponds to the transformation of the 4-potentials of the atom to the gauge which is related to the Lorentz gauge by the transformation $A^\mu = A^\mu_{Lor} - \partial^\mu f$ where the gauge function f is defined by $\frac{\partial f}{\partial t} = \frac{v^2}{c} A^0_{Lor}$.

In order to derive Eqs.(98) and (100) from Eq.(93) we used the continuity equation for the ion current. Therefore, the cross sections (93), (98) and (100) will yield identical results only if exact electronic states of the ion are used. Approximate electronic states cannot in general provide the near cancellation occurring in the Lorentz gauge between the contributions of the scalar and vector potentials to the term (94). Consequently, if in calculations one needs to apply approximations for the states ψ_n and ψ_0, then Eq.(98) or Eq.(100), where the 'near-cancellation problem' is already not present, should be used as a starting point. Of course, the cross sections (98) and (100) in general are not expected to yield identical results if any approximations are employed for the electron states of the ion. Therefore, we attempted to compare Eqs.(98) and (100) by using them for calculations of the total loss cross sections with semirelativistic states for the electron of the ion: In cases tested both these cross sections yielded quite similar results.

3.10 Where are first order considerations valid ?

In general, this question is not easy to answer. Of course, one expects that first order theories should represent a reasonable tool for treating those ion-atom collisions, where the ion-atom

interaction is weak. However, without comparing first order results with those following from more sophisticated treatments, it is not always clear whether the interaction is already weak enough in order that first order considerations could yield a proper description for a certain process occurring in the collision.

If we restrict our consideration to collisions between a hydrogen-like ion and a neutral atom, where no more than one electron of the atom makes a transition in the collision process, then first order approaches should be very well suited for describing various cross sections including the fully differential ones provided the conditions $\frac{Z_I}{v} \ll 1$, $\frac{Z_A}{v} \ll 1$ and $\frac{Z_I Z_A}{v} \ll 1$ are fulfilled. The latter condition may be especially restrictive. It, however, can be ignored if we do not intend to describe the projectile scattering and target recoil and are only interested in treating electron transitions. Further, if we focus our attention on cross sections for excitation of the ion or on the total cross section for the electron loss and do not ask ourselves about what precisely happens to electrons of the atom, then one can expect that results of first order approaches will not strongly deviate from reality if Z_A is substantially smaller than Z_I and/or v. [11]

We will return to the discussion of the validity of first order treatments in sections 5 and 6 where predictions of first order considerations will be compared to results obtained by using approximations discussed in the next section.

4 Projectile-electron excitation and loss in ultrarelativistic collisions with atoms: considerations beyond first order

4.1 Preliminary remarks

In high-velocity collisions deviations from first order predictions are often discussed [1] in terms of the so called binding and polarization effects [39]. Although here we consider excitation and loss of the projectile electron in collisions at very high energies, where these effects are not expected to play any noticeable role, the first order treatment may still not always be well suited for this consideration. On one hand, even at very high collision velocities a highly charged projectile can strongly affect a target in not very distant collisions. On the other hand, the contribution to the excitation or loss of the projectile's electron in collisions with neutral atoms arises mainly from relatively small impact parameters where the atomic field can reach very large values.

If we study electron transitions in the projectile-ion and are not interested in what can happen to the atomic target in the projectile-target collision, then cross sections for the projectile-electron excitation and loss can be evaluated by noting the following point. Although it is

[11] See pp. 278-280 of [5] for a discussion of why first order theories can still yield reasonable results for the projectile-electron excitation and loss in cases where the projectile-target interaction is already rather strong for the target.

unlikely that the initial quantum state of the atomic target will not be changed by such collisions with a highly charged projectile, where the latter penetrates the target electron cloud, it is still quite reasonable to assume that the spatial distribution of the target electrons will not be altered considerably during the very short effective collision time when the target field acts on the projectile electron. Therefore, the projectile-electron excitation and loss cross sections can be evaluated using the assumptions that the electrons of the atomic target are 'frozen' during the effective collision time and that the spatial distribution of these electrons during this time can be represented by the wavefunction of the initial atomic state [12].

It is evident that higher-order effects in projectile-electron excitation and loss should be more pronounced for collisions with heavy atomic targets. According to the first order consideration the screening mode is by far the dominant one in collisions with heavy targets, which contain very many electrons, provided the dimension of the electron orbit in the projectile is much less than the dimension of the neutral target. In addition, the deviation from results of the first order consideration is first of all expected for very small impact parameters where, as it will be discussed in detail in section 5, the relative contribution of the antiscreening mode is even weaker compared to that in the total excitation or loss cross section. Therefore, in what follows we will neglect the antiscreening contribution and concentrate on a better description, compared to the first order one, of the screening mode only.

4.2 General

In the screening mode the action of the atom on the electron of the ion is represented by an external potential and the many-electron problem of two colliding atomic particles reduces to the much simpler problem of the motion of the electron of the ion in two fields, the field of the ion nucleus and the field of the atom 'frozen' in its ground state. In the rest frame of the nucleus of the ion the motion of its electron is described by the Dirac equation

$$i\frac{\partial\psi(\mathbf{r},t)}{\partial t} = \left(c\boldsymbol{\alpha}\cdot\left(\mathbf{p}+\frac{1}{c}\mathbf{A}(\mathbf{r},t)\right)+\beta c^2-\frac{Z_I}{r}-\Phi(\mathbf{r},t)\right)\psi(\mathbf{r},t), \tag{101}$$

where $\boldsymbol{\alpha}$ and β are the Dirac's matrices, $\mathbf{r}$ is the coordinate of the electron with respect to the nucleus of the ion, Φ and $\mathbf{A}$ are the scalar and vector potentials of the incident neutral atom. We assume that in the rest frame of the atom its scalar potential is well approximated by a short-range interaction

$$\Phi' = \frac{Z_A\phi(r')}{r'}, \tag{102}$$

[12] The assumption that the spatial distribution of the atomic electrons is 'frozen' during the collision does not imply that these electrons will finally remain in the atomic initial state. Therefore, the *screening* mode, as it is regarded in this section, is no longer equivalent to the *elastic* mode (see also [22]).

where

$$\phi = \sum_j A_j \exp(-\kappa_j r') \tag{103}$$

with the screening parameters A_j ($\sum_j A_j = 1$) and κ_j which have already been introduced in 3.2. An interaction of the type (102)-(103) can be regarded as originating from the exchange of 'massive photons' with masses $M_j = \kappa_j$: a photon with mass M_j has the source characterized by a charge $Z_j = Z_A A_j$ ($\sum_j Z_j = Z_A$).

The scalar and vector potentials of a source Z_j of massive photons with mass M_j, which moves with relativistic velocity v, are described by the Proca equation [35]

$$\begin{aligned} \Delta\Phi_j - \frac{1}{c^2}\frac{\partial^2\Phi_j}{\partial t^2} - M_j^2\Phi_j &= -4\pi Z_j \delta(\mathbf{r} - \mathbf{R}(t)) \\ \mathbf{A}_j &= \frac{\mathbf{v}}{c}\Phi_j. \end{aligned} \tag{104}$$

We will assume that in the projectile frame the atom moves along a straight-line trajectory $\mathbf{R} = \mathbf{b} + \mathbf{v}t$, where $\mathbf{b} = (b_x, b_y)$ is the impact parameter and $\mathbf{v} = (0, 0, v)$ is the velocity of the atom.

With the help of the Fourier transformation the solution of (104) can be written as

$$\Phi_j(\mathbf{r}, t) = \frac{Z_j}{2\pi^2}\int d^2\mathbf{k}_\perp \exp(i\mathbf{k}_\perp(\mathbf{r}_\perp - \mathbf{b}))\int_{-\infty}^{+\infty} dk_z \frac{\exp(ik_z(z - vt))}{k_\perp^2 + \frac{k_z^2}{\gamma^2} + M_j^2}, \tag{105}$$

where $\mathbf{r} = (\mathbf{r}_\perp, z)$ with $\mathbf{r}_\perp \cdot \mathbf{v} = 0$.

The straightforward integration of (105) results in

$$\Phi_j(\mathbf{r}, t) = \frac{\gamma Z_j}{\sqrt{\gamma^2(z - vt)^2 + (\mathbf{r}_\perp - \mathbf{b})^2}} \exp\left(-M_j\sqrt{\gamma^2(z - vt)^2 + (\mathbf{r}_\perp - \mathbf{b})^2}\right). \tag{106}$$

The potential (106) could be easily derived directly from (102) and (103) by using the Lorentz transformation. However, the advantage of the Fourier representation (105) is that, for collision velocities v which very closely approach the speed of light, it allows one to obtain straightforwardly the essential simplification for the form of the scalar and vector potentials, whereas the limit $v \to c$ of (106) is rather delicate.

4.2.1 Light-cone (eikonal) approximation

For infinite γ one can drop the term $\frac{k_z^2}{\gamma^2}$ in the integrand of (105) and obtain

$$\begin{aligned} \Phi_j(\mathbf{r}, t) &= \frac{Z_j}{2\pi^2}\int d^2\mathbf{k}_\perp \exp(i\mathbf{k}_\perp(\mathbf{r}_\perp - \mathbf{b}))\int_{-\infty}^{+\infty} dk_z \frac{\exp(ik_z(z - ct))}{k_\perp^2 + M_j^2} \\ &= \frac{2Z_j}{c}\delta\left(t - \frac{z}{c}\right) K_0\left(M_j \mid \mathbf{r}_\perp - \mathbf{b} \mid\right), \end{aligned} \tag{107}$$

where δ is the delta-function and K_0 is a modified Bessel function. Then the scalar and vector potentials created by the incident atom in the rest frame of the ion are given by

$$\begin{aligned} \Phi(\mathbf{r},t) &= \frac{2Z_A}{c}\delta\left(t-\frac{z}{c}\right)\sum_j A_j K_0\left(M_j \mid \mathbf{r}_\perp - \mathbf{b} \mid\right) \\ A_z(\mathbf{r},t) &= \Phi(\mathbf{r},t),\ A_x = A_y = 0. \end{aligned} \tag{108}$$

For the potentials (108) the Dirac equation (101) can be solved exactly using a method proposed in [40] to calculate electron transitions caused by collisions with a point-like charge moving at the speed of light. In the case under consideration, where the perturbing atomic field is short-ranged, the exact probability amplitude a_{0n} for the electron of the ion to make a transition $\psi_0 \to \psi_n$ between the electron states ψ_0 and ψ_n of the projectile is given by [41]

$$\begin{aligned} a_{0n}^{eik}(\mathbf{b}) &= \delta_{0n} + \left\langle \psi_n \left| (1-\alpha_z)\exp\left(i\frac{\omega_{n0}z}{c}\right)\left(\exp\left(-\frac{2iZ_A}{c}\sum_j A_j K_0\left(M_j \mid \mathbf{r}_\perp - \mathbf{b} \mid\right)\right) - 1\right)\right| \psi_0 \right\rangle \\ &\equiv \left\langle \psi_n \left| (1-\alpha_z)\exp\left(i\frac{\omega_{n0}z}{c}\right)\exp\left(-\frac{2iZ_A}{c}\sum_j A_j K_0\left(M_j \mid \mathbf{r}_\perp - \mathbf{b} \mid\right)\right)\right| \psi_0 \right\rangle, \end{aligned} \tag{109}$$

where ω_{n0} is the transition frequency. The second line in (109) follows directly from the first one if the identity $< \psi_n \mid \alpha_z \exp\left(i\frac{\omega_{n0}z}{v}\right) \mid \psi_0 > \equiv \frac{v}{c} < \psi_n \mid \exp\left(i\frac{\omega_{n0}z}{v}\right) \mid \psi_0 >$ $(n \neq 0)$ is used. One can prove analytically that the amplitude (109) preserves the unitarity condition $\sum_n \mid a_{0n}(\mathbf{b}) \mid^2 \equiv 1$, as it should be for an exact solution. The transition amplitude (109) can be seen as the eikonal formula [42] in the case of the exchange of massive photons. Below, the transition amplitude (109) is referred to as the eikonal or 'light-cone' amplitude.

In the limit of vanishing screening ($M_j \to 0$) one can use the relation $K_0(x) \approx -\ln\left(\frac{x}{2}\right) - \Gamma$ for $\mid x \mid \ll 1$ (see e.g. [43]), where Γ is Euler's constant. Then, neglecting an inessential coordinate-independent phase factor, the transition amplitude (109) reduces to

$$a_{0n}^{eik-coul}(\mathbf{b}) = < \psi_n \mid (1-\alpha_z)\exp\left(i\frac{\omega_{n0}z}{c}\right)\exp\left(\frac{iZ_A}{c}\ln\left(\frac{\mathbf{r}_\perp - \mathbf{b}}{b}\right)^2\right) \mid \psi_0 > . \tag{110}$$

The transition amplitude (110) coincides with that derived in [40] for the electron transition in collisions with a point-like charge [13].

For finite values of γ the transition amplitude (109) is expected to give good results if the effective duration time of the interaction $T(b) \sim b/(v\gamma)$ is small compared to the characteristic electron transition time in the ion $\tau \sim \omega_{n0}^{-1}$, i.e. for impact parameters $b \ll b_0 = v\gamma/\omega_{n0}$ where the collision is 'sudden' for the electron. For collisions with neutral atoms there is another characteristic distance, the dimension of the neutral atom a_0. If $b_0 \gg a_0$ then the amplitude

[13] Eq.(10) of [40] reads: $a_{0n}(\mathbf{b}) = \delta_{0n} + < \psi_n \mid (1-\alpha_z)\exp\left(i\frac{\omega_{n0}z}{c}\right)\left(\exp\left(-i\frac{Z_A}{c}\ln(\mathbf{r}_\perp - \mathbf{b})^2\right) - 1\right) \mid \psi_0 >$. The transformation of the latter amplitude into Eq.(110) is similar to that used for obtaining the second line in Eq.(109).

(109) can be used for any impact parameter because for larger impact parameters $b \gtrsim b_0$, where collisions are no longer 'sudden' for the electron, the electron-atom interaction is already negligible.

The eikonal amplitude (109) is to be compared with the transition amplitude for the screening mode, which is obtained in the first order semiclassical perturbation theory (see Eq.(120) of the next section),

$$a_{0n}^{p}(\mathbf{b}) = \frac{2iZ_A}{v} \sum_j A_j < \psi_n \mid \left(1 - \frac{v}{c}\alpha_z\right) \exp\left(i\frac{\omega_{n0}z}{v}\right) K_0\left(B_j \mid \mathbf{r}_\perp - \mathbf{b} \mid\right) \mid \psi_0 >, \qquad (111)$$

where $B_j = \sqrt{\frac{\omega_{n0}^2}{v^2\gamma^2} + M_j^2}$.

For collisions at infinite γ the transition amplitude, given by (109), is valid for any impact parameter b. For collisions with light atoms, where $\frac{2Z_A}{c} \ll 1$, or at large impact parameters, where the condition $\frac{2Z_A}{c}\sum_j A_j K_0\left(M_j \mid \mathbf{r}_\perp - \mathbf{b} \mid\right) \ll 1$ holds for any atom, the transition amplitude (109) reduces to the first order amplitude (111).

4.2.2 Collisions at high but finite γ: combination of the eikonal and first order approaches

For collisions with high but finite values of γ both transition amplitudes (109) and (111) are not exact. In such a case the expressions (109) and (111), in general, are better suited to describe the transition amplitude at small and large impact parameters, respectively. In a comparative analysis for these two amplitudes we first consider colliding systems where $b_0 = \frac{\gamma v}{\omega_{n0}} \gg a_0$. In such a case one has $B_j \simeq M_j$ since $M_j \gtrsim 1$. For large impact parameters $b \gg \frac{Z_A}{Z_I c}$, where the atomic field acting on the electron of the ion is weak compared to the interaction between the electron and the nucleus of the ion, the exponent in Eq.(109) can be expanded in series and one sees that the transition amplitude (109) is approximately equivalent to the first order transition amplitude for these impact parameters (if in the latter one neglects terms proportional to $\frac{1}{\gamma^2}$). For collisions with smaller impact parameters, where the atomic field can reach considerable magnitudes during the collisions, the first order transition amplitude (111) is inferior to the amplitude (109). Therefore, for colliding systems, which satisfy the condition $b_0 \gg a_0 \sim 1$, the eikonal transition amplitude (109) should be used for all impact parameters.

Let us now consider colliding systems where $b_0 \lesssim a_0$. One should note that in ultrarelativistic collisions such a condition can be fulfilled only for very heavy ions. If, in addition, $b_0 \gg a_I$, where $a_I \sim \frac{1}{Z_I}$ is the typical dimension of the ground state of the electron in the ion, then a simple method can be applied to calculate cross sections (see e.g. [44]- [46]). Namely, for collisions with small impact parameters $b \ll b_0$, where the atom-electron interaction can be strong, the transition probability is calculated according to the nonperturbative expression (109). For collisions with larger impact parameters $b \gg \frac{1}{Z_I} \gtrsim \frac{Z_A}{Z_I c}$, where the perturbation is already weak, the first order perturbation theory can be used to calculate the transition probability. This method of combining the eikonal and first-order treatments can be employed if there exists an

overlap between the regions $b \ll b_0$ and $b \gg \frac{1}{Z_I}$, i.e. when $Z_I b_0 \gg 1$. Then, taking into account (109) and (111), the screening contribution to the cross section can be written as

$$\sigma_{0\to n} = 2\pi \int_0^{b_1} db\, b \mid a_{0n}^{eik}(b) \mid^2 + 2\pi \int_{b_1}^{\infty} db\, b \mid a_{0n}^{p}(b) \mid^2 \tag{112}$$

where b_1 has to be in the range of impact parameters where transition probabilities, calculated according to (109) and (111), are approximately equal. The existence of the 'overlap' region is very important because only in such a case the cross section (112) becomes independent of a particular choice made for the value of b_1. This point is discussed in detail in Appendix B where it is shown that, for the electron loss in ultrarelativistic collisions with a point-like charged particle, one can always find a range of impact parameters where the eikonal and first order transition amplitudes are approximately equal and that in collisions with neutral atoms a similar range of impact parameters does exist for the loss from very heavy ions.

5 Impact parameter dependence of projectile-electron excitation and loss in relativistic collisions

For a collision in which the electron of the projectile ion makes a transition $0 \to n$ and those of the target atom make a transition $0 \to m$, the semiclassical transition probability [14] reads

$$P_{0\to n}^{0\to m}(\mathbf{b}) = \mid a_{0\to n}^{0\to m}(\mathbf{b}) \mid^2, \tag{113}$$

where the transition amplitude $a_{0\to n}^{0\to m}(\mathbf{b})$ is given by Eq.(79).

Usually in collision experiments on the projectile-electron excitation and loss a final internal state of the atom is not observed. In such a case one has to sum over all possible states of the atom. The total probability for the ion to make a transition $0 \to n$ in the collision then reads

$$P_{0\to n}(\mathbf{b}) = \sum_m \mid a_{0\to n}^{0\to m}(\mathbf{b}) \mid^2 . \tag{114}$$

This transition probability can be split into the sum of the screening

$$P_{0\to n}^{s}(\mathbf{b}) = \mid a_{0\to n}^{0\to 0}(\mathbf{b}) \mid^2 \tag{115}$$

and antiscreening

$$P_{0\to n}^{a}(\mathbf{b}) = \sum_{m\neq 0} \mid a_{0\to n}^{0\to m}(\mathbf{b}) \mid^2 \tag{116}$$

parts.

[14] If the final state of the projectile or of the target is a continuum state, then Eq.(113) represents the probability density.

In what follows the probability $P_{0\to n}(\mathbf{b})$ will be evaluated within the nonrelativistic atom approximation. Within this approximation the semiclassical first order transition amplitude (79) is substantially simplified and reduces to

$$a_{0\to n}^{0\to m}(\mathbf{b}) = -\frac{i}{\pi v}\int d^2\mathbf{q}_\perp \exp(-i\mathbf{q}_\perp\mathbf{b}) < u_m \mid Z_A - \sum_{j=1}^{N_A}\exp(-i\mathbf{Q}\cdot\boldsymbol{\xi}_j) \mid u_0 > \times\frac{< \psi_n \mid \left(1-\frac{v}{c}\alpha_z\right)\exp(i\mathbf{q}\cdot\mathbf{r}) \mid \psi_0 >}{q_\perp^2 + \frac{(\varepsilon_n-\varepsilon_0+\epsilon_m-\epsilon_0)^2}{v^2\gamma^2} + 2(\gamma-1)\frac{(\varepsilon_n-\varepsilon_0)(\epsilon_m-\epsilon_0)}{v^2\gamma^2}}. \quad (117)$$

Here, $\mathbf{q} = (\mathbf{q}_\perp, q_{min})$ and $\mathbf{Q} = (-\mathbf{q}_\perp, -Q_{min})$ are the momenta transferred to the ion (in the ion frame) and to the atom (in the atom frame), respectively, with q_{min} and Q_{min} given by Eqs.(61) and (62).

5.1 Screening mode

In this case $m = 0$ and the corresponding transition amplitude is given by

$$a_{0\to n}^{0\to 0}(\mathbf{b}) = -\frac{i}{\pi v}\int d^2\mathbf{q}_\perp \exp(-i\mathbf{q}_\perp\mathbf{b}) Z_{A,eff}(\mathbf{Q}) \times\frac{< \psi_n \mid \left(1-\frac{v}{c}\alpha_z\right)\exp(i\mathbf{q}\cdot\mathbf{r}) \mid \psi_0 >}{q_\perp^2 + \frac{(\varepsilon_n-\varepsilon_0)^2}{v^2\gamma^2}}. \quad (118)$$

Here,

$$Z_{A,eff}(\mathbf{Q}) = Z_A - \langle u_0 \left| \sum_{j=1}^{N_A}\exp(i\mathbf{Q}\cdot\boldsymbol{\xi}_j)\right| u_0\rangle \quad (119)$$

represents the effective charge of the atom which is 'seen' by the electron of the ion (in the ion frame) in collisions where the momentum $\mathbf{Q} = (-\mathbf{q}_\perp, -(\varepsilon_n - \varepsilon_0)/v\gamma))$ is transferred to the atom (in the atom frame). Using the analytical Dirac-Hartree-Fock-Slater functions from Salvat et al [33] and performing the integration over the transverse part $\mathbf{q}_\perp$ of the momentum transfer, the expression (118) for the elastic transition amplitude can be transformed into

$$a_{0\to n}^{0\to 0}(\mathbf{b}) = \frac{2iZ_A}{v}\sum_{j=1}^{3} A_j \times \langle\psi_n \left|\exp\left(i\frac{\varepsilon_n-\varepsilon_0}{v}z\right)\left(1-\frac{v}{c}\alpha_z\right) K_0(\mid \mathbf{b}-\mathbf{r}_\perp \mid B_0)\right| \psi_0\rangle, \quad (120)$$

where K_0 is the modified Bessel function, $\mathbf{r} = (\mathbf{r}_\perp, z)$ with $\mathbf{r}_\perp\cdot\mathbf{v} = 0$ are the coordinates of the electron of the ion, $B_{0,n} = \sqrt{\frac{(\varepsilon_n-\varepsilon_0)^2}{v^2\gamma^2} + \kappa_j^2}$, A_j and κ_j are the screening parameters tabulated for neutral atoms in [33]. Note that if we neglect in (120) the screening effect of the atomic electrons

by setting all $\kappa_j = 0$ then, taking into account that $\sum_j A_j = 1$, we obtain the amplitude for a transition $0 \to n$ of the electron of the ion in collisions with a bare nucleus with a charge Z_A

$$a_{0\to n}^{0\to 0}(\mathbf{b}) = \frac{2iZ_A}{v} \times \langle \psi_n \left| \exp\left(i\frac{\varepsilon_n - \varepsilon_0}{v} z \right) \left(1 - \frac{v}{c}\alpha_z \right) K_0 \left(\frac{(\varepsilon_n - \varepsilon_0)}{\gamma v} \mid \mathbf{b} - \mathbf{r}_\perp \mid \right) \right| \psi_0 \rangle. \quad (121)$$

5.2 Antiscreening mode

In this case $m \neq 0$. Taking into account that

$$\int d^2\mathbf{q}_\perp \frac{\exp(-i\mathbf{q}_\perp(\mathbf{b} - \mathbf{r}_\perp + \boldsymbol{\xi}_{\perp,j}))}{\mathbf{q}_\perp^2 + B_{m,n}^2} = 2\pi K_0(\mid \mathbf{b} - \mathbf{r}_\perp + \boldsymbol{\xi}_{\perp,j} \mid B_{mn}),\ B_{m,n} > 0, \quad (122)$$

where $\boldsymbol{\xi}_j = (\boldsymbol{\xi}_{\perp,j}, \xi_{z,j})$ with $\boldsymbol{\xi}_{\perp,j} \cdot \mathbf{v} = 0$ are the coordinates of the atomic electrons with respect to the atomic nucleus [15], the transition amplitude can be written as

$$a_{0\to n}^{0\to m}(\mathbf{b}) = < u_m \mid \sum_{j=1}^{N_A} e^{-i\left(\frac{\epsilon_m - \epsilon_0}{v} + \frac{\varepsilon_n - \varepsilon_0}{v\gamma}\right)\xi_{z,j}} \alpha_{n0}^j(\mathbf{b} + \boldsymbol{\xi}_{\perp,j}, m0) \mid u_0 > . \quad (123)$$

In the above formula

$$\alpha_{n0}^j(\mathbf{b} + \boldsymbol{\xi}_{\perp,j}, m0) = \frac{2i}{v} < \psi_n \mid e^{-i\left(\frac{\varepsilon_n - \varepsilon_0}{v} + \frac{\epsilon_m - \epsilon_0}{v\gamma}\right)z} \left(1 - \frac{v}{c}\alpha_z \right) \times K_0 \left(\mid \mathbf{b} - \mathbf{r}_\perp + \boldsymbol{\xi}_{\perp,j} \mid B_{m,n} \right) \mid \psi_0 >, \quad (124)$$

where $B_{m,n} = \sqrt{\frac{(\varepsilon_n - \varepsilon_0 + \epsilon_m - \epsilon_0)^2}{v^2\gamma^2} + 2(\gamma - 1)\frac{(\varepsilon_n - \varepsilon_0)(\epsilon_m - \epsilon_0)}{v^2\gamma^2}}$. The form of the expression (124) resembles the semi-classical transition amplitude for the electron of the ion in collisions with a point-like particle with a charge -1 which moves along a classical straight-line trajectory with the velocity v and the impact parameter $\mathbf{b} + \boldsymbol{\xi}_{\perp,j}$.

In order to find the total probability of the electron transition in the ion from all collisions, where the atom can finally be in any of its excited states including the atomic continuum, one has to perform the summation in (116). This can be done by using the closure method (see [5] and references therein). In the simplest form of this method the same averaged energy $\Delta\epsilon$ is assumed for all possible transitions of the atomic electrons. In nonrelativistic collisions this approximation yields good results for the electron loss at collision velocities well above the energy threshold for the projectile ionization by a beam of free electrons. Therefore, one can expect this approximation to give reasonable results for relativistic collisions when the kinetic energy T of an equivelocity electron is much larger than the transition energy of the electron in the ion: $T = m_e c^2(\gamma - 1) \gg \varepsilon_n - \varepsilon_0$. Starting with $\gamma \sim 2-3$ the latter condition is fulfilled even for the heaviest single-electron ions. Since we already have the condition $\gamma \geq 3 - 4$ imposed

[15] as they are viewed in the atomic frame.

by the application of the nonrelativistic atom approximation for the antiscreening mode, no additional restrictions on the collision energies are introduced here.

Within the closure approximation the closure relation for the electron states of the atom

$$\sum_m \mid u_m >< u_m \mid = \mathbf{I} \tag{125}$$

is applied in order to perform the summation over the final states of the atom. In addition, if the antisymmetrization in the ground state of the atom is ignored and the wavefunction of the ground state is expressed as

$$u_0 = \prod_\lambda \phi_\lambda(\boldsymbol{\xi}_\lambda), \tag{126}$$

where $\phi_\lambda(\boldsymbol{\xi})$ are the single electron orbitals, the antiscreening probability takes the much simpler form

$$\begin{aligned} P^a_{0\to n}(\mathbf{b}) &= \sum_{m\neq 0} \mid a^{0\to m}_{0\to n}(\mathbf{b}) \mid^2 \\ &= \sum_\lambda < \phi_\lambda \mid\mid e^{-i\left(\frac{\Delta\epsilon}{v}+\frac{\varepsilon_n-\varepsilon_0}{v\gamma}\right)\xi_z} \alpha_{n0}(\mathbf{b}+\boldsymbol{\xi}_\perp) \mid^2 \mid \phi_\lambda > \\ &\quad - \sum_\lambda \mid < \phi_\lambda \mid e^{-i\left(\frac{\Delta\epsilon}{v}+\frac{\varepsilon_n-\varepsilon_0}{v\gamma}\right)\xi_z} \alpha_{n0}(\mathbf{b}+\boldsymbol{\xi}_\perp) \mid \phi_\lambda > \mid^2 . \end{aligned} \tag{127}$$

Here $\alpha_{n0}(\mathbf{b}+\boldsymbol{\xi}_\perp)$ is defined by Eq.(124) with the replacements $\epsilon_m - \epsilon_0 \to \Delta\epsilon$ and $B_{mn} \to \sqrt{\frac{(\varepsilon_n-\varepsilon_0+\Delta\epsilon)^2}{v^2\gamma^2} + 2(\gamma-1)\frac{(\varepsilon_n-\varepsilon_0)\Delta\epsilon}{v^2\gamma^2}}$. The expression (127) still contains the sixfold integration over the electronic coordinates and an additional threefold integration needs to be performed if one considers the electron loss.

5.3 Results and discussion

In this subsection we will discuss probabilities for the electron excitation in Bi^{82+} in relativistic collisions with two neutral atoms, Cu and He. For a comparison the excitation of Bi^{82+} in collisions with the corresponding bare nuclei, Cu^{29+} and He^{2+}, will also be considered. In addition, results will be presented for the antiscreening probability of the projectile-electron excitation in collisions with helium. Helium as a target was chosen because of three main reasons. First, helium is a few-electron system where the contribution from the antiscreening mode is expected to be comparable in magnitude with that of the screening mode. Second, helium target is widely used in experiments on atomic collision physics. Third, in the helium case orbitals $\phi_\lambda(\boldsymbol{\xi})$ are $1s$-orbitals and the sixfold integral in (127) can be reduced analytically to a fourfold integration [18]. The latter, however, has to be done numerically.

In contrast to helium, a copper atom has many electrons. Therefore, in collisions of Bi^{82+}, which has a very tightly bound electron, with copper the antiscreening mode is of minor importance and will not be considered here.

Throughout this subsection relativistic units $\hbar = m_e = c = 1$ are used except in figure 8 where the impact parameter is given in fermi (1 rel. unit. $\simeq$ 386 fm).

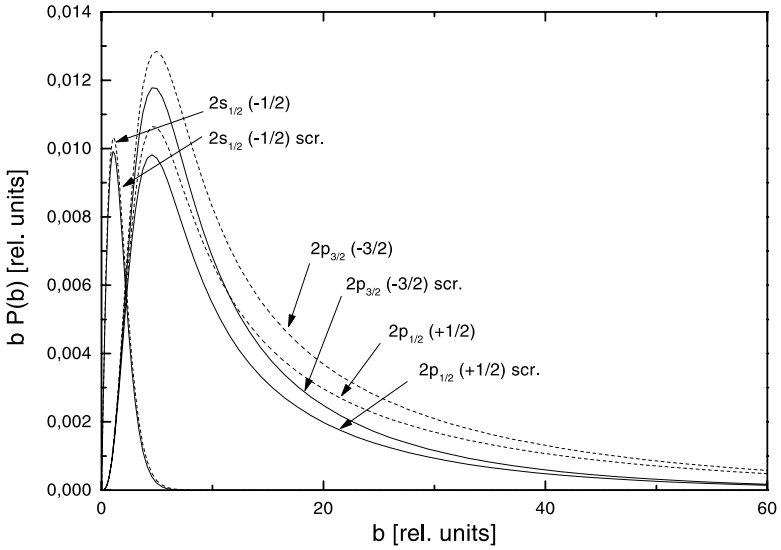

Figure 4: Weighted probabilities for projectile excitation in collisions of a Bi^{82+} projectile with Cu at a collision energy corresponding to $\gamma = 10$. Solid lines: the screening mode, dashed lines: collisions with a bare atomic nucleus Cu^{29+}. The numbers in brackets denote the magnetic quantum numbers of the final electron states in the Bi^{82+} ion. From [12].

5.3.1 Screening in ultrarelativistic collisions with moderately heavy atoms

In figure 4 weighted probabilities $bP(b)$ are shown for the excitation of a $1s_{1/2}(m_j = -1/2)$ electron of a Bi^{82+} projectile incident on Cu at a collision energy corresponding to $\gamma = 10$. The different full curves show results for excitation to different states of Bi^{82+} where the screening effect has been included. The dashed curves show the excitation without any screening, i.e. in collisions with a bare nucleus Cu^{29+}. It can be seen from this figure that the main effect of the screening is to reduce the transition probabilities at larger impact parameters. For transitions to the $2s_{1/2}(m_j = -1/2)$-state the screening effect plays almost no role. This suggests that these transitions occur effectively at very small impact parameters where the electrons of the neutral copper atom cannot screen their nucleus.

In figure 5 results of similar calculations are displayed for the same projectile-target system but at a collision energy corresponding to $\gamma = 100$. Because of the retardation effect, in collisions with Cu^{29+} the probabilities of transitions to p-states have considerably longer tails at large b compared to the previous case. However, in collisions with a neutral atom the screening of the nucleus of Cu by its electrons reduces the transition probabilities in collisions with larger impact parameters. Thus, one obtains almost the same results for the screened probabilities at $\gamma = 10$ and $\gamma = 100$. For a many-electron atom like Cu the antiscreening mode is not expected to play a noticeable role. Therefore, one may conclude that at $\gamma \gtrsim 10$ the corresponding cross sections for the excitation, considered as a function of collision energy, are very close to or already have entered the 'saturation' region where the cross sections become γ-independent

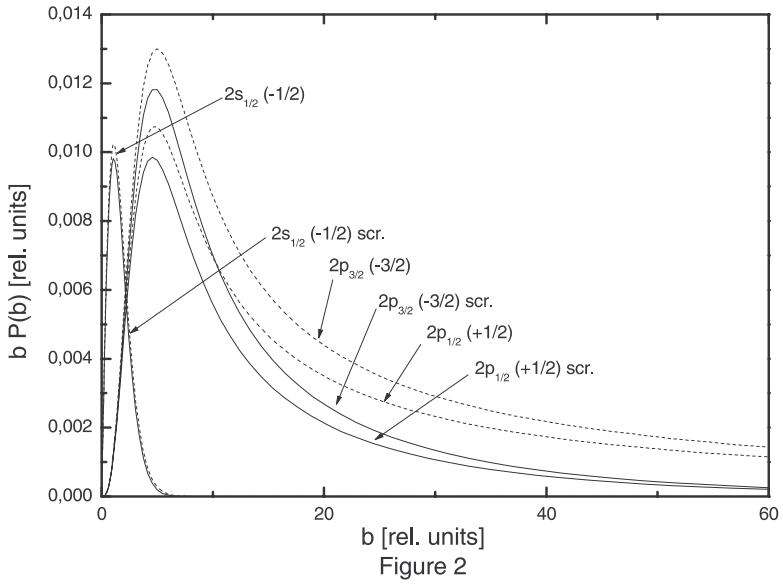

Figure 5: As in figure 4 but at a collision energy corresponding to $\gamma = 100$. From [12].

(for more discussion of the cross section saturation see 6.1.5).

5.3.2 Screening and antiscreening in ultrarelativistic collisions with very light atoms. 'Separation' of the screening and antiscreening modes in the impact parameter space

In figure 6 the weighted probabilities are depicted for the excitation of a $1s_{1/2}(m_j = -1/2)$ electron of a Bi^{82+} projectile incident on He at a collision energy corresponding to $\gamma = 10$. Similarly to the case of Bi^{82+}-Cu collisions, the full and dashed lines represent results of calculations with and without the screening, respectively. The helium atom is much lighter than copper and the orbits of helium electrons are much larger than the orbits of inner electrons in copper. Therefore, in contrast to collisions with Cu, in collisions with He the screening effect plays a very modest role at $\gamma = 10$ for all transitions shown in the figure.

The situation changes drastically for Bi^{82+}-He collisions at $\gamma = 100$ (see figure 7). In collisions with He^{2+} at $\gamma = 100$, larger impact parameters (compared to the case with $\gamma = 10$) considerably contribute to transitions to the p-states in Bi^{82+}. These impact parameters are already comparable in magnitude with the dimension of the electron orbits in the ground state of neutral He. Therefore, in collisions at such impact parameters, electrons of He are able to effectively screen their nucleus and considerably reduce the transition probabilities.

In figure 7 we compare the screening and antiscreening effects in the probabilities of the electron transitions in Bi^{82+} in collisions with He at a collision energy corresponding to $\gamma = 100$. There are some interesting features in the antiscreening probabilities, which should be mentioned. First, at small impact parameters these probabilities are much lower than the

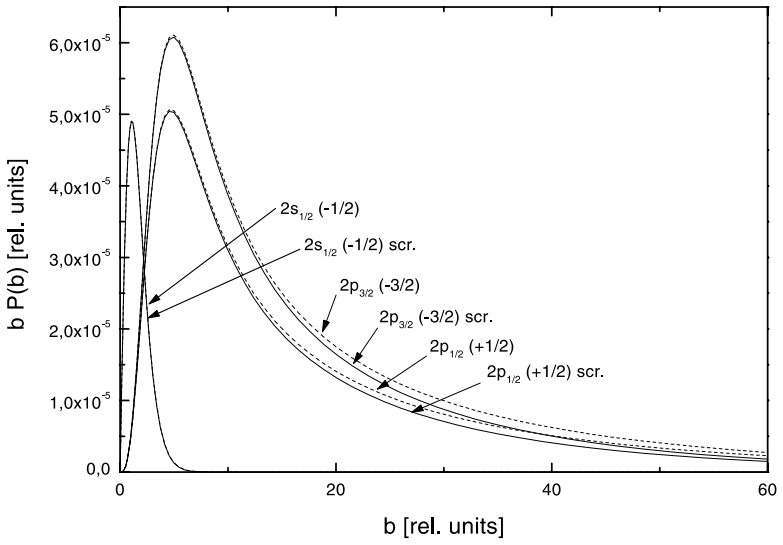

Figure 6: As in figure 4 but for collisions with He. From [12].

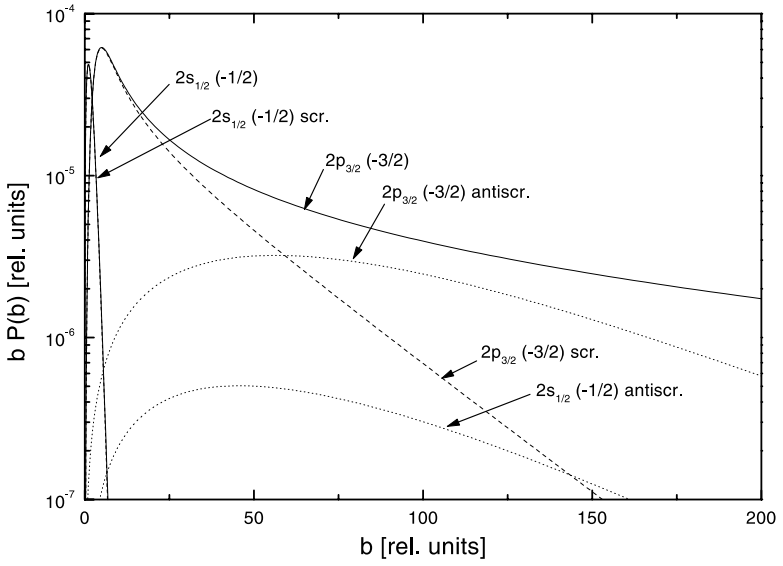

Figure 7: Weighted probabilities for projectile excitation in collisions of a Bi^{82+} projectile with He. Dashed lines: the screening mode, dotted lines: the antiscreening mode, solid lines: collisions with He^{2+}. The numbers in brackets denote the magnetic quantum numbers of the final states of the Bi^{82+} ion. From [12].

screening probabilities. Second, the antiscreening probabilities spread to much larger impact parameters. At $b \sim 100$ the antiscreening probabilities for the $1s$-$2p$ transitions are comparable in magnitude to the probabilities in collisions with the unscreened helium nucleus. And only at $b \gtrsim 300$ (which is not shown in the figure) the antiscreening probabilities become much smaller

than the probabilities in collisions with the unscreened helium nucleus. Thus, it turns out that the screening and antiscreening contributions to the excitation are to large extent separated in the b-space.

This relationship between the screening and antiscreening contributions can be understood by noting that, whereas the atomic nucleus is point-like (on a typical atomic scale), the atomic electrons spread over a large volume. Because of this reason in collisions with small impact parameters the action of the atomic electrons on the electron, which is bound in a highly charged ion, cannot effectively compete with that of the atomic nucleus. However, due to the same reason, the atomic electrons become more effective, compared to the atomic nucleus, at larger impact parameters.

Estimates show that, because of the long tails at large impact parameters, the antiscreening mode contributes considerably (about 25-30 %) to the total cross sections for the (electric) dipole allowed electron transitions in Bi^{82+} in collisions with He at $\gamma = 100$. The relative contribution of the antiscreening mode to the total cross section for the $1s$-$2s$ transition is about 15%, i.e. it is considerably smaller. The latter point can be understood by noting that the contribution of large impact parameters, where the antiscreening mode could become more important, to the $1s_{1/2}(-1/2) \rightarrow 2s_{1/2}(-1/2)$ transition is strongly suppressed compared to the case of the excitation of the dipole allowed transitions.

5.3.3 Comparison between excitation of heavy ions in collisions with neutral atoms at low and high γ

Excitation of hydrogen-like Bi ions in collisions with copper at a collision energy of 119 MeV/u corresponding to $\gamma = 1.13$ was studied in [47]- [48]. Since the excitation energies of Bi^{82+} are very big and the value of γ is quite low, only collisions with momentum transfers which are large on the atomic scale of copper can effectively excite the ion. Therefore, under these conditions the screening effect is expected to be very weak and, as our calculations show, can be neglected. In addition, the collision velocity corresponding to the energy 119 MeV/u is below the threshold for the ionization of Bi^{82+} by a free electron having the same velocity in the ion frame as the atom. Therefore, under the experimental conditions of [47]- [48] the antiscreening effect is very weak as well and the main contribution to the excitation is given by the interaction with the unscreened target nucleus. Thus, the physics of the excitation of 119 MeV/u Bi^{82+} in collisions with a neutral copper atom is basically reduced to that in collisions with a bare copper nucleus.

Probabilities for the excitation of 119 MeV/u Bi^{82+} in collisions with a point-like copper nucleus Cu^{29+} were calculated in [47]- [48] within the first order of the perturbation theory (see figure 8). As was just discussed above, at this collision energy these results can be directly applied for collisions with neutral atoms of copper. It is of interest to state briefly the main differences between the excitation of very heavy hydrogen-like ions in collisions at low γ and in ultrarelativistic collisions. First, in contrast to collisions at low γ, at high values of γ the screening effect of the atomic electrons becomes important even for very light atomic targets. Second, the antiscreening mode is always of considerable importance in ultrarelativistic col-

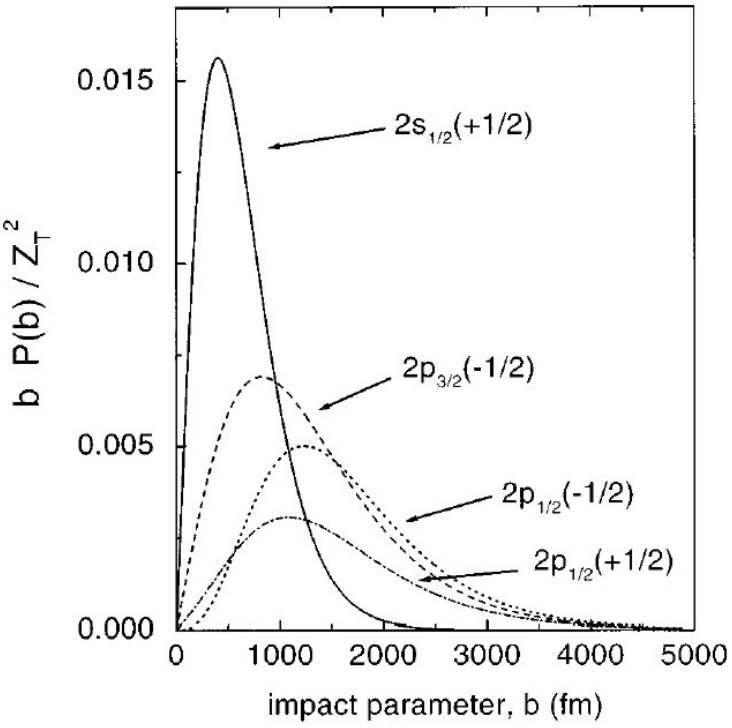

Figure 8: Weighted probabilities for excitation of a 119 MeV/u Bi^{82+} divided by Z_T where Z_T is the target atomic number. The numbers in brackets denote the magnetic quantum numbers of the final states of the Bi^{82+} ion. From [48].

lisions with few-electron targets. Third, in collisions at low γ the $1s$-$2s$ transition in Bi^{82+} were shown to dominate over the transitions to $2p$-states [48]. In ultrarelativistic collisions this situation is changed. Now the $1s$-$2p$ transitions contribute most to the excitation with the transition $1s_{1/2}(m_j = -1/2) \rightarrow 2p_{3/2}(m_j = -3/2)$ being the most probable one. Compared to collisions with $\gamma = 1.13$, in collisions with $\gamma = 10$ the maximum of the distribution $bP(b)$ for transition to $2s$ state is reduced by a factor of about 4 and the position of the maximum and the width of this distribution are practically unchanged. In contrast, the distributions $bP(b)$ for the main transitions to $2p$ states are not reduced in height but are shifted towards larger b and acquire larger widths. This behaviour of the probabilities for transitions to $2s$ and $2p$ states is connected with the increase of the collision velocity (energy). At $\gamma = 1.13$ the collision velocity is considerably less than the speed of light ($v/c = 0.46$) and the increase of this velocity leads to a decrease of all the transition probabilities at small impact parameters. However, when the collision velocity approaches the light velocity and cannot be noticeably increased further, the retardation effect is the only important effect and it increases the transition probabilities for the dipole-allowed transitions. For large enough values of γ the retardation effect, which would lead to longer and longer tails for the probabilities of the dipole-allowed transitions, is neutralized by the screening effects discussed earlier in this section.

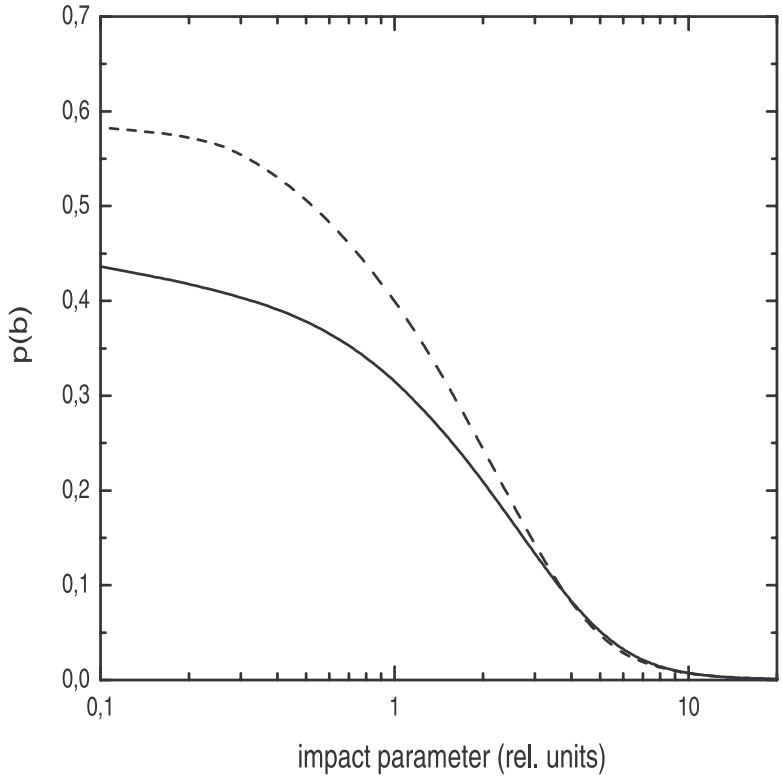

Figure 9: Probabilities for the electron loss from a 160 GeV/u Pb^{81+} projectile colliding with atomic gold. Dashed line: first order result, solid line: calculation in the eikonal approximation.

Since a $2s$-state can be effectively excited in collisions with very small impact parameters only, the influence of the retardation effect on the excitation to a $2s$-state is quite weak.

5.3.4 Higher-order effects in the loss probability in collisions at large γ

In figure 9 the probability for the electron loss from Pb^{81+} in collisions with Au is presented for a collision energy of 160 GeV/u. Two results for the loss probability are shown in this figure. One was obtained using the first order theory and considering only the screening contribution (because Au has a very large number of electrons the antiscreening contribution is of negligible importance and is not considered here). The second was calculated within the 'light-cone' approximation, discussed in section 4. The latter becomes exact at $\gamma \to \infty$ but also represents an excellent approximation at very high but finite collision energies for collisions with not too large impact parameters where the effective interaction time is much shorter than the typical electron transition time in the ion [41], [49].

The deviation from the first order prediction is clearly seen at the impact parameters of the order or smaller than the typical dimension of the electron orbit in the ground state of Pb^{81+}. These impact parameters, however, are so small that, as we will see in section 6, they contribute very little to the loss cross section and the 'exact' and first order loss cross sections

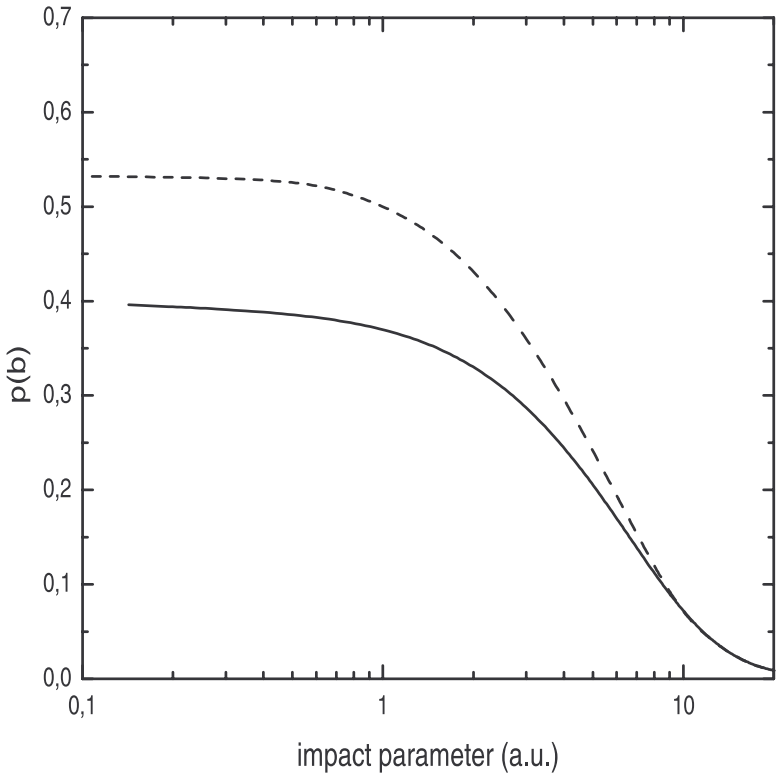

Figure 10: Same as in figure 9 but for the electron loss from Kr^{35+}.

do not differ considerably.

In figure 10 the probability for the electron loss from a much lighter ion, Kr^{35+}, in collisions with the same target and at the same energy per nucleon is presented. Compared to the electron in Pb^{81+} the electron in Kr^{35+} is much weaker bound and now the deviation from the first order prediction for the loss probability becomes more substantial and can result in a considerable difference between the first order and 'exact' loss cross sections.

By comparing figures 9 and 10 one can also draw the conclusion that the loss probability in collisions with very small impact parameter is larger for the heavier ion. Note that this relation between the probabilities is suggested by both the first order and the light-cone approximations. For ionization of a hydrogen-like ion with a charge $Z_1 > 12-15$ by a nucleus with a charge Z_2 at collision energies corresponding to $\gamma > 5$, it was found in [37] and [50] that the ionization(loss) probability at $b = 0$ is weakly dependent on γ and Z_1. Taking this into account it is plausible to assume that the values of the loss probability, observed in figure 10 for the lighter ion, are due to the larger screening effect of the atomic electrons in the latter case. Indeed, since the dimension of the electron orbit increases with decrease of the ion charge, the screening of the atomic nucleus by the atomic electrons at small impact parameters should become more effective in collisions with lighter ions.

6 Cross sections

6.1 Electron loss from hydrogen-like projectiles: total loss cross section

6.1.1 Preliminary remarks

If the final state of the target is not observed then, by using the first order perturbation theory of section 3 and applying the nonrelativistic atom approximation, the total loss cross section is given by

$$\begin{aligned}\sigma &= \frac{4}{v^2}\sum_m \int d^3\mathbf{k} \int d^2\mathbf{q}_\perp \left| Z_A\delta_{m0} - \langle u_m(\boldsymbol{\tau}) \left| \sum_{j=1}^{Z_A} \exp(i\mathbf{Q}\cdot\boldsymbol{\xi}_j) \right| u_0(\boldsymbol{\tau})\rangle \right|^2 \\ &\times \frac{\left|\left\langle \psi_{\mathbf{k}}(\mathbf{r}) \left| \left(1-\frac{v}{c}\alpha_z\right) \exp(i\mathbf{q}\cdot\mathbf{r}) \right| \psi_0(\mathbf{r})\right\rangle\right|^2}{\left(q_\perp^2 + \frac{(\varepsilon_k-\varepsilon_0+\epsilon_m-\epsilon_0)^2}{v^2\gamma^2} + 2(\gamma-1)\frac{(\varepsilon_k-\varepsilon_0)(\epsilon_m-\epsilon_0)}{v^2\gamma^2}\right)^2}. \end{aligned} \tag{128}$$

Here, $\psi_0(\mathbf{r})$ and $\psi_{\mathbf{k}}(\mathbf{r})$ are the initial and final continuum states of the electron in the projectile with energies ε_0 and ε_k, respectively, $\mathbf{r}$ is the coordinate of the electron of the projectile with respect to the projectile nucleus. The initial and final states, $\psi_0(\mathbf{r})$ and $\psi_{\mathbf{k}}(\mathbf{r})$, and the coordinate $\mathbf{r}$ are given in the rest frame of the projectile. The final continuum states are normalized according to $\langle\psi_{\mathbf{k}}|\psi_{\mathbf{k}'}\rangle = \delta^3(\mathbf{k}-\mathbf{k}')$. It is implied in (128) and throughout the section that an averaging over the initial and sum over the final spin states of the electron of the ion is performed. Further, $u_0(\boldsymbol{\tau})$ and $u_m(\boldsymbol{\tau})$ are the initial and final internal states of the atom with energies ϵ_0 and ϵ_m, the set of coordinates of the atomic electrons with respect to the target nucleus is denoted by $\boldsymbol{\tau} = \{\boldsymbol{\xi}_1, ..., \boldsymbol{\xi}_{Z_A}\}$. All atomic quantities are given in the rest frame of the atom. Z_A is the atomic number and α_z is the Dirac matrix. Further, $\mathbf{q} = (\mathbf{q}_\perp, q_{min})$, $\mathbf{Q} = (-\mathbf{q}_\perp, -Q_{min})$, where q_{min} and Q_{min} are given by Eqs.(61) and (62), respectively. In Eq.(128) the summation runs over all internal atomic states, including the atomic continuum.

The cross section (128) can be split into the screening($m = 0$) and antiscreening (all $m \neq 0$) contributions. The screening part reads

$$\sigma_s = \frac{4}{v^2}\int d^3\mathbf{k}\int d^2\mathbf{q}_\perp\, Z_{A,eff}^2(\mathbf{Q}_0)\frac{|<\psi_{\mathbf{k}}(\mathbf{r}) \mid \left(1-\frac{v}{c}\alpha_z\right)\exp(i\mathbf{q}_0\cdot\mathbf{r}) \mid \psi_0(\mathbf{r})>|^2}{\left(q_\perp^2 + \frac{(\varepsilon-\varepsilon_0)^2}{v^2\gamma^2}\right)^2}, \tag{129}$$

where $\mathbf{q}_0 = (\mathbf{q}_\perp, \frac{\varepsilon_k-\varepsilon_0}{v})$, $\mathbf{Q}_0 = (-\mathbf{q}_\perp, -\frac{\varepsilon_k-\varepsilon_0}{v\gamma})$. The effective charge of the atom in the ground state is defined by Eq.(119). Using the analytical Dirac-Hartree-Fock-Slater screening functions given for all neutral atoms by Salvat et al [33] or the Moliere parametrization of the Thomas-Fermi potential [51], we obtain

$$Z_{A,eff}(\mathbf{Q}_0) = Z_A Q_0^2 \sum_{i=1}^{3} \frac{A_i}{\kappa_i^2 + Q_0^2}, \tag{130}$$

where A_i and κ_i are given in [33] and [51]. [16]

Using the closure approximation, the antiscreening contribution to the loss cross section can be written as [68]

$$\sigma_a = \frac{4}{v^2}\int d^3\mathbf{k}\int d^2\mathbf{q}_\perp S(\mathbf{Q}_1)\frac{|< \psi_{\mathbf{k}}(\mathbf{r}) \mid (1-\frac{v}{c}\alpha_z)\exp(i\mathbf{q}_1\cdot\mathbf{r}) \mid \psi_0(\mathbf{r}) >|^2}{\left(q_\perp^2+\frac{(\varepsilon_k-\varepsilon_0+\Delta\epsilon)^2}{v^2\gamma^2}+2(\gamma-1)\frac{\varepsilon_k-\varepsilon_0+\Delta\epsilon}{v^2\gamma^2}\right)^2}. \tag{131}$$

In (131) $\mathbf{q}_1 = \left(\mathbf{q}_\perp, \frac{\varepsilon_k-\varepsilon_0}{v}+\frac{\Delta\epsilon}{v\gamma}\right)$, $\mathbf{Q}_1 = (-\mathbf{q}_\perp, -\frac{\Delta\epsilon}{v}-\frac{\varepsilon_k-\varepsilon_0}{v\gamma})$, where $\Delta\epsilon$ is the mean excitation energy for transitions of atomic electrons, and

$$S(\mathbf{Q}) = \sum_{m\neq 0}\left|\langle u_m(\boldsymbol{\tau})\left|\sum_{j=1}^{Z_A}\exp(i\mathbf{Q}\cdot\boldsymbol{\xi}_j)\right|u_0(\boldsymbol{\tau})\rangle\right|^2 \tag{132}$$

is the so called incoherent scattering function. These functions are tabulated in [52], [53] for all atomic elements. The mean energy, which is used in calculations of the stopping power and is tabulated for a variety of atoms (see e.g. [54]), has been taken as the mean excitation energy, $\Delta\epsilon$.

Eqs.(129) and (131) have been obtained using the Lorentz gauge and, therefore, can be directly applied only in calculations which employ the exact Coulomb-Dirac states ψ_0 and $\psi_{\mathbf{k}}$. In calculations with approximate states of the electron of the ion, Eqs.(129) and (131) must be replaced by the corresponding screening and antiscreening cross sections resulting from Eq.(98) or Eq.(100). In our calculations with the semirelativistic approximations for the ion states, discussed below, we used the loss cross sections obtained from Eq.(98), i.e. the loss cross section written in the Coulomb gauge. The screening and antiscreening parts of this cross section are given by

$$\begin{aligned}\sigma_s &= \frac{4}{v^2}\int d^3\mathbf{k}\int d^2\mathbf{q}_\perp Z_{A,eff}^2(\mathbf{Q}_0)\\ &\times\left|\frac{\langle\psi_{\mathbf{k}}(\mathbf{r})\,|\exp(i\mathbf{q}_0\cdot\mathbf{r})|\,\psi_0(\mathbf{r})\rangle}{\mathbf{q}_0^2}-\frac{1}{c}\frac{\langle\psi_{\mathbf{k}}(\mathbf{r})\,|\boldsymbol{\lambda}_0\cdot\boldsymbol{\alpha}\,\exp(i\mathbf{q}_0\cdot\mathbf{r})|\,\psi_0(\mathbf{r})\rangle}{\mathbf{q}_0^2-\frac{\omega_{k0}^2}{c^2}}\right|^2\end{aligned} \tag{133}$$

and

$$\begin{aligned}\sigma_a &= \frac{4}{v^2}\int d^3\mathbf{k}\int d^2\mathbf{q}_\perp S(\mathbf{Q}_1)\\ &\times\left|\frac{\langle\psi_{\mathbf{k}}(\mathbf{r})\,|\exp(i\mathbf{q}_1\cdot\mathbf{r})|\,\psi_0(\mathbf{r})\rangle}{\mathbf{q}_1^2}-\frac{1}{c}\frac{\langle\psi_{\mathbf{k}}(\mathbf{r})\,|\boldsymbol{\lambda}_1\cdot\boldsymbol{\alpha}\,\exp(i\mathbf{q}_1\cdot\mathbf{r})|\,\psi_0(\mathbf{r})\rangle}{\mathbf{q}_1^2-\frac{\omega_{k0}^2}{c^2}}\right|^2,\end{aligned} \tag{134}$$

respectively. In Eqs.(133) and (134) $\boldsymbol{\lambda}_0 = \mathbf{v}-\frac{\omega_{k0}}{q_0^2}\mathbf{q}_0$, $\boldsymbol{\lambda}_1 = \mathbf{v}-\frac{\omega_{k0}}{q_1^2}\mathbf{q}_1$ and $\omega_{k0} = \varepsilon_k-\varepsilon_0$.

In the screening mode the 'polarization' vector $\boldsymbol{\lambda}_0$ is strictly transverse since one has $\boldsymbol{\lambda}_0\cdot\mathbf{q}_0 = 0$. If we choose the quantization axis for the electron of the ion to be directed along $\mathbf{q}_0$ then,

[16] In our calculations reported in this section we used results of [33].

as was discussed in section 3.9, the terms in the integrand of (133) proportional to $1/q_0^2$ and $1/(q_0^2 - \omega_{k0}^2/c^2)$ can be squared separately resulting in the screening cross section written as the sum of the longitudinal and transverse contributions.

In the antiscreening mode one has $\boldsymbol{\lambda}_1 \cdot \mathbf{q}_1 = \Delta\epsilon/\gamma$ and the vector $\boldsymbol{\lambda}_1$ is not strictly transverse. Its deviation from the transverse direction is given by the angle $\vartheta \sim \Delta\epsilon/(\gamma\omega_{k0})$. In the process of the electron loss from highly charged ions moving with relativistic velocities this angle will be very small. Therefore, one can assume that $\boldsymbol{\lambda}_1 \cdot \mathbf{q}_1 \approx 0$ and, similarly to the case with the screening mode, present the antiscreening cross section as the sum of the longitudinal and transverse parts.

6.1.2 Loss in collisions at low γ

There exists a substantial amount of experimental data for the total cross sections for the electron loss from very heavy hydrogen-like ions, like e.g. Au^{78+} and U^{91+}, in collisions with gas and solid state targets at collision energies $\sim 0.1 - 1$ GeV/u. [17] At these relatively low collision energies the process of the electron loss from such very heavy ions is characterized by very large momentum transfers to the target atom in the target frame. This means that the collisional impact parameters of importance are effectively so small that, as test calculations show, the screening effect for these energies is rather weak even for collisions with very heavy atoms. For example, for 1 GeV/u Au^{78+} on Au^0 collisions the screening effect reduces the loss cross section by less than 10 % and becomes even weaker when the collision energy decreases. Therefore, in the elastic mode the action of the electrons of the target can be neglected and the physics of the elastic mode of the loss process in collisions with neutral atoms is basically the same as in collisions with bare atomic nuclei and will not be discussed here.

Concerning the antiscreening mode of these collisions one should note that the lower energy part of the interval $0.1 - 1$ GeV/u covers the range where the energy of a free electron, having the same velocity in the ion frame as the incident atom, is close to the binding energy of the electron in a very heavy ion. In this energy range the treatment of the antiscreening mode is most difficult. We are not aware about any rigorous calculations for the antiscreening mode for these collision energies.

For collision energies of 0.082, 0.14 and 0.2 GeV/u there are experimental data for the electron loss from a hydrogen-like Xe^{53+} in collisions with several solid targets ranging from Be to Au. Compared to the case with the tightly bound electron in very heavy hydrogen-like ions, briefly discussed above, the binding of the electron in Xe^{53+} is much weaker. Therefore, as first-order calculations suggest, the shielding effect of the atomic electrons may become rather substantial for the electron loss from Xe^{53+} by collisions with very heavy atoms (see figure 11).

There seems to be yet another effect which is due to contributions of the higher-order terms in the ion-atom interaction. According to our estimates, at these collision energies this effect

[17] The reader interested in experimental data on loss cross sections from very heavy hydrogen-like ions at collision energies below 1 GeV/u can be referred to [55]- [58].

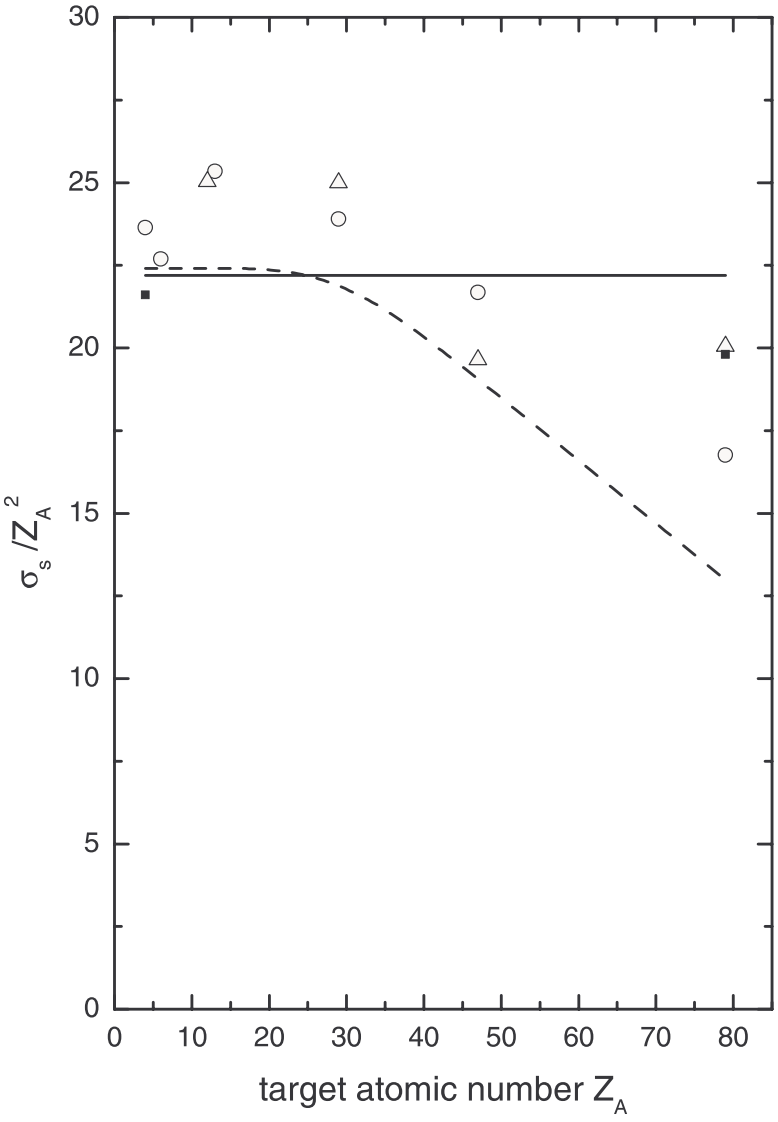

Figure 11: Screening part of the cross section for the electron loss from 0.2 GeV/u Xe^{53+} divided by Z_A^2. Open circles and triangles: experimental data from [55] (in addition to the statistical errors these results have possible systematic errors up to 20% [4]). Solid line: results of the first order calculation for the loss by the bare atomic nuclei. Dash curve: CDW-EIS results. Solid squares: results of the first order calculation for the loss by the screened nuclei of C and Au.

may reduce the calculated first order cross section much stronger than the shielding of the atomic nucleus by the atomic electrons (see figure 11). A rough estimate for this effect can be obtained as follows. According to the first order calculations the transverse contribution to the total electron loss from Xe^{53+} at these collision energies does not exceed 2%. Therefore, the instantaneous (nonrelativistic) Coulomb interaction between the ion and atom can be taken as the only interaction responsible for the electron loss from the ion. Further, in our first-order cal-

Atom	Z_2	Experiment	[29]	[30]	I	II
C	6	0.31	0.31	0.27	0.29	0.25
Al	13	1.18	1.28	1.15	1.21	1.0
Cu	29	5.26	5.8	5.37	5.59	4.8
Ag	47	16.2	14.4	13.7	13.8	11.9
Au	79	38.2	38.8	38	36.6	31.7

Table 1: Experimental and theoretical cross sections (in kb) for the electron loss from 10.8 GeV/u Au^{78+} penetrating various solid targets. The ion is initially in its ground state.

culations we used two options to describe the electron in Xe^{53+}, the semirelativistic Darwin and the fully nonrelativistic Schrödinger wavefunctions, and found that the corresponding first-order results are quite close. Therefore, disregarding for the moment the effect of the atomic electrons, the influence of the higher-order terms in the interaction between the electron of the ion and the atom can be estimated within the nonrelativistic Continuum-Distorted-Wave-Eikonal-Initial-State (CDW-EIS) model where the electron of the ion is treated fully nonrelativistically and its interaction with the atomic nucleus is the nonrelativistic Coulomb interaction. Results of our calculations using the CDW-EIS model are shown in figure 11. For the loss by collisions with Au they predict a strong reduction of the cross section by $\simeq 70\%$ compared to that of our first order results where the screening effect was ignored. This suggests that for relatively low collision energies the effect of the higher-order terms in the interaction between the electron of the ion and the nucleus of a very heavy atom can be much more important for the loss process than the screening effect of the atomic electrons.

6.1.3 Loss in collisions at moderately high γ

Table 1 shows a comparison between the experimental data of Claytor et al [59] and different theoretical results. In the experiment [59] the loss cross sections for Au^{78+} ions were measured at a collision energy of 10.8 GeV/u corresponding to $\gamma = 12.6$.

The theoretical results include those of Anholt and Becker [29], of Sørensen [30] and results obtained by using Eqs.(128)-(134). The latter results are given in columns denoted by I and II.

Column I presents results of calculations where the semi-relativistic Darwin wavefunctions were used to approximate the initial and final electron state in Au^{78+}.

Column II displays results of the first order calculations where the relativistic (Coulomb-Dirac) wavefunctions for the ground and continuum states of the electron in Au^{78+} were used. These loss cross sections were obtained by taking into account the continuum states with angular momentum κ up to ± 7 and energies up to $\varepsilon_k = 5mc^2$. The inspection of cross sections differential in energy and the inclusion of states with higher κ showed that these regions of the continuum energies and the angular momenta give practically the total contribution to the loss cross sections. The results of the column II are noticeably lower than those in the first column. This difference shows that a proper description of the relativistic effects in the motion

of the electron in the initial and final states of Au^{78+} may considerably reduce the calculated loss cross section.

Since both the results of Anholt and Becker [29] and those given in the column I were obtained by using similar semi-relativistic descriptions for the initial and final electron states in Au^{78+}, it is instructive to compare them. According to the table the difference between these results is relatively modest for all targets considered. This means that at not very large values of the collision Lorentz factor γ the fitting formula for the total loss cross section $\sigma_{loss} \sim A+B\ln\gamma$, which was suggested by Anholt and Becker, may still be rather accurate (see also figure 2).

As suggested by Table 1 all the theoretical results seem to be in relatively good agreement with the experimental data, except those of Column II which are considerably lower than all other theoretical data. At the first glance it is quite surprising that the most rigorous calculation yields the biggest deviation from the experiment. One should take into account, however, that all the reported calculations have been done for the projectile colliding with atoms whereas in the experiment the projectile was stripped in solids. As it was found in [9] measured electron loss cross sections in collisions with solids may be considerably larger than those in collisions with gas targets. Therefore, a definite answer to the question, which calculation gives a better agreement with reality, could be made only after comparing with experimental data obtained for gas targets.

6.1.4 Loss in collisions at high γ

Let us now turn to the case studied experimentally in [8] and [9], where a much higher collision energy was considered. In these experiments the loss cross sections for Pb^{81+} ions were measured in collisions with solid and gas targets at a collision energy of $\simeq 160$ GeV/u where the corresponding collisional Lorentz factor is very high.

Figure 12 shows a comparison between experimental data of [8], [9] and results of different calculations for the loss cross sections for Pb^{81+} penetrating various solid and gas targets at a collision energy of 160 GeV/u. Results of Anholt and Becker are depicted by open squares. First order results for the total loss cross section obtained with Eqs.(128)-(131) are shown by small solid circles and triangles. [18] Corresponding connecting lines are given just to guide the eye.

Solid circles present results of the first order calculations where the semi-relativistic Darwin wavefunctions were used to describe the motion of the electron in the ground and continuum states of Pb^{81+}. Solid triangles show results of the first-order calculations where the electron motion in the ground and continuum states of Pb^{81+} was described by the Coulomb-Dirac wavefunctions. Comparing these two calculations we again observe that the results obtained with the fully relativistic description of the electron in Pb^{81+} yields noticeably lower loss cross sections. We also note that the results of the fully relativistic description are roughly by a factor of 2 lower than those of [29].

[18] Results of Sørensen [30] turned out to be rather close to that set of our results, which was obtained by using the semi-relativistic states for describing the electron motion in Pb^{81+}, and are not shown in the figure.

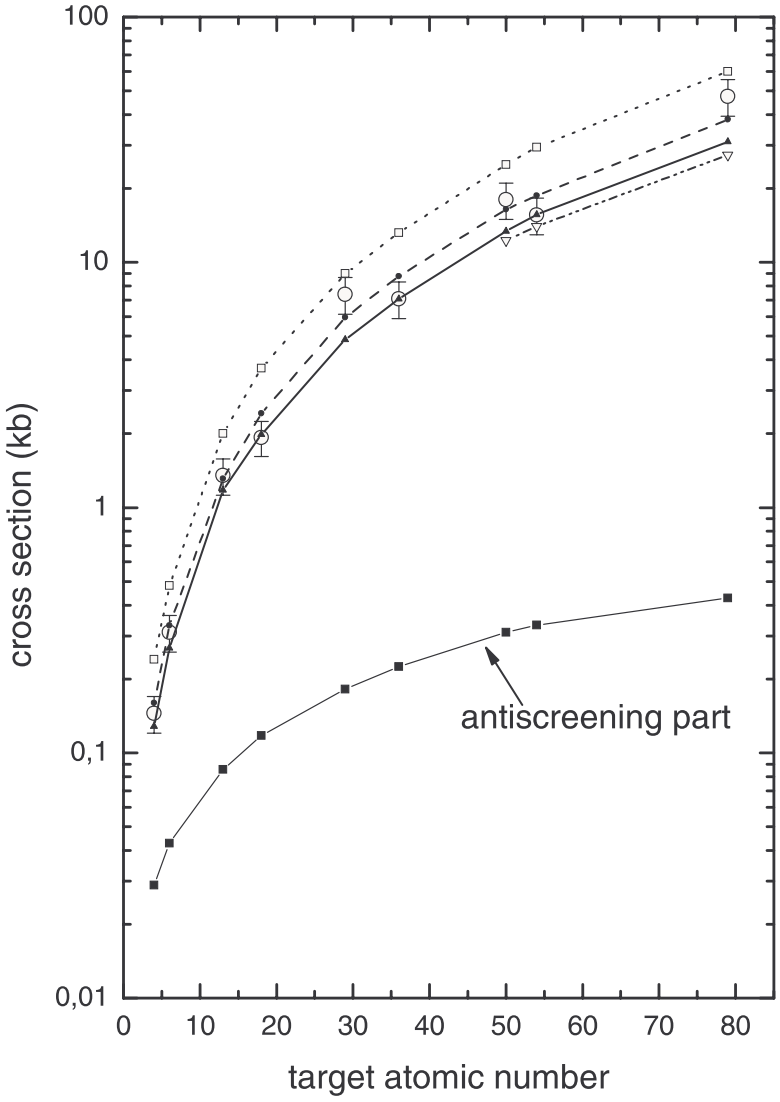

Figure 12: Cross section for the electron loss from 160 GeV/u $Pb^{81+}(1s)$ in collisions with neutral atoms of Be, C, Al, Ar, Cu, Kr, Sn, Xe and Au. Open circles with error bars: experimental data from [8] (solid targets) and [9] (gas targets). Open squares connected by dot lines: results of [29]. Solid circles connected by dash lines and solid triangles connected by solid lines: results of the first order calculations where the semirelativistic and relativistic wavefunctions, respectively, were used to describe the electron in Pb^{81+}. Open triangles: results of the application of the 'nonperturbative' approach, discussed in section 4. Lines connecting the theory points are intended just to guide the eye. For more explanations see the text.

Most of the measured data shown in figure 12 are from the experiment [8] where the loss cross sections were obtained for collisions with solids. There are just three points (Ar, Kr, Xe) in the figure which represent results from the experiment of [9] where gas targets were used. However, strictly speaking, only the latter results can be directly compared with calculations

since all the calculations were performed for collisions with atomic targets.

An important feature of the loss cross sections measured in gases in [9] is that their values were found to be substantially lower (by 30-50 %) than those which one could obtain by interpolating the loss cross sections measured in solids [8]. Since all calculations were performed for the loss in collisions with atoms it would be instructive to compare them with a larger set of experimental results for atomic (gas) targets. At the moment this is not possible because no new experimental results for gas targets have been reported since the article [9] was published. However, one can still get some ideas about 'real' values of the loss cross sections for a large number of atomic targets by 'correcting' data measured in solids to values which are consistent with experimental data obtained for gas targets. Since gas targets used in [9] have atomic numbers $18 \leq Z_A \leq 54$ and the loss cross section, as a function of the target atomic number, behaves rather smoothly, such a 'scaling' procedure is expected to be rather accurate ($\pm 10\%$) for, say, $13-15 \lesssim Z_A \lesssim 65-75$. With such a 'correction' we obtain results shown in figure 13.

The antiscreening contribution to the total loss cross section is shown separately in figure 12. This contribution was calculated using the Coulomb-Dirac wavefunctions for the ground and continuum states of the electron in Pb^{81+} and it corresponds to the total loss cross section depicted by the solid triangles. Comparing the results for the total loss cross section and its antiscreening part one may conclude that the antiscreening contribution represents a small correction to the screening contribution and that, as of course expected, this correction is relatively more important for collisions with few-electron atoms like Be and C. For collisions with heavy targets, like Sn, Xe and Au, the antiscreening contribution is very small ($\lesssim 2\%$).

6.1.5 Saturation of loss cross sections at asymptotically high γ

In figures 14 and 15 the cross sections for the electron loss from $1-1000$ GeV/u Au^{78+} and $1-100$ Fe^{25+} ions in collisions with neutral atoms are shown as functions of the collision energy.

For a comparison we also display the loss cross section in collisions with bare nuclei. In the latter case the cross sections show a continuous logarithmic increase with energy. Such an increase of ionization cross sections in ultrarelativistic collisions is well known and is due to the Lorentz contraction of the electromagnetic field generated by a bare nucleus moving at velocities approaching the speed of light. Because of this contraction the effective time for a collision with a point-like charge is not given by $T(b) \sim b/v$ as in the nonrelativistic case but is estimated according to $T(b) \sim b/(\gamma v)$ (b is the impact parameter) and this time continues to decrease with increase of the collision energy even at $v \approx c$ where the collision velocity cannot be noticeably increased further. The external time-dependent field of the incident nucleus is effective in inducing electron transitions in the ion only provided this field contains high enough frequency components. Therefore, the electron can make a transition with a noticeable probability only if the typical transition time $\tau \sim \omega_{n0}^{-1}$, where $\omega_{n0} = \varepsilon_n - \varepsilon_0$ is the energy transfer to the electron, does not exceed substantially the effective collision time T(b). The latter condition means that

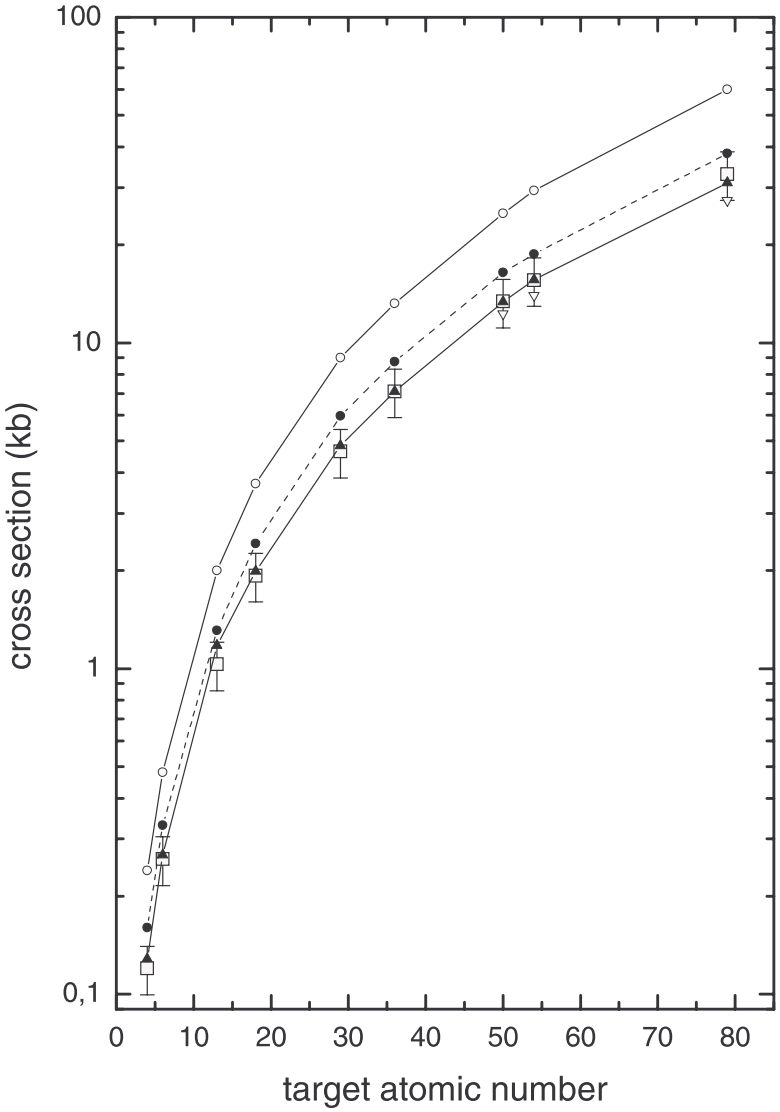

Figure 13: Same as in figure 12 but the experimental loss cross sections measured in solid state targets [8] have been shifted to values obtained by interpolating loss cross sections measured in gases [9].

the impact parameter range contributing most to the loss is given by $b \lesssim \gamma v/\omega_{eff}$, where ω_{eff} is of the order of the binding energy of the electron in the ion. This range of impact parameters gives rise to the dependence $\sigma_{loss} \sim \ln \gamma$ (see e.g. [45]- [46], [60]- [61], [65]).

Compared to the electron loss from ions colliding with bare nuclei, the distinct feature of the loss process in collisions with a neutral atom is the saturation of the loss cross section at high enough collision energies where this cross section becomes practically independent of the collisional Lorentz factor γ. One can denote this domain of collision energies as the region of asymptotically high γ. The saturation of the loss cross section at asymptotically high γ is the

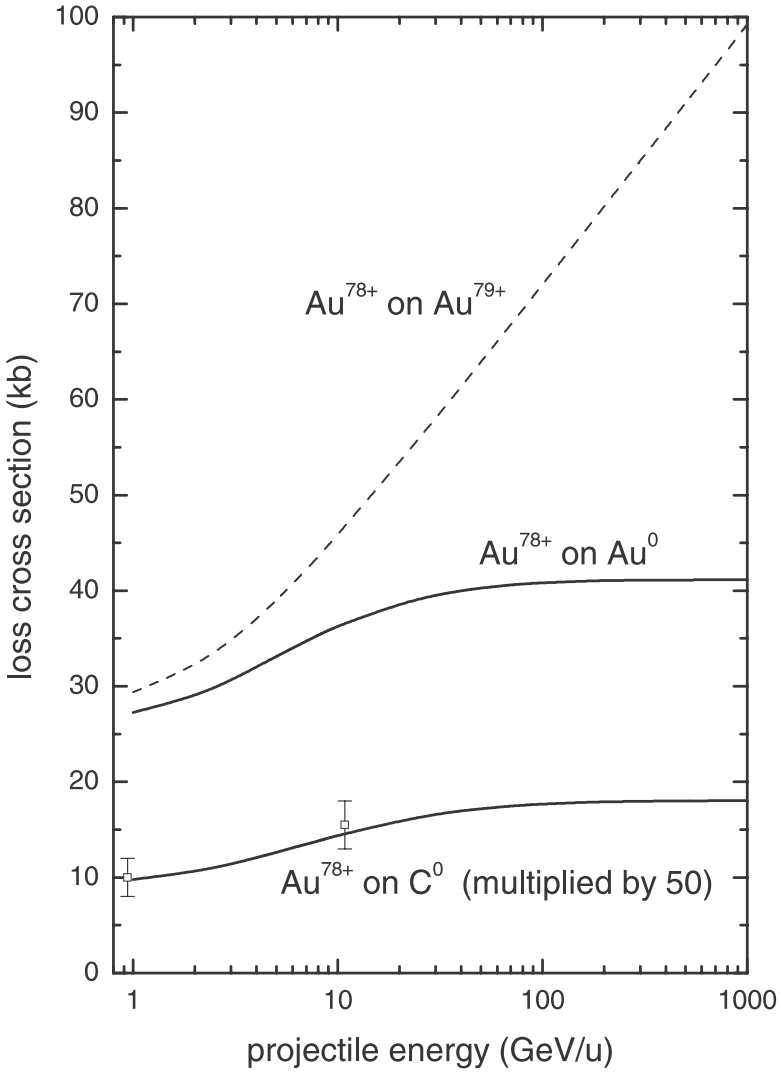

Figure 14: Cross section for the electron loss from Au^{78+} shown as a function of the incident energy (per nucleon) for collisions with neutral atoms of carbon and gold. The experimental points for lower and higher energies are from [56] and [59], respectively. For a comparison the loss cross section by a bare gold nucleus, Au^{79+}, is also displayed. All results shown in this figure were obtained by using the Darwin approximation for the electron states in Au^{78+}.

clear signature of the screening effect of the atomic electrons which in essence 'puts out of play' collisions with impact parameters larger than the size of a neutral atom.

Roughly speaking, the screening effect becomes very substantial only in such collisions where the impact parameters of importance are not too small and the electron of the ion, when penetrating the atom, 'sees' that a considerable part of the atomic electron cloud is situated between this electron and the atomic nucleus. In the electron loss from different ions, colliding with the same atom and at the same value of γ, relatively smaller impact parameters would

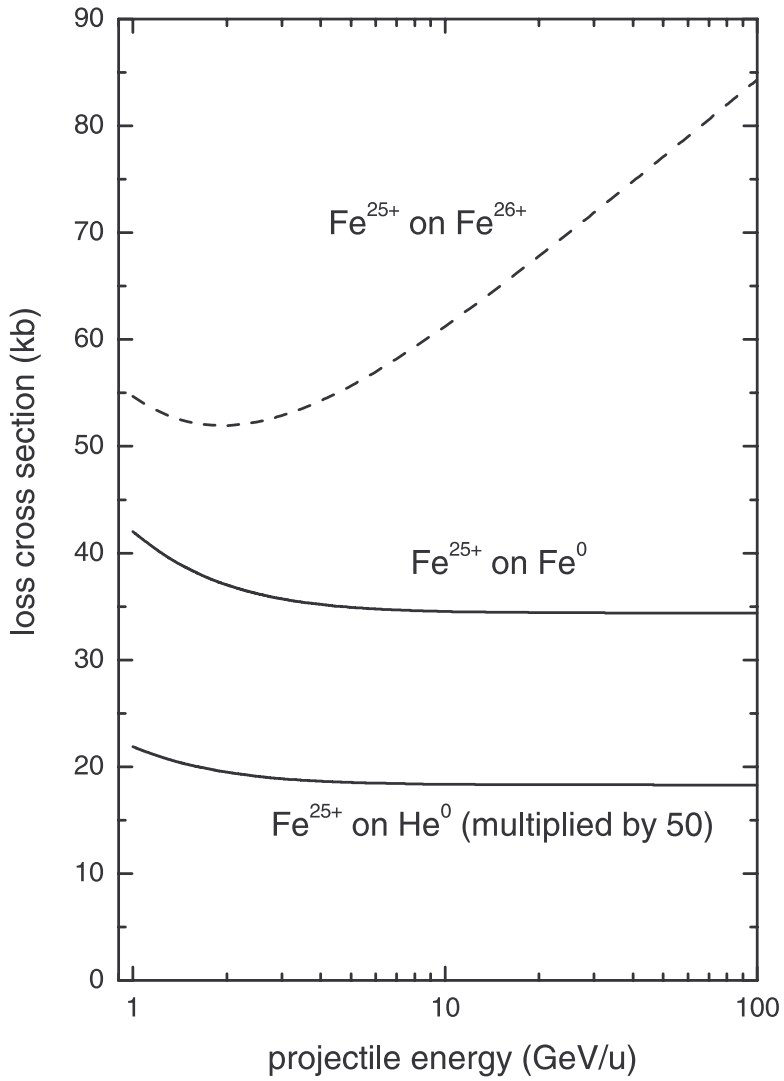

Figure 15: Cross section for the electron loss from Fe^{25+} shown as a function of the incident energy (per nucleon) for collisions with neutral atoms of helium and iron. For a comparison the loss cross section by a bare iron nucleus, Fe^{26+}, is also displayed. All results shown were obtained by using the Darwin approximation for the electron states in Fe^{25+}.

contribute to the loss from a heavier ion. Therefore, it is obvious that the screening effect in such collisions is smaller for heavier ions. On the other hand, if the electron loss from an ion occurs in collisions with different atoms but at the same collision energy per nucleon, then the screening effect is strongest for collisions with the heaviest atom. All that can be observed in figures 14 and 15 where: i) different ion-atom pairs enter the saturation region at different values of γ, ii) for the loss from the lighter ion, Fe^{25+}, this region begins at smaller energies and iii) for the loss from the same ion the saturation is reached first for collisions with a heavier atom.

Figure 14 also suggests that for the collision energies under consideration the cross section for the loss from very heavy ions increases with increase of the collision energy before this cross section enters the saturation region. In contrast, for the loss from much lighter ions like Fe^{25+} the loss cross section decreases before reaching a constant value.

6.1.6 On the longitudinal and transverse contributions to the total loss cross section. Is the incoherent addition of these contributions incorrect?

An attempt to find a reason for the substantial disagreement between the experimental data of [8] and theoretical predictions of [29] was made in [47], [8]. It was suggested there that the disagreement might be attributed to the fact that Anholt and Becker [29], following an earlier paper of Anholt [28], added incoherently the longitudinal and transverse contributions to the loss cross section. Since this, quite surprising, point of view has been insistently repeated in the literature, it is worth while to briefly comment on it here.

As was mentioned in section 5.3.3 , in [47] and [48] semiclassical first order calculations were performed for the excitation of hydrogen-like Bi ions by a point-like charged particle. Considering the collision in the reference frame of the Bi ion and using the *Lorentz* gauge to treat the field of the incident point-like particle the authors of [47]- [48] found a substantial interference between the contributions to the excitation of the Bi ion which arises due to the interaction of the electron of the ion with the scalar and vector potentials of the incident particle. Because of this interference the above contributions must be added in the transition amplitude, i.e. coherently.

Having in mind such an interference effect it has been suggested in a number of publications (see [47]- [48], [62]- [63]) that the incoherent adding of the longitudinal and transverse contributions to the ionization cross section is incorrect. However, the longitudinal and transverse parts of the ionization transition amplitude are the contributions due to the scalar and vector potentials taken in the *Coulomb* gauge [19] and not in the *Lorentz* one! Since the 4-potential is gauge dependent, it is not a surprise that the longitudinal contribution is not equivalent to the contribution arising due to the scalar potential taken in the *Lorentz* gauge as well as the transverse contribution differs from that due to the vector potential taken in the *Lorentz* gauge.

In sections 3.7 and 3.9 we discussed in detail the correspondence between the descriptions of relativistic collisions which employ the *Lorentz* and *Coulomb* gauges. In particular, we stressed that in calculations of the total ionization/loss cross section, where the quantization axis can be chosen along the vector of the momentum transfer, the contributions from the interaction with the scalar and vector potentials, taken in the *Coulomb* gauge, to the ionization/loss transition amplitudes can be squared separately because the absorption of the longitudinal and transverse virtual photons leads to electron transitions into different final states and no interference occurs.

Thus, one can conclude that the criticism, undertaken in papers [47]- [48], [62]- [63] with respect to the incoherent addition of the longitudinal and transverse contributions to the total

[19] For the process of atom excitation/ionization by collisions with unstructured point-like charges the longitudinal and transverse parts were defined many years ago [64], [65], [54] and later on used by Anholt [28].

ionization/loss cross section [20], has no grounds. In our calculations with the Darwin approximation for the electron states in the ion, reported in this section, we did add incoherently the longitudinal and transverse contributions and the difference between these calculations and those of [29] should be attributed to the fact that the model of [29] failed to properly describe the action of the target electrons in ultrarelativistic collisions.

In fact, by calculating separately the longitudinal and transverse contributions to cross sections, some additional information of interest on the process of projectile-electron loss in collisions with neutral atoms can be obtained. For example, for the electron loss from 200 GeV/u Pb^{81+} in collisions with Au^0 the exchange of the transverse photon accounts for more than 60% of the total loss. However, for the electron loss from 200 GeV/u S^{15+} and 200 GeV/u O^{7+} ions the transverse part contributes only about 4% and less than 1%, respectively, to the total loss cross section. In collisions of light hydrogen-like ions with neutral atoms the exchange of the transverse virtual photon always represents the minor mechanism for the total electron loss from the ions. For collisions at low γ ($\gamma \sim 1$) the exchange of the longitudinal photon dominates in the total loss because *in the ion frame* the motion of the electron of the ion is nonrelativistic in both the initial and final ion states [21] and γ is small compared to v/v_e where $v_e \sim Z_I$ is a 'typical velocity' of the electron of the ion in the process. For collisions at larger γ the relative contribution to the loss cross section due to the exchange of the transverse photon could strongly increase in collisions with charged particles but in collisions with neutral atoms the coupling of the electron of a light ion with the incident atom via the transverse photon, emitted by the atom, is essentially cut off by the screening effect of the atomic electrons. This, in particular, means that, in order to estimate the total electron loss from light ions in collisions with neutral atoms at any collision energy, one can take the interaction with the instantaneous (unretarded) scalar potential of the incident atom as the full interaction acting on the electron of the ion. Of course, this is in sharp contrast to what is known for the loss (ionization) in collisions with relativistic charged particles. In the latter collisions the exchange of the transverse virtual photon gives the very important contribution, which is asymptotically dominant at $\gamma \to \infty$ for the loss from both heavy and light ions.

6.1.7 Higher-order effects in the loss cross sections at asymptotically large γ

The open triangles in figures 12 and 13 display results of the method considered in section 4 which allows one to take into account higher-order contributions in the projectile electron-target interaction and becomes 'exact' when $\gamma \to \infty$. We will term these results as nonperturbative. Since the higher-order contributions in collisions with velocities closely approaching the speed of light are expected to be important only for collisions with very heavy atoms, the nonperturbative results are shown only for the heaviest targets, used in experiments [8] and [9]. The antiscreening contribution was neglected in this calculation since, as was already mentioned, it

[20] In some of the above references this addition is called 'Anholt's model' although Anholt just followed Fano who was the first to realize that these contributions might be squared separately [65].

[21] Formally the electron in the final state could acquire a relativistic velocity with respect to the ion nucleus. Such a situation, however, is rather unlikely and contributes negligibly to the total loss cross section.

is very small for these targets. For details about how the nonperturbative calculation can be performed we refer to [41].

As it follows from these figures, the difference between the results of the first order and 'exact' calculations for the loss cross section is rather small, even for collisions with Au. This is consistent with what was discussed in subsection 5.3.4 where the impact parameter dependence for the loss probability P(b) was considered. Indeed, it was noted there that only for very small impact parameters b, which do not contribute appreciably to the loss, there is a considerable difference between the first order and the nonperturbative calculations for the loss probability P(b) for such a heavy ion like P^{81+} (see figure 9). Such a small difference between the 'exact' and first order loss cross sections should be attributed to both the very high collision energy and the very tight binding of the electron in Pb^{81+}. There are some indications (see e.g. [66] and also figure 11 of the present article) that in relativistic collisions with heavy atoms at much lower energies ($\gamma \sim 1-2$) the difference between the experimental data and first order results for the electron loss cross sections may reach $50-100\%$ even for very heavy projectile-ions. In addition, even at extremely high collision energies there still remains a substantial deviation between the first order and eikonal results for the total cross section for the loss from relatively light projectiles, where the electron is not so tightly bound, colliding with heavy targets. For example, for the electron loss from S^{15+} colliding with Au at asymptotically high collision energies $\gamma \to \infty$ one finds that the first-order loss cross section still overestimates the 'exact' one by about 15%.

Thus, even at asymptotically high collision energies the higher-order effects can still be rather important even for the total loss cross section provided a relatively light projectile collides with a heavy neutral target. This is in sharp contrast to the loss (ionization) in ultrarelativistic collisions with charged particles where, due to the crucial importance of the contribution from very large impact parameters, any difference with first order predictions for the total cross section tends to disappear when $\gamma \to \infty$, even for ionization of hydrogen by U^{92+} [45].

6.2 Electron loss from hydrogen-like projectiles: differential loss cross sections

In general, much more information about the projectile-electron loss process can be obtained by considering differential loss cross sections.

In this subsection we shall discuss spectra of electrons emitted from ultrarelativistic projectiles colliding with neutral atoms. These spectra will be considered for both the laboratory and projectile reference frames. Such explorations may reveal some interesting features in the projectile-electron loss process which are not evident when one deals exclusively with the total loss cross sections.

Results of the first measurement of the spectrum of electrons emitted by projectiles in collisions of $\simeq$ 160 GeV/u Pb^{81+} ions with solid Al target were reported in [10]. Having in mind this experiment, we restrict here our attention to highly charged hydrogen-like ions colliding with Al atoms. The first order perturbation theory for treating the loss process in

such collisions is justified and will be used below.

In order to obtain the differential cross section in the laboratory frame K_A it is convenient to calculate first the differential cross section in the rest frame K_I of the projectile ion and then, by using the known relation (see e.g. [67], [4])

$$\frac{d^2\sigma'(\varepsilon',\Omega')}{d\varepsilon' d\Omega'} = \frac{k'}{k}\frac{d^2\sigma(\varepsilon,\Omega)}{d\varepsilon d\Omega}, \tag{135}$$

to transform the results into the laboratory frame. Here ε, k, $d\Omega$ and $\frac{d^2\sigma}{d\varepsilon d\Omega}$ are the total energy of the electron, the absolute value of the electron momentum, the solid electron emission angle and the cross section, respectively. Primed and unprimed quantities in (135) refer to the laboratory and projectile frames, respectively.

If a final state of the target, which rests in the laboratory frame, is not observed, the double differential loss cross section in the rest frame of the projectile is given within the nonrelativistic atom approximation by

$$\begin{aligned}\frac{d^2\sigma}{d\varepsilon d\Omega} &= \frac{4}{v^2}\sum_m \int d^2\mathbf{q}_\perp \mid Z_A - < u_m(\boldsymbol{\tau}) \mid \sum_{j=1}^{Z_A} \exp(i\mathbf{Q}\cdot\boldsymbol{\xi}_j) \mid u_0(\boldsymbol{\tau}) > |^2 \\ &\times \frac{|< \psi_{\mathbf{k}}(\mathbf{r}) \mid \left(1 - \frac{v}{c}\alpha_z\right) \exp(i\mathbf{q}\cdot\mathbf{r}) \mid \psi_0(\mathbf{r}) > |^2}{\left(q_\perp^2 + \frac{(\varepsilon_k - \varepsilon_0 + \epsilon_m - \epsilon_0)^2}{v^2\gamma^2} + 2(\gamma-1)\frac{(\varepsilon_k - \varepsilon_0)(\epsilon_m - \epsilon_0)}{v^2\gamma^2}\right)^2}.\end{aligned} \tag{136}$$

As in the case with the total loss cross section, the differential cross section (136) can be split into the screening and antiscreening contributions. The latter ones are evaluated using exactly the same approximations as in the calculation of the total loss cross section.

Below we shall discuss loss spectra for electrons emitted in collisions of 160 GeV/u Pb^{81+} and S^{15+} ions with Al. These spectra were calculated in [68]. In [68] the relativistic Coulomb-Dirac wavefunctions were used for the ground ψ_0 and continuum $\psi_{\mathbf{k}}$ states of the electron in the Pb^{81+} ion and the cross sections for the electron loss were obtained by taking into account the continuum states with angular momentum κ up to ± 7 and energies up to $\epsilon_{max} = 5mc^2$. The electron motion in the initial and final states of S^{15+} was treated by using the semirelativistic Darwin wavefunctions.

Figure 16a shows the cross section differential in energy in the laboratory frame for the electron loss from the Pb^{81+} projectiles colliding with Al atoms. The following main features of the calculated spectrum can be noted. First, the electron energy distribution has a maximum at an electron energy $\varepsilon'_{max} = mc^2\gamma$ which corresponds to the emitted electron moving with a velocity equal to the velocity of the projectile. Second, this distribution is asymmetric with the majority of the lost electrons having energies lower than ε'_{max}. Third, the width of the distribution is much larger (about a factor $2.5-3$) than it was measured experimentally in [10] for 33 TeV Pb^{81+} projectiles penetrating aluminium foils (figure 1b). Fourth, this distribution also differs rather strongly from that given in [10] (see figure 1b) where, as the authors of [10] state, a $Pb^{81+}(1s)$ Compton profile was mapped into the laboratory frame assuming that the angular emission distribution in the projectile frame is of a dipole form.

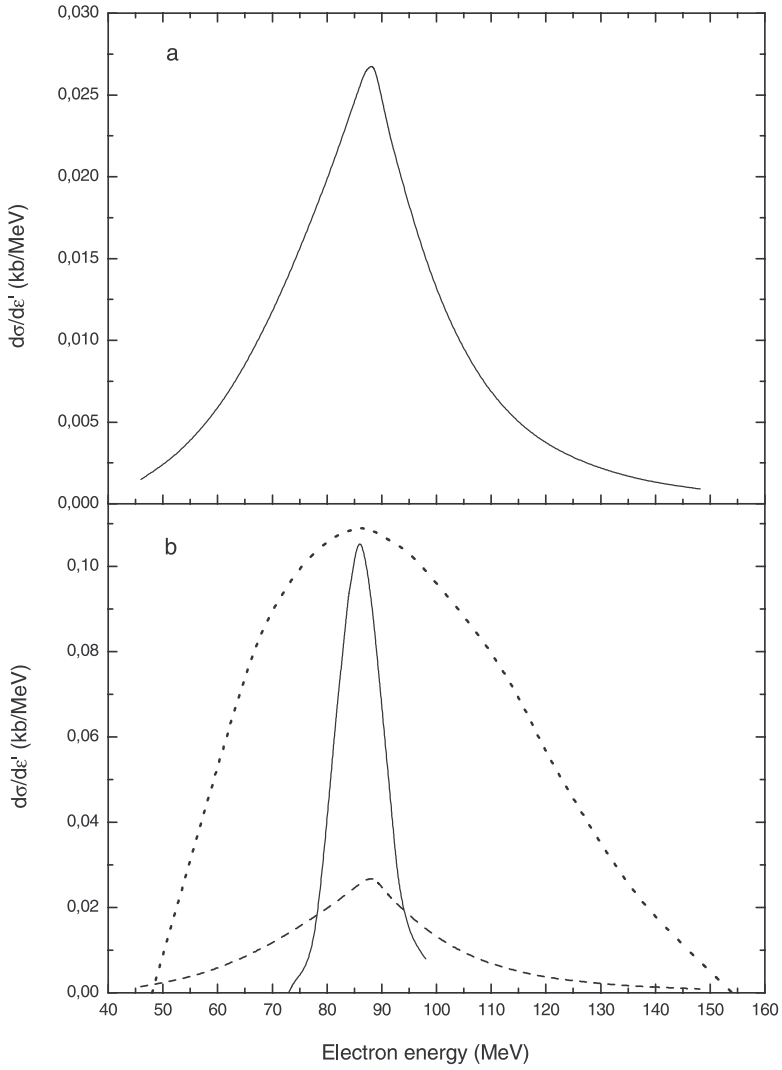

Figure 16: Cross section differential in energy for the electron loss from 160 GeV/u Pb^{81+} colliding with Al atoms. The cross section is given in the laboratory frame, where the atoms are at rest. a) Calculations of [68] based on Eqs.(135) and (136). b) Full curve: experimental results of [10] which we normalised according to the total cross section for the electron loss from 33 TeV Pb^{81+} colliding with Al solid target reported in [8]; dashed curve: our calculation; dotted curve: the Compton profile of Pb^{81+} mapped into the laboratory frame [10]. From [68].

In order to obtain some insight into the origin of the shape of the calculated loss peak in the laboratory frame, results for the double differential loss cross sections for 160 GeV/u Pb^{81+} in the projectile rest frame are shown in figure 17. The following points are worth to mention. First, the angular distribution of the emitted electrons in the projectile frame is rather asymmetric: the main part of the electrons in this frame is emitted in the direction of the motion of the incident neutral atom. The angular asymmetry in the emission increases with

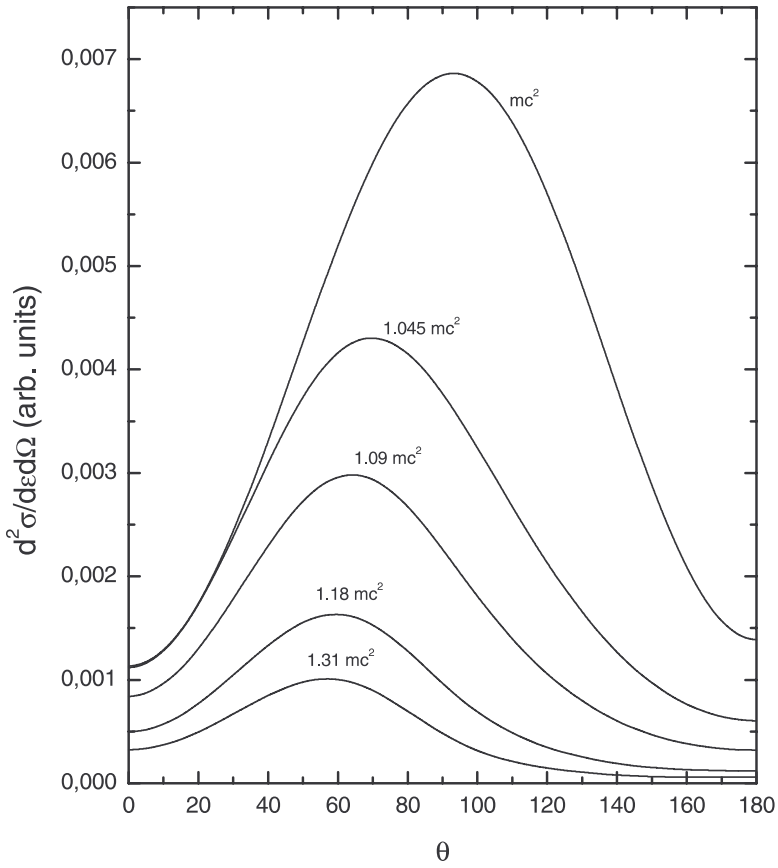

Figure 17: Doubly differential cross section for the electron emission from 160 GeV/u Pb^{81+} colliding with Al atoms. The cross section is given in the projectile frame as a function of the electron emission angle for several electron energies. The zero angle corresponds to the direction of the velocity of the incident atom. From [68].

increasing electron kinetic energy. Second, the number of the emitted electrons rapidly decreases with increasing this energy and the main part of the emitted electrons has kinetic energies not substantially higher than the electron binding energy ($\approx 0.2mc^2$ in Pb^{81+}). The first point allows one to understand the asymmetry in the electron energy spectra in the laboratory frame: since the majority of the electrons in the projectile frame is emitted in the direction of the motion of the incident atom then the main part of the electrons in the laboratory frame has energies which are less than $\varepsilon'_{max} = mc^2\gamma$. The second point states that a considerable part of the emitted electrons in the projectile frame has relatively low kinetic energies and this makes it clearer why the electron spectrum in the laboratory frame has a maximum near $\varepsilon'_{max} = mc^2\gamma$. In addition, the fact that the main part of the emitted electrons has low energies in the rest frame of the projectile shows that the Compton profile of $Pb^{81+}(1s)$ is not a relevant physical quantity for the loss process. The Compton profile of an initial state would be reflected directly in the ionization (loss) spectra only if the electron would be ejected mainly in collisions

where the momentum transfer to the electron (in the projectile frame) is large compared to the typical electron momentum in the initial bound state. This would lead to the population of high-energy continuum states of the ion which could be approximated by plane waves. As a result, the Compton profile of the initial state would follow from the corresponding transition matrix elements. However, since according to figure 17 the emitted electrons have relatively low energies, the above scenario is certainly not the case here.

The reason for the large difference between the calculated and measured electron loss spectra for the Pb^{81+} ions colliding with Al is still not clear. This difference is especially surprising because the calculated result for the total cross section for the electron loss $\sigma_{loss} = 1.15$ kb is in reasonable agreement with the total loss cross section of $1.3 - 1.4$ kb measured in [8] by means of counting the residual ions Pb^{82+}. In the experiment [10] only the lost electrons were counted which were emitted in the laboratory frame within the cone with half-angle 0.55. If the same restriction on the electrons is set in calculations the calculated spectrum becomes slightly narrower but the difference, compared to the spectrum shown in figure 16a, is quite small.

As a typical example of the electron loss from relatively light ions, let us now consider the electron loss from 160 GeV/u S^{15+} colliding with Al atoms. The electron loss spectrum in the laboratory frame is displayed in figure 18. One can note two main differences between the spectra displayed in figures 16a and 18. First, the width of the energy distribution of the electrons emitted from the sulphur ions is much smaller than that shown in figure 16a. Second, the spectrum given in figure 18 is more symmetric compared to that shown in figure 16a. The origin of these differences can be found by inspecting the double differential loss spectra in the rest frame of the projectile which are shown in figure 19. Similarly to the loss from the Pb^{81+} ions the number of the emitted electrons rapidly decreases with increasing electron kinetic energy. Again the main part of the emitted electrons has kinetic energies smaller or of the order of the initial binding energy of the electron. Since now this energy (≈ 3.5 keV) is much less than that in Pb^{81+} (≈ 100 keV) the spectrum of the electron emitted from 160 GeV/u S^{15+} is much narrower in energy than that originating from 160 GeV/u Pb^{81+}. In figure 19 one also sees that the angular spectra of the emitted electrons are nearly symmetrical in the rest frame of the projectile with respect to the direction $\theta = \pi/2$ and that this is the case for the whole range of emission energies of importance which gives practically all the contribution to the total loss. This is in contrast to the angular spectra displayed in figure 17. The reason for this contrast is the following. The energy and minimum momentum which are transferred to the ion in an ultrarelativistic collision are related by $q_{min} = \frac{\varepsilon_k - \varepsilon_0}{c}$, where one has $\varepsilon_k - \varepsilon_0 \sim Z_I^2$ for the majority of electrons emitted from the ions with a charge Z_I. For light ions one has $q_{min}/\overline{k_z} \sim Z_I/c \ll 1$, where $\overline{k_z} \sim Z_I$ is the typical absolute value for the z-component of the momentum of the emitted electron. A similar relation also holds between the absolute value of the transverse momentum transfer $q_\perp$ and the typical absolute value of the transverse component of the electron momentum. Therefore, in the case of the emission from light ions the electron momentum is balanced mainly by the recoil of the residual ion resulting in dipole-like angular spectra in the rest frame of the ion [60]. For very heavy ions, where $Z_I \sim c$, typical values of the momentum transfers to the ion are already rather close to typical values

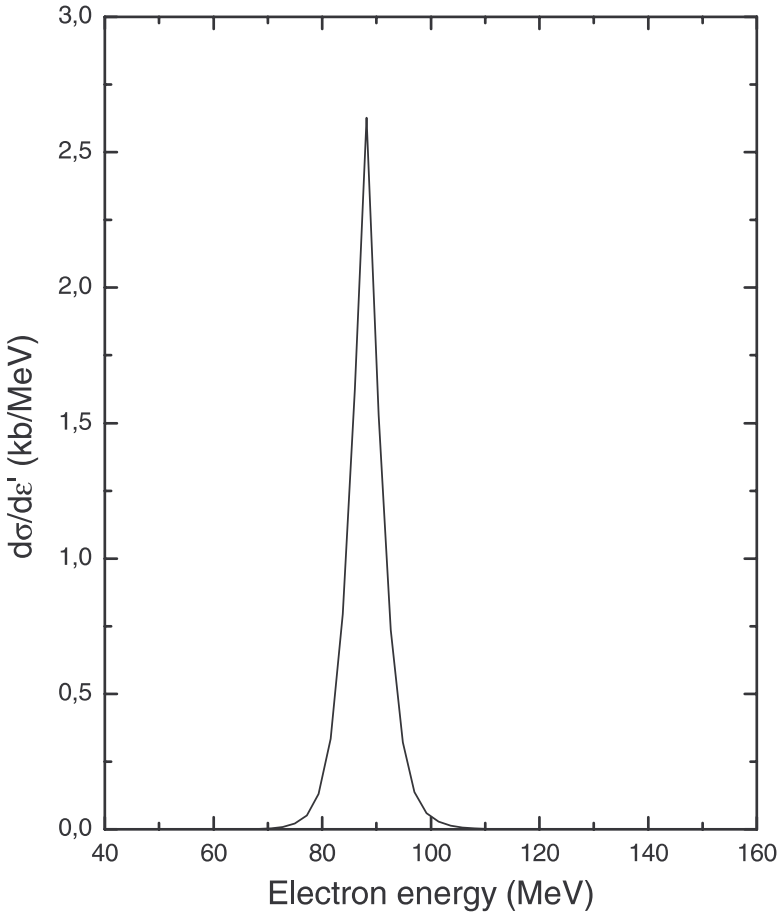

Figure 18: Cross section differential in energy for the electron loss from 160 GeV/u S^{15+} colliding with Al atoms. The cross section is given in the laboratory frame, where the atoms are at rest. From [68].

of the momentum of the emitted electron in the ion frame. Therefore, the emitted electron momentum is no longer balanced by the recoil of the residual nucleus and the angular spectra show considerable shifts to angles less than $\pi/2$.

The nearly symmetrical shape of the loss spectra in the rest frame of the projectile for light projectiles is reflected in the electron loss spectrum in the laboratory frame resulting in a nearly symmetrical distribution of the electron energies with respect to the 'central' energy $\varepsilon'_{max} = mc^2\gamma$ (figure 18).

6.3 Excitation and simultaneous excitation-loss cross sections

Experimental data for cross sections for excitation of 119 MeV/u $Bi^{82+}(1s)$ ions into $2s_{1/2}$, $2p_{1/2}$ and $2p_{3/2}$ states in collisions with neutral atomic targets were reported in [56] and [47]-[48]. The atomic numbers of the targets used in this experiment were much lower than that

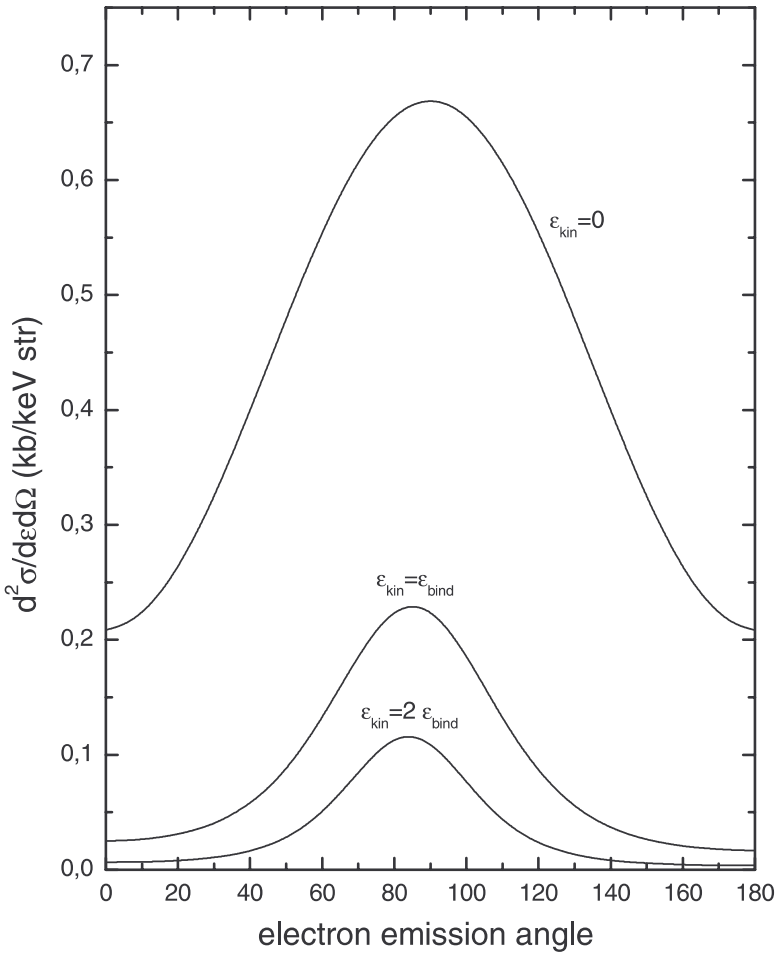

Figure 19: Doubly differential cross section for the electron emission from 160 GeV/u S^{15+} colliding with Al atoms. The cross section is given in the projectile frame as a function of the emission angle for several kinetic energies of the emitted electron. The zero angle corresponds to the direction of the velocity of the incident atom. From [68].

of the projectile and at this collision energy the excitation of $Bi^{82+}(1s)$ by the 'active' target electrons is not possible [22]. Therefore, neither the screening nor the antiscreening effects of the target electrons could noticeably influence the excitation process and the physics of the latter is basically reduced to excitation in collisions with bare target nuclei. The comparison between experiment and calculations, performed in [47]- [48] by using the first order of perturbation theory for excitation by a point-like heavy charged particle, suggested that the first order theory is quite adequate for these collision systems (see figure 20).

If a heavy ion initially carries several electrons then more than one electron of the ion can be simultaneously excited and/or lost in a collision with a neutral atom. In [62] simultaneous

[22]The energy 'threshold' for the antiscreening mode for excitation of $Bi^{82+}(1s)$ is $\approx$ 140 MeV/u. Although this 'threshold' is smeared out due to the electron motion inside the targets it still is far from 119 MeV/u.

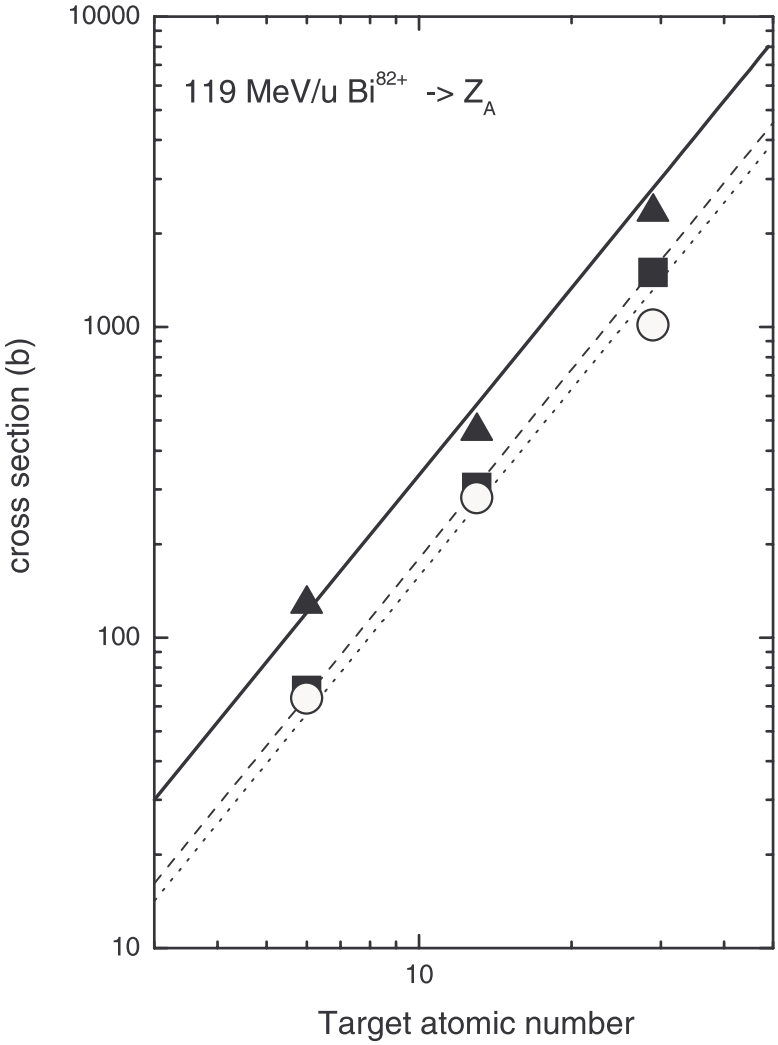

Figure 20: K shell excitation cross section for a 119 MeV/u hydrogen-like Bi ion given as a function of the target nuclear charge. Open circles, solid squares and solid triangles are experimental data for cross sections for Ly-α_1, Ly-α_2 and total Ly-α transitions, respectively. Dot, dash and solid lines represent theoretical results for cross sections of Ly-α_1, Ly-α_2 and total Ly-α transitions, respectively. Adapted from [47].

excitation and ionization of 223.2 MeV/u U^{90+} ions impinging on atomic targets of Ar, Kr and Xe was investigated experimentally. In the studied process one of the electrons of U^{90+} was ejected and the other was simultaneously excited into the L-subshell states of U^{91+} (see figure 21). In [62] also results of calculations for this process were reported. These calculations were done by assuming: (i) that the effect of the target electrons can be neglected and, thus, the action of the neutral targets can be replaced by that of their bare nuclei; (ii) that the main effect resulting in the simultaneous excitation and ionization is represented by independent interactions between the target nucleus and each of the projectile electrons; and (iii) that each

of these interactions involves just a single photon exchange where the corresponding probability can be evaluated within the first order of perturbation theory in the interaction between the target nucleus and projectile electron. While the assumptions (i) and (ii) seem to be well justified for the collision systems considered in [62], one may question (see [62]) whether the last assumption is met since the double electron process occurs at effectively very small impact parameters where the deviation of the corresponding excitation and ionization probabilities from predictions of the first order consideration can be already substantial even for such a heavy ions like U^{90+}. The fact that the point (iii) may not be fulfilled is seen in figure 21 where the theoretical predictions agree with the experiment for the case of collisions with Ar, where the interaction of the electron of the ion with the target nucleus is relatively weak, but do not fit experimental data for collisions with Kr and especially Xe where this interaction is much stronger.

The process of simultaneous excitation and loss considered in [62] represents one of the simplest and basic processes which can occur in collisions with projectiles having initially more than one electron. In the next subsection we shall discuss in great detail another basic two-electron process: the double electron loss from heavy helium-like projectiles. In particular, it will be clear that the above assumption (iii) is quite restrictive since it may not be fulfilled even for collisions at $\gamma \to \infty$ provided the target atom is heavy enough.

6.4 Single and double electron loss from heavy helium-like ions in collisions with many-electron atoms at high γ

6.4.1 General

Here we will consider single and double electron loss from a heavy helium-like projectile which initially is in the ground state and collides with a neutral many-electron atomic target at asymptotically high energies, where the loss cross sections become practically independent of the collision Lorentz factor. Two main points will be addressed in detail. The first one is the asymptotic high-energy double-to-single electron loss ratio. The second point concerns the deviation in the single and double electron loss cross sections from predictions of the lowest-order perturbation theory.

A full description of electron loss from helium-like ions in relativistic collisions with neutral atoms beyond the first order of perturbation theory seems to be prohibitory difficult. However, if one is concerned with the electron loss from heavy ions in collisions with heavy neutral atoms then, by invoking some reasonable approximations, the treatment of this problem can be greatly simplified.

As was already discussed, the antiscreening mode is rather a weak mechanism for the projectile-electron excitation and loss processes provided the colliding ion and neutral atom are heavy enough. Then the antiscreening mode may be neglected and in the target frame the effect of the atom on the projectile electron can be well approximated as caused by a superposition of short-ranged Yukawa-type potentials given by Eqs.(102)-(103). Thus, the problem of the

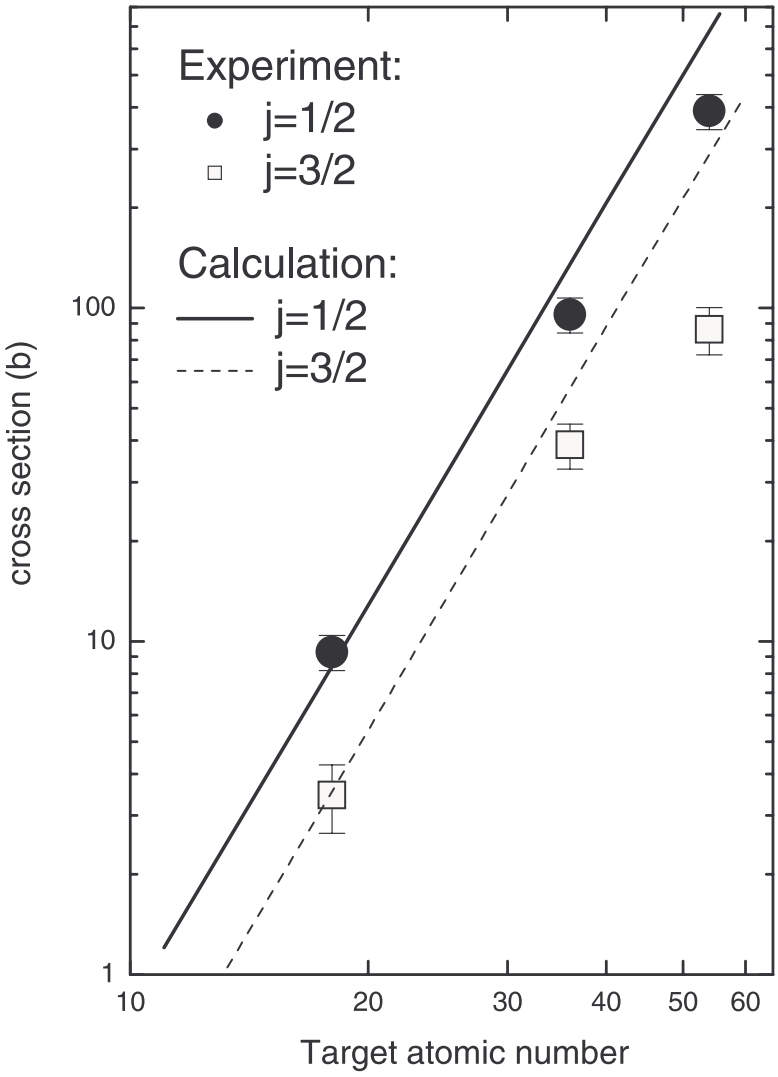

Figure 21: Total cross sections for simultaneous excitation-loss from 223.2 U^{90+} ions in collisions with Ar, Kr and Xe gas targets. Solid circles and open squares are experimental data for excitation into the $j = 1/2$ and $j = 3/2$ L-shell states, respectively, of the residual U^{91+} ions. Solid and dash lines show theoretical results. Adapted from [62].

electron loss from a heavy helium-like projectile in collisions with a many-electron target can be reduced to the electron loss from the projectile by the action of an external potential.

In general, the process of removal of two electrons is substantially more complicated compared to that of single ionization which is often regarded as a basically uncorrelated single-electron process. There are essentially two possibilities to get the double loss. The first is that the target potential simultaneously influences the motion of both projectile electrons and this influence directly leads to their loss. Below this process will be referred to as the two-step-2

process (or TS-2) [23].

The other possibility to remove two electrons from the projectile in a single collision is that effectively only one projectile-electron interacts with the target and is removed by this interaction from the projectile, and the other one is lost either due to electron-electron-correlations within the projectile or due to rearrangement in the projectile final state. These processes can be referred to as the two-step-1 (TS-1) and shake-off (SO), respectively.

It was shown in [69] that the double electron loss from heavy helium-like ions in collisions with neutral atoms will occur predominantly via the TS-2 mechanism provided the condition

$$\frac{Z_A Z_I}{v} > 0.4 \tag{137}$$

is fulfilled. Therefore, in the range (137) of the collision parameters the electron loss from the projectile can be dealt with within the independent electron model (IEM), which has been proved to be quite successful in describing cross sections in cases of strong external perturbations (see e.g. [7], [4] and references therein).

Within the IEM the single and double electron loss cross sections, respectively, read

$$\begin{aligned} \sigma^{(1)} &= \int d^2\mathbf{b}\ P_1(\mathbf{b}) = 2\int d^2\mathbf{b}\ p(\mathbf{b})\Big(1-p(\mathbf{b})\Big) \\ \sigma^{(2)} &= \int d^2\mathbf{b}\ P_2(\mathbf{b}) = \int d^2\mathbf{b}\ \Big(p(\mathbf{b})\Big)^2 . \end{aligned} \tag{138}$$

Here, $P_1(\mathbf{b})$ and $P_2(\mathbf{b})$ are the impact parameter dependent probabilities for single and double electron loss, respectively, and the one-electron transition probability $p(\mathbf{b})$ is given by

$$p(\mathbf{b}) = \int d^3\mathbf{k}\ |a_{0\to\mathbf{k}}(\mathbf{b})|^2 , \tag{139}$$

where $a_{0\to\mathbf{k}}$ denotes the amplitude for the collision-induced transition from the ground-state ψ_0 to a continuum-state $\psi_\mathbf{k}$ of a hydrogen-like ion with an effective nuclear charge Z_{eff}. It is convenient to calculate $a_{0\to\mathbf{k}}$, $p(\mathbf{b})$ and the corresponding cross sections in the projectile reference frame and this frame will be used below.

According to the considerations of the sections 4 and 5 the semiclassical first-order and eikonal transition amplitudes are given by

$$a^{pert}_{0\to\mathbf{k}}(\mathbf{b}) = \frac{2iZ_A}{v}\sum_{j=1}^{3} A_j \langle\psi_\mathbf{k}(\mathbf{r})|(1-\beta\alpha_z)\exp\left(i\frac{\omega_{k0}}{v}z\right)K_0\big(B_{k,j}|\mathbf{b}-\mathbf{r}_\perp|\big)|\psi_0(\mathbf{r})\rangle \tag{140}$$

[23] Note that the target interaction with each of the projectile electrons in a single collision event can involve both single- and many-virtual-photon exchanges. Therefore, the TS-2, as it is defined in the present subsection, represents a more general process compared to that which is usually called the 'TS-2' in the literature on double ionization of helium atoms by the impact of multiply charged ions. In the latter 'TS-2' only the two-photon exchange between the target and projectile (or, more exactly, one photon per one electron) is taken into account. The present TS-2 reduces to the latter only in the case of not too strong interactions.

and

$$a_{0\to\mathbf{k}}^{eik}(\mathbf{b}) = \langle\psi_{\mathbf{k}}(\mathbf{r})|(1-\alpha_z)\exp\Big(i\frac{\omega_{k0}}{c}z\Big)\exp\left(\frac{2iZ_A}{c}\sum_j A_j K_0(\kappa_j|\mathbf{b}-\mathbf{r}_\perp|)\right)|\psi_0(\mathbf{r})\rangle, \qquad (141)$$

respectively, where $B_{k,j} = \sqrt{\frac{\omega_{k0}^2}{v^2\gamma^2}+\kappa_j^2}$.

By using Eqs.(138)-(141) the cross sections for single and double electron loss were calculated in [69] for collisions of helium-like ions Kr^{34+}, Xe^{52+} and Pb^{80+} with neutral Kr,Xe and Au at asymptotically high γ. These nine collision pairs are quite representative since they cover all possible situations, where the projectile-ion is 'light-heavy', 'intermediate-heavy' or 'very heavy' and collides with a 'light-heavy', 'intermediate-heavy' or 'very heavy' target-atom. In obtaining the cross sections (138) relativistic Coulomb-Dirac wave-functions were used to calculate the first-order and eikonal transition amplitudes (140) and (141). In [69] the projectile nuclear charge Z_I was taken as an effective projectile charge Z_{eff} for calculating both single and double electron loss.

Following [69] we will refer to the approach, which uses the IEM with the first order one-electron transition amplitude (140) and, thus, takes into account only the one-photon exchange between the target and each of the projectile electrons, as to the *perturbative* treatment. Correspondingly, results, obtained in this way, will be termed as *perturbative*. The *nonperturbative* approach, which for the asymptotically high collision energies fully accounts for the many-photon exchange between the 'frozen' target and the projectile electrons, is based on the IEM and (141). Results of the latter calculations will be termed *nonperturbative*.

Table 2 shows the single and double loss cross sections.

6.4.2 High-energy limit for the double-to-single loss ratio

According to the table the calculated ratios are weakly dependent on the atomic number of the projectile-ion and, thus, are essentially determined only by the target-atom. An additional calculation performed in [69] for the loss from S^{14+} confirms this result: the ratios of 1.8 %, 3.7 % and 7.1 % were found for collisions with Kr, Xe and Au, respectively. Figures 22 and 23 offer some insight why the ratios are nearly independent of the projectile atomic number Z_I. They show the loss probabilities as a function of the impact parameter, which is given in units of $1/Z_I$. It is seen that the curves for different projectiles look rather similar. This means that both the single and double loss cross sections scale approximately like Z_I^{-2}. Thus, the influence of the projectile nucleus charge on the loss process is, basically, to set the length scale that does not affect much the ratio.

These predictions, that the double-to-single loss ratio is strongly dependent on the atomic number Z_A of the ionizing agent and is nearly independent of the nuclear charge Z_I of the electron binding center, are in sharp contrast to what is expected in the high-energy limit ($\gamma \to \infty$) for the double-to-single ionization ratio in the case of ionization of helium and helium-like positive ions in collisions with charged particles. In the latter case the TS-1 and SO mechanisms would always dominate in the double ionization at $\gamma \to \infty$ and the predicted

Target	Z_T	Projectile	$\sigma^{(1)}_{pert}$	$\sigma^{(2)}_{pert}$	$\sigma^{(1)}_{eik}$	$\sigma^{(2)}_{eik}$	$\frac{\sigma^{(2)}_{eik}}{\sigma^{(1)}_{eik}}$
Kr^0	36	Kr^{34+}	62.5	1.15	62.4	1.13	1.8 %
Kr^0	36	Xe^{52+}	29.1	0.497	29.1	0.495	1.7 %
Kr^0	36	Pb^{80+}	12.5	0.184	12.5	0.184	1.5 %
Xe^0	54	Kr^{34+}	125	5.29	123	4.77	3.9 %
Xe^0	54	Xe^{52+}	59.6	2.42	58.9	2.19	3.7 %
Xe^0	54	Pb^{80+}	25.1	0.903	24.9	0.817	3.3 %
Au^0	79	Kr^{34+}	234	23.0	224	16.3	7.3 %
Au^0	79	Xe^{52+}	113	10.6	110	7.63	6.9 %
Au^0	79	Pb^{80+}	49.2	3.98	48.9	2.94	6.0 %

Table 2: Cross sections (in kb) for single and double electron loss from helium-like projectiles in ultrarelativistic collisions with neutral targets. The projectiles are initially in their ground states. The fourth and fifth columns display cross sections obtained within the perturbative treatment. The sixth, seventh and eighth columns contain the nonperturbative results. From [69].

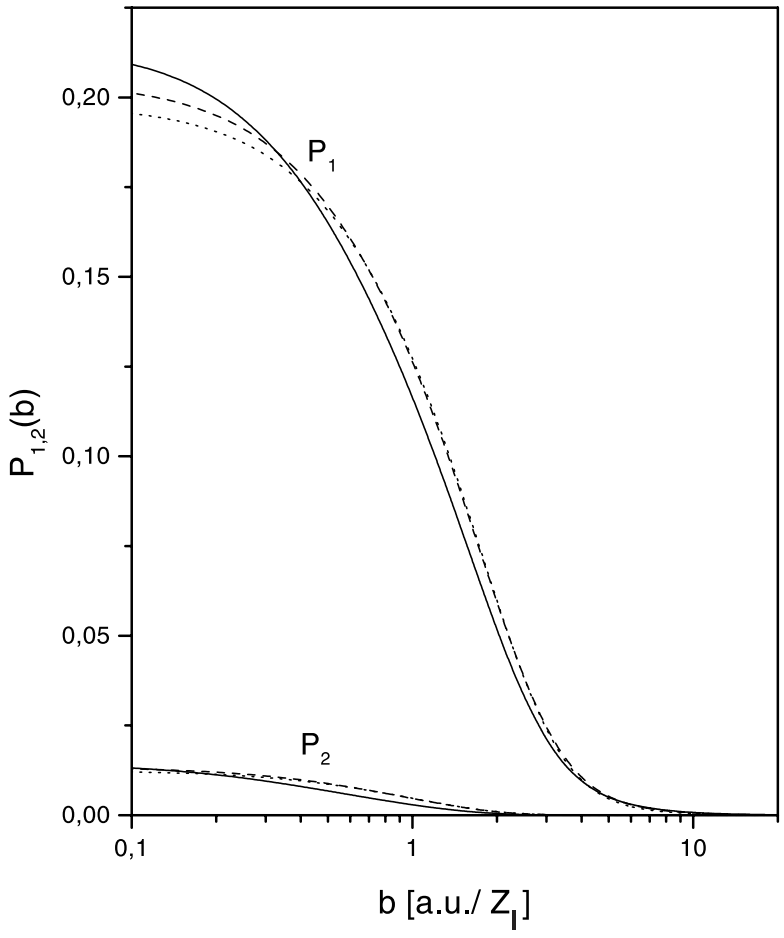

Figure 22: Nonperturbative asymptotic high-energy probabilities $P_1(b)$ and $P_2(b)$ for single and double electron loss from helium-like Pb, Xe and Kr ions by impact on neutral Kr atoms. Solid lines: results for Pb^{80+}; dashed lines: results for Xe^{52+}; dotted lines: results for Kr^{34+}. From [69].

features ([70]- [71]) of the ratio are: i) the strong dependence on the atomic number of the binding center (helium, helium-like ion), ii) the independence of the charge of the ionizing agent (a point-like charged particle) and iii) in the high-energy limit both the single and double ionization cross sections depend on the collision energy and behave as $\ln \gamma$. It is the fundamental difference between the influence of a short-range potential in the case of the electron removal by the action of a neutral atom and that of the long-range Coulomb potential in the case of ionization by a charged particle which is responsible for this contrast.

6.4.3 Nonperturbative behaviour of the loss process

The TS-2 mechanism dominates, provided the condition (137) is fulfilled, which is the case for all projectile-target pairs given in table 2. The TS-2, however, involves the exchange of at least

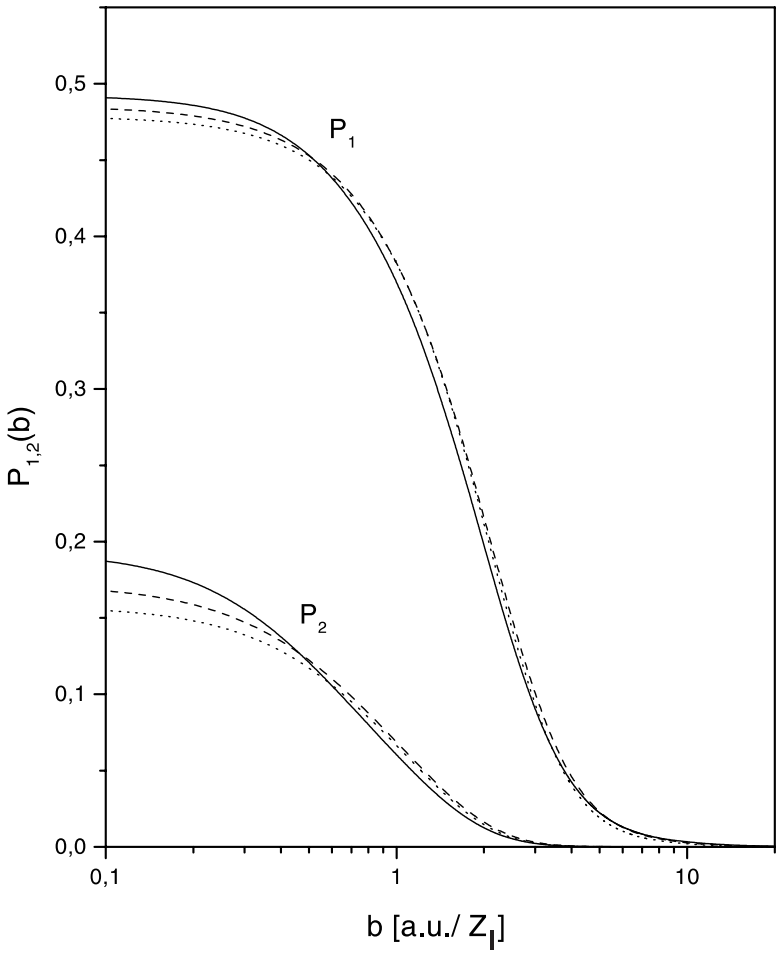

Figure 23: Same as Fig. 23, but for impact on neutral Au atoms. From [69].

two virtual photons (one photon per one electron) and, thus, is not a first order mechanism. Moreover, the influence of many-photon processes, where the target exchanges with each of the projectile electrons more than one photon, can also be substantial.

According to the definition of 'perturbative' and 'nonperturbative', given at the end of 6.4.1, one can generally refer to the difference between results, obtained with the first order (140) and 'exact' (141) transition amplitudes as to the *nonperturbative behaviour* of the loss process.

It was found in [69] that the double loss cross sections for Pb^{80+}, Xe^{52+} and Kr^{34+} ions impinging on Au atoms, calculated using the first order transition amplitude (140), are by 35-42% larger than the nonperturbative results. Figure 24 shows the corresponding loss probabilities as a function of the impact parameter. It is seen that the region of small impact parameters is responsible for the pronounced nonperturbative behaviour.

Regarding single loss from helium-like Kr, Xe and Pb ions by impact on neutral Au, table 2

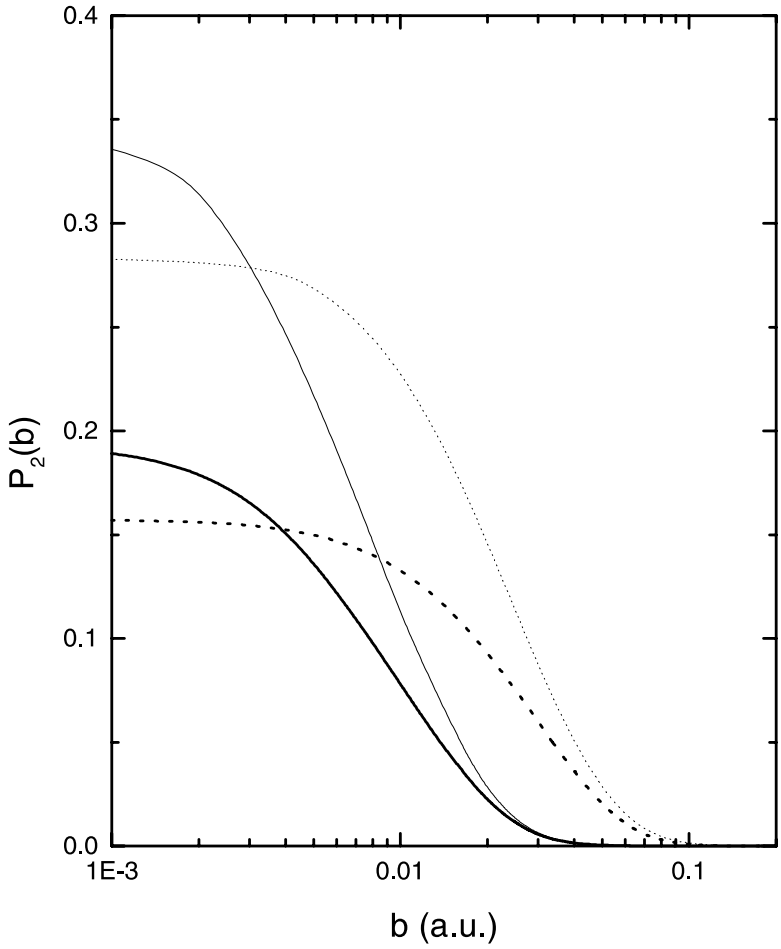

Figure 24: Perturbative versus nonperturbative probabilities $P_2(b)$ for double loss from helium-like Pb and Kr ions by ultrarelativistic impact on neutral Au atoms. Thick solid line: nonperturbative result for Pb^{80+}; thin solid line: perturbative result for Pb^{80+}; thick dotted line: nonperturbative result for Kr^{34+}; thin dotted line: perturbative result for Kr^{34+}. From [69].

suggests that the influence of the many-photon exchange on the cross section is even weaker compared to that for the electron-loss from the corresponding hydrogen-like projectiles. This observation can be explained if one notes that within the IEM the identity $\sigma^{(1)} = 2(\sigma_{loss} - \sigma^{(2)})$ holds, where σ_{loss} denotes the cross section for the electron-loss from the corresponding hydrogen-like projectile. Hence the weaker signs of the nonperturbative behaviour in single electron loss are due to a partial compensation of the contributions of the many-photon exchanges to σ_{loss} and $\sigma^{(2)}$. As the collision system Pb + Au shows, this compensation can be almost complete.

The perturbative calculations predict that for $40 \lesssim Z_I \lesssim 90$ the double loss cross sections should approximately scale according to Z_A^4-dependence. Such a dependence would be the exact scaling-law within the IEM for collisions with bare target nuclei. Thus, according to the perturbative treatment, the screening of the target-nucleus by the target-electrons does

not affect much the double loss even for not very heavy projectile-ions. This suggests that the double loss mainly occurs at so small impact parameters where the projectile-electrons interact, in essence, with the unscreened target-nucleus. In the nonperturbative treatment the scaling Z_A^4 gets lost and the double loss cross sections increase slower with Z_A. This slower increase is a signature of the many-photon exchange, which for strong interactions is known to reduce ionization probabilities compared to perturbative results. According to figure 24 the main difference between the perturbative and 'exact' results appears at very small impact parameters where the screening effects are of minor importance.

Some conclusions can be drawn from the above discussion of the electron loss from heavy helium-like projectiles.

First, even in the asymptotic region $\gamma \to \infty$ the many-photon exchange between the target and each of the projectile electrons play an important role in the double loss in collisions with heavy neutral targets.

Second, the double loss from very heavy and even not very heavy helium-like ions occurs mainly in collisions at so small impact parameters, where the screening effects of the target nucleus by the target electrons are already rather weak.

Third, the double-to-single loss ratio is strongly dependent on the atomic number Z_A of the target but is nearly independent of the nuclear charge Z_I of the projectile.

Fourth, it is rather obvious that, within the IEM, cross sections for multiple-electron loss from heavy projectiles, having several electrons, should in general be even more sensitive to the form of the single-electron transition probability $p(\mathbf{b})$ than the cross section for double electron loss from heavy helium-like projectiles. Therefore, contrary to usual assumptions (see e.g. [4], p.204), the application of perturbation theory for obtaining the one-electron transition probability $p(\mathbf{b})$ might result in large errors in calculated cross sections for multiple electron loss from projectiles.

6.5 Screening effects in electron-positron pair production in high-energy collisions

In the Dirac sea picture the electron-positron pair production is considered as a transition of a negative-energy electron to a state with a positive energy. If this final state is in the continuum then the process is termed as free pair production. The created electron can also be captured by an ion into a bound state. The latter process is called bound-free pair production.

The collisional electron-positron pair production is usually considered for the case where two colliding particles are bare nuclei. However, in some experimental situations only one of the colliding partners can be a bare nucleus whereas the second is represented by a neutral atom. Pair production in collisions between a bare nucleus and a neutral atom is the topic of the present section.

This process can be considered in the rest frame of the nucleus and viewed as a transition, stimulated by the atom impact, between electron states with negative and positive (total)

energy which are solutions of the Dirac equation for an electron moving in the field of the nucleus. Such a picture was adopted in [72] to treat bound-free pair production in nucleus-atom collisions. In this picture a close analogy between pair production and the 'normal' ionization or the electron loss process is rather obvious. Therefore, the methods for considering electron loss from ions colliding with atoms, which were discussed in the previous sections, can be rather straightforwardly used to treat pair production in nucleus-atom collisions.

6.5.1 Pair production with capture

We will focus our attention on the screening effect of atomic electrons and describe the influence of a neutral atom on the pair production process in the first order of the perturbation theory. Below we will see that, because of large momentum transfers necessary to produce a pair, the screening effect becomes important only when γ is very large. Besides, since the cross section for pair production with capture scales approximately as Z_I^5 where Z_I is the charge of a bare nucleus, we will consider collisions only with very heavy bare nuclei. For such collisions (high γ and Z_I) one can expect that the difference between results of the first order treatment and of more refined theories is already not very substantial [40]. In addition, the screening effect manifests itself in collisions with impact parameters, which are large compared to the electron Compton wave-length, where the first-order approach should yield a reasonable description.

Assuming that the positron states are normalized on the 'energy' scale and choosing the quantization axis (z-axis) to be along the total momentum transfer $\mathbf{q}$, the cross section for the bound-free pair production, where the electron is captured into the ground state of the ion, is given by (see [72])

$$\sigma_s(1s) = \frac{4}{v^2}\sum_{s_p,s_e}\int d^2\mathbf{q}_\perp \int d\Omega_k \int_{mc^2}^{\infty} d\varepsilon_k \, Z_{A,eff}^2(\mathbf{Q_0}) \left\{ \frac{|\langle\psi_0(\mathbf{r})\,|\exp(iq_0z)|\,\psi_{\mathbf{k}}(\mathbf{r})\rangle|^2}{q_0^4} + \frac{v^2\,q_\perp^2}{c^2\,q_0^2}\frac{|\langle\psi_0(\mathbf{r})\,|\exp(iq_0z)\,\alpha_x|\,\psi_{\mathbf{k}}(\mathbf{r})\rangle|^2}{\left(q_0^2-\frac{\omega_{0,k}^2}{c^2}\right)^2} \right\}. \quad (142)$$

Here $\mathbf{q}_0 = \left(\mathbf{q}_\perp, \frac{\omega_{0,k}}{v}\right)$, $\mathbf{Q}_0 = \left(-\mathbf{q}_\perp, -\frac{\omega_{0,k}}{v\gamma}\right)$, ε_k is the energy of the positron, ε_0 is the electron energy in the ground state of the ion and $\omega_{0,k} = \varepsilon_k + \varepsilon_0$. Further, $Z_{A,eff}$ is the effective atomic charge for the screening mode of the collision, defined similarly as in the case of the electron loss, and $d\Omega_k$ is the element of the solid angle for the positron. The sum in (142) is over the electron and positron spins. Equation (142) represents the cross section for the bound-free pair production written in the Coulomb gauge as sum of the 'longitudinal' and 'transverse' contributions.

For the pair production process, where the typical momentum transfers to the atom are much larger compared to those in the electron loss process, the antiscreening part of the bound-free cross section can be estimated as $\sigma_a \approx \frac{1}{Z_A}\sigma_s$. Thus, the total cross section for the pair production with electron capture into a bound state is given by $\sigma = \left(1+\frac{1}{Z_A}\right)\sigma_s$, where for the

capture to the ground state the screening cross section is defined by Eq.(142).

In an experiment [73] the cross section for bound-free pair production in collisions of 10 GeV/u Au^{79+} projectiles with Al, Cu, Ag and Au atomic targets were measured. Calculations for the bound-free pair production, performed in [72] show that at this collision energy the screening effect does not exceed few per cent even for the heaviest target.

Figure 25 shows a comparison between the experimental data of Krause et al. [8] and theoretical results. In this experiment cross sections were measured for total electron capture by 160 GeV/uPb^{82+} projectiles colliding with different solid state targets and the bound-free pair production cross sections were extracted from the measured data. The theoretical results include those obtained by using Eq.(142) [72] and results of [29]. In the latter paper cross sections for bound-free pair production were given for a variety of projectile-target pairs for collisions with energies corresponding to $\gamma \leq 1000$. The authors [29], however, neglected the screening effect of the atomic electrons arguing that at $\gamma \leq 1000$ it still should be negligible because of large momentum transfers needed to excite the positron-electron vacuum.

Theoretical results in figure 25 include a multiplication of the cross section for the capture to the ground state by a factor of 1.2. This correction aims at taking into account (approximately) the possibility for the electron to be captured into excited states of the ion. In both [29] and [72] semi-relativistic approximations to describe the electron and positron states were used and, therefore, the difference between the theoretical results shown in figure 25 is solely due to the screening effect of the atomic electrons. With the screening included, the cross section is reduced by 2.5 percent for collisions with Be and C targets. The screening effect increases with the atomic number of the target and reduces the cross section by 14% for collisions with Au target.

In [72] cross sections for bound-free pair production in collisions with Be and Au targets was also estimated for 1000 GeV/u Pb^{82+} projectiles. For this collision energy, neglecting the screening effect, values $\sigma(1s) = 0.18$ and 56b were found for Be and Au targets, respectively. Including the screening effect these cross sections reduce to $\sigma(1s) = 0.15$ and 37b, respectively. Thus, at this collision energy the screening reduces the cross section by 16% for Be targets and by 33% for Au targets.

6.5.2 Free pair production

The screening effect of atomic electrons in free pair production in collisions between a bare nucleus and a neutral atom was estimated in [2] in the lowest (second) order of perturbation theory by using the Weizsäcker-Williams approximation of equivalent photons. The main conclusions of [2] were: (i) the screening effect is important at all energies (where the Weizsäcker-Williams approximation is valid) reducing the free pair production by at least a factor of 1.5-2 and (ii) the screening effect decreases when the collision energy increases. These findings, both the absolute size of the predicted screening effect and its suggested dependence on the collision energy, seem to be difficult to understand.

The results of [2] were not supported by a more recent study performed in [74]. In the latter

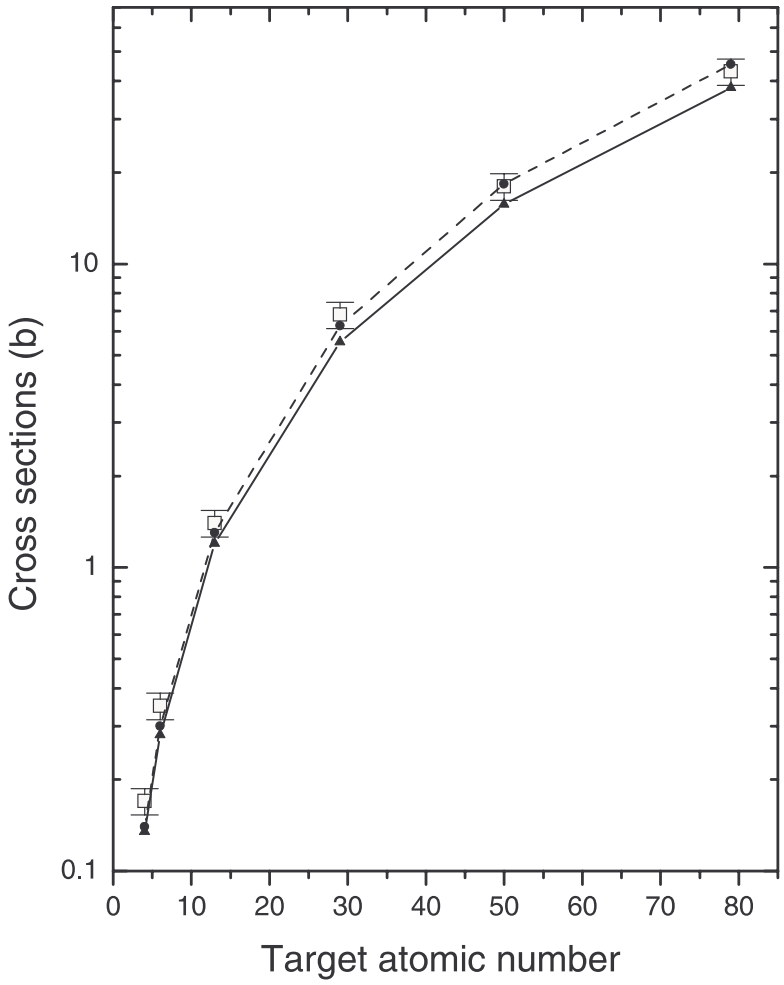

Figure 25: Cross sections for bound-free pair production in collisions of 160 GeV/uPb^{82+} with solid state targets as a function of the target atomic number. Open squares with error bars: experimental data from [8], solid circles connected by dashed curve: calculations of [29], solid triangles connected by solid curve: calculations including the screening [72]. The curves are just to guide the eye. Adapted from [72].

paper free pair production in nucleus-atom collisions was also calculated in the second order of perturbation theory (without using the Weizsäcker-Williams approximation). The authors of [74] predict that (i) the screening effect increases with increasing the collision energy and (ii) it is larger for collisions with heavier atoms. Thus, with respect to these two points the screening effect in bound-free and free-free pair production is similar. However, the reduction of cross sections by the screening effect was found in [74] to be substantially lower compared to what we discussed for the bound-free pair production. According to [74] in Au^{79+} on Au^0 collisions the screening effect reduces the cross section for the free pair production by 4.5% at a collision energy of $E = 200$ GeV/u, by 13.5% at $E = 2$ TeV/u and by 31.4% at $E = 200$

TeV/u.

The relatively weaker screening effect in free pair production can be attributed to the fact that this process, compared to the bound-free pair creation, involves on average substantially larger momentum transfers.

6.6 Excitation and break-up of pionium in relativistic collisions with neutral atoms

The DIRAC experiment at CERN, aimed at measuring the lifetime of pionium [75], has sparked considerable interest in the study of excitation and break-up of pionium colliding with neutral atoms at relativistic velocities ($\gamma \sim 15 - 20$). Since the pionium-atom collisions occur predominantly via the electromagnetic interaction, the excitation and break-up of pionium in such collisions are closely related to the topic of the present review and we will briefly comment on these processes.

From the point of view of usual atomic physics pionium, which is a bound state of π^+ and π^- both having zero spin, represents rather an exotic object. The lifetime of pionium in the ground state is of the order of 10^{-15} s. Compared to a 'normal' hydrogen-like system, consisting of a heavy nucleus and a light electron, pionium has other important differences. The masses of π^+ and π^- are equal, $m_{\pi^\pm} \simeq 270 m_e$ ($m_e = 1$ is the electron mass), that may bring in considerable features into the dynamics of excitation and break-up of pionium, which would be absent in the case of excitation or 'ionization' of a hydrogen-like ion. Since the reduced mass of pionium is large, $\mu_\pi \simeq 137 m_e$, the typical dimension of the pionium ground state is even smaller than that of the electron orbit in the ground state of U^{91+}. However, the relative velocity of π^+ and π^- in the ground state of pionium is of the order of 1 a.u. and, thus, despite the small size this system is still very far from being relativistic.

Excitation and break-up of pionium is conveniently described in the pionium frame [76]-[81]. In this frame the motion of the π^+ and π^- is practically always nonrelativistic [24]. Because of this, in collisions with neutral atoms, the exchange of the transverse virtual photon affects pionium transitions much weaker than the exchange of the longitudinal photon. For collisions at low γ the influence of the transverse photon would be weak due to the purely nonrelativistic motion of the π^+ and π^- in both initial and final states of pionium. With increasing γ this influence could strongly increase in collisions with bare nuclei but in collisions with neutral atoms it is essentially removed by the screening effect of the atomic electrons. It was shown in [78] and [80] that the relative contributions of the exchange of the transverse photon for pionium transitions is substantially less than 1%.

In [78]- [80] it was argued that, within the first order approximation, one can calculate cross sections for pionium with accuracy better than 1% for both the elastic and inelastic modes. However, substantial deviations from predictions of the first order consideration can occur due to exchanges of many longitudinal photons between pionium and the incident atom. Using the

[24] In the process of pionium break-up the fragments, π^+ and π^-, can in principle attain relativistic velocities in the pionium frame but the contribution of such collision events into the total break-up cross section is negligible.

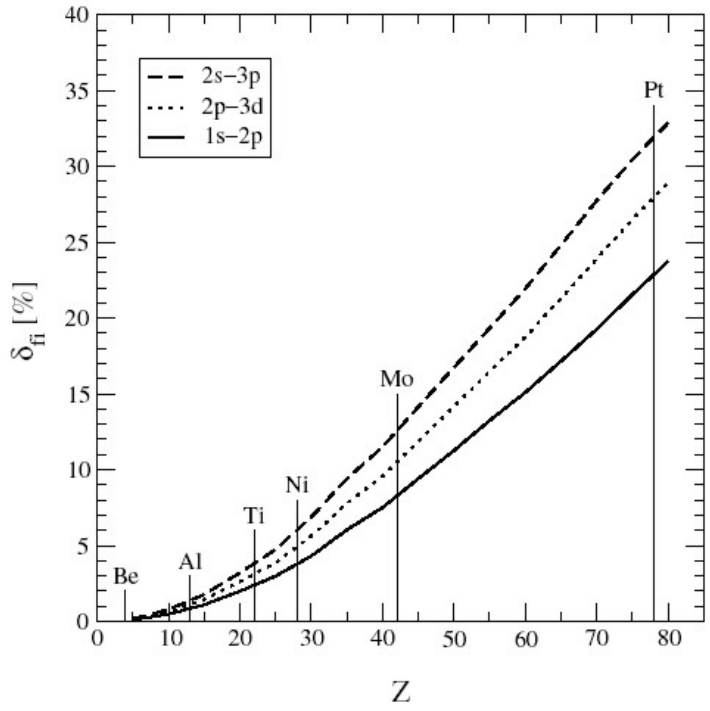

Figure 26: The relative correction δ_{fi} to the excitation cross sections as a function of the atomic number Z of the target. The correction δ_{fi} is the difference between the first-order and Glauber cross sections normalized to the first-order cross section. In the figure this correction is shown for the $1s$-$2p$, $2p-3d$ and $2s$-$3p$ transitions by solid, dot and dash curves, respectively. From [81].

Glauber approximation it was shown in [76]- [77] and [81] that the account of the many-photon exchanges may reduce cross sections by more than 10% in collisions with heavy atoms (see figure 26).

7 Summary and outlook

In this article we have attempted to present an overview of the current state of the research in the field of projectile-electron excitation and loss in relativistic collisions with neutral atoms. Although considerable efforts have been devoted to the experimental and theoretical investigations in this field, there remain many topics yet to be explored in detail. Below we list some of them.

1. Two-center electron-electron interaction.

There have been substantial experimental and theoretical activities in the study of the interaction between 'active' electrons which belong to different colliding centers moving at nonrelativistic velocities with respect to each other, including a sophisticated recent experiment [82]

where very detailed information about final states of the projectile and target was obtained. By performing similar studies in the domain of relativistic collision velocities one can learn about how the relativistic effects could affect this interaction. As an example of the reaction, where the two-center electron-electron interaction plays a crucial role and, therefore, might be explored in detail, one could mention mutual ionization in collisions between multiply charged hydrogen-like ions, $Z_I \sim 3 - 10$, and helium or hydrogen atoms [25] at collision energies starting with ~ 1 GeV/u and higher.

2. Excitation of a hydrogen-like projectile in ultrarelativistic collisions with neutral atoms.

There are no experimental data about projectile-electron excitation in relativistic collisions with neutral targets at such conditions where the excitation process can be strongly influenced by the screening and antiscreening effects of the target electrons and where the screening and antiscreening themselves can already be profoundly modified by the relativistic effects arising due to collision velocities approaching the speed of light.

3. Simultaneous excitation-loss and double loss in relativistic collisions between helium-like ions and neutral atoms.

These two processes are the simplest processes which involve more than one 'active' projectile electron. Amongst interesting points to address here are: the higher-order effects in collisions with heavy targets, the excitation-loss and double loss mechanisms in collisions with light targets, the role of the target electrons in collisions with few-electron targets e.t.c..

4. Differential loss spectra.

The study of differential cross sections can unveil valuable information about the collision process which might remain 'hidden' when only the total cross section is explored. In particular, we remind that the puzzling disagreement between the experimental and theoretical data for the electron cusp produced in collisions of 160 GeV/u Pb^{81+} with Al is yet to be resolved.

The extension of the investigations of the projectile-electron excitation and loss to the domain of relativistic collision velocities can bring new and important knowledge about the field of relativistic atomic collision physics. Besides, since such studies yield a more broad and general picture of collisions, they might sometimes give a better insight into the physics of corresponding processes occurring in nonrelativistic collisions. We hope that experimental studies of relativistic collisions of two structured atomic particles, both carrying active electrons, could get strong boosts after upgrading the accelerator facilities at the GSI (Darmstadt, Germany), that will allow to explore experimentally the ion-atom interactions at collision energies corresponding to the Lorentz factor $1 < \gamma \lesssim 40$.

Acknowledgment

The author is grateful to N. Grün for useful discussions and careful reading of this manuscript.

[25] COLTRIMS experiments with atomic hydrogen target might very soon become possible [83].

A Nonrelativistic atom approximation for the screening mode

For simplicity we shall restrict our discussion to single electron targets. In such a case we have to consider the following three matrix elements

$$\langle \phi_0 \left| \alpha_x \exp(i\mathbf{Q}_0 \cdot \boldsymbol{\xi}) \right| \phi_0 \rangle ,$$

$$\langle \phi_0 \left| \alpha_y \exp(i\mathbf{Q}_0 \cdot \boldsymbol{\xi}) \right| \phi_0 \rangle ,$$

and

$$\frac{1}{c} \langle \phi_0 \left| v\alpha_z \exp(i\mathbf{Q}_0 \cdot \boldsymbol{\xi}) \right| \phi_0 \rangle ,$$

where $\mathbf{Q}_0 = (-\mathbf{q}_\perp, -(\varepsilon_n - \varepsilon_0)/(v\gamma))$.

Let us start with the matrix element containing α_z. First we rewrite the term $v\alpha_z$ as follows

$$v\alpha_z = \mathbf{v} \cdot \boldsymbol{\alpha} = \left(\mathbf{v} - \frac{\Omega}{Q_0^2} \mathbf{Q}_0 \right) \cdot \boldsymbol{\alpha} + \frac{\Omega}{Q_0^2} \mathbf{Q}_0 \cdot \boldsymbol{\alpha}, \tag{143}$$

where Ω is a parameter to be determined below. Taking into account Eq.(86) we immediately see that $\langle \phi_0 \left| \mathbf{Q}_0 \cdot \boldsymbol{\alpha} \exp(i\mathbf{Q}_0 \cdot \boldsymbol{\xi}) \right| \phi_0 \rangle = 0$ and obtain

$$\frac{1}{c} \langle \phi_0 \left| v\alpha_z \exp(i\mathbf{Q}_0 \cdot \boldsymbol{\xi}) \right| \phi_0 \rangle = \frac{1}{c} \langle \phi_0 \left| \mathbf{e} \cdot \boldsymbol{\alpha} \exp(i\mathbf{Q}_0 \cdot \boldsymbol{\xi}) \right| \phi_0 \rangle , \tag{144}$$

where $\mathbf{e} = \mathbf{v} - \frac{\Omega}{Q_0^2} \mathbf{Q}_0$. Now we define the parameter Ω by demanding that the vector $\mathbf{e}$ is perpendicular to the momentum transfer $\mathbf{Q}_0$ that yields $\Omega = \mathbf{v} \cdot \mathbf{Q}_0 = -\frac{\varepsilon_n - \varepsilon_0}{\gamma}$. With such a choice of the 'polarization' vector $\mathbf{e}$ the structure of the matrix element on the right-hand side of Eq.(144) becomes quite similar to that appearing in the study of the interaction between the atom and a real photon which has linear polarization $\sim \mathbf{e}$ and momentum $\mathbf{Q}_0$.

Let us now turn to the consideration of $\langle \phi_0 \left| \alpha_y \exp(i\mathbf{Q}_0 \cdot \boldsymbol{\xi}) \right| \phi_0 \rangle$. Without any loss of generality we can assume that the total momentum transfer $\mathbf{Q}_0$ is in the plane xz. But then, by writing $\alpha_y = \boldsymbol{\lambda} \cdot \boldsymbol{\alpha}$ with $\boldsymbol{\lambda} = (0, 1, 0)$ and, thus, $\boldsymbol{\lambda} \perp \mathbf{Q}_0$, we arrive at the same situation as that discussed in the previous paragraph.

The continuity equation (86) for the atomic current in the elastic mode reads

$$\begin{aligned} \langle \phi_0 \left| Q_{0x} \alpha_x \exp(i\mathbf{Q}_0 \cdot \boldsymbol{\xi}) \right| \phi_0 \rangle + \quad & \langle \phi_0 \left| Q_{0y} \alpha_y \exp(i\mathbf{Q}_0 \cdot \boldsymbol{\xi}) \right| \phi_0 \rangle + \\ & \langle \phi_0 \left| Q_{0z} \alpha_z \exp(i\mathbf{Q}_0 \cdot \boldsymbol{\xi}) \right| \phi_0 \rangle = 0. \end{aligned} \tag{145}$$

Taking into account that the ratio Q_x/Q_z can be arbitrary we conclude that the x-component of the elastic atomic form-factor will not be zero provided that the z component is also not zero.

Thus, for the elastic mode all three space parts of the atomic form-factor of hydrogen-like targets will not be zero only when the known selection rules for the interaction with a real photon permit the 'transition' $\phi_0 \to \phi_0$. If such a 'transition' is forbidden, then the nonrelativistic atom 'approximation' becomes in fact exact for the elastic mode.

B On the existence of the 'overlap' region

I.*Collisions with a point-like charge.*
Let us first consider collisions with a point-like charge Z_A. In this case the eikonal transition amplitude is given by Eq.(109), the first order amplitude is given by Eq.(111) where one should set $M_j = 0$. Due to the presence of the ground state in the transition matrix element, the electron coordinates are effectively restricted to $r \stackrel{<}{\sim} \frac{1}{Z_I}$. Therefore, for collisions with impact parameters $b \gg \frac{1}{Z_I}$ one can approximately write

$$K_0\left(B_0 \mid \mathbf{r}_\perp - \mathbf{b} \mid\right) \approx K_0(B_0 b) + \frac{B_0 K_1(B_0 b)}{b} \mathbf{b} \cdot \mathbf{r}_\perp, \tag{146}$$

where $B_0 = \frac{\omega_{n0}}{\gamma v}$ and K_1 is a modified Bessel function. Further, one can also expand

$$\ln \frac{\mid \mathbf{b} - \mathbf{r}_\perp \mid}{b} \;\; \approx \;\; -\frac{\mathbf{b} \cdot \mathbf{r}_\perp}{b^2}. \tag{147}$$

Using (146) and the condition $\sum_j A_j = 1$ one obtains for the first order transition amplitude (111)

$$\begin{aligned} a_{0n}^p(\mathbf{b}) \;\; &\approx \;\; \frac{2iZ_A}{v} K_0(B_0 b) < \psi_n \mid \left(1 - \frac{v}{c}\alpha_z\right) \exp\left(i\frac{\omega_{n0} z}{v}\right) \mid \psi_0 > \\ &+ \;\; \frac{2iZ_A}{vb} B_0 K_1(B_0 b) < \psi_n \mid \left(1 - \frac{v}{c}\alpha_z\right) \exp\left(i\frac{\omega_{n0} z}{v}\right) (\mathbf{r}_\perp \cdot \mathbf{b}) \mid \psi_0 > . \end{aligned} \tag{148}$$

Applying the identity $< \psi_n \mid \alpha_z \exp\left(i\frac{\omega_{n0} z}{v}\right) \mid \psi_0 > \equiv \frac{v}{c} < \psi_n \mid \exp\left(i\frac{\omega_{n0} z}{v}\right) \mid \psi_0 >$ one sees that the first term in (148) is proportional to $\frac{1}{\gamma^2}$. We will neglect this term and choose b to satisfy not only the relation $b \gg \frac{1}{Z_I}$ but also $b \ll \frac{\gamma v}{\omega_{n0}}$. Estimating $\omega_{n0} \sim Z_I^2$ one can see that it is always possible to find the range $\frac{1}{Z_I} \ll b \ll \frac{\gamma v}{\omega_{n0}}$ for ultrarelativistic collisions when one has $\gamma c \gg Z_I$ for any Z_I. Since $B_0 = \frac{\omega_{n0}}{\gamma v}$, it is easy to see that in this range of impact parameters $B_0 b \ll 1$. Correspondingly, one can approximate $K_1(B_0 b) \approx \frac{1}{B_0 b}$ [43] and the first order transition amplitude reads

$$a_{0n}^p(\mathbf{b}) \approx \frac{2iZ_A}{cb^2} < \psi_n \mid (1 - \alpha_z) \exp\left(i\frac{\omega_{n0} z}{c}\right) (\mathbf{r}_\perp \cdot \mathbf{b}) \mid \psi_0 >, \tag{149}$$

where we set $v \approx c$.

On the other hand, taking into account Eq.(147), the eikonal transition amplitude (109) becomes

$$a_{0n}^{Coul}(\mathbf{b}) \approx < \psi_n \mid (1 - \alpha_z) \exp\left(i\frac{\omega_{n0} z}{c}\right) \exp\left(\frac{i2Z_A}{c} \frac{\mathbf{b} \cdot \mathbf{r}_\perp}{b^2}\right) \mid \psi_0 > . \tag{150}$$

Since $r_\perp \sim \frac{1}{Z_I}$, then, for $b \gg \frac{Z_A}{Z_I c}$, one can expand the exponential function in (150) and the eikonal transition amplitude (150) recovers the first order transition amplitude (149). Thus,

one can conclude that, for collisions with a point-like charge,
i) the first order perturbation theory can be used for $b \gg \frac{Z_A}{Z_I c}$ and
ii) the eikonal and first order transition amplitudes are approximately equal at $\frac{1}{Z_I} \ll b \ll \frac{\gamma v}{\omega_{n0}}$.

II. *Collisions with a neutral atom.*

Let us now discuss briefly the electron excitation and loss in ultrarelativistic collisions with neutral atoms. Since for collisions with a neutral atom having atomic number Z_A the screened atomic field for any impact parameter is not stronger than the field of a point-like charge Z_A then the conclusion i) is applicable for collisions with neutral atoms as well. In the eikonal amplitude

$$a_{0n}^{eik}(\mathbf{b}) = < \psi_n \mid (1-\alpha_z) \exp\left(i\frac{\omega_{n0} z}{c}\right) \exp\left(\frac{2iZ_A}{c} \sum_j A_j K_0\left(M_j \mid \mathbf{r}_\perp - \mathbf{b} \mid\right)\right) \mid \psi_0 > . \quad (151)$$

we expand the functions $K_0(M_j \mid \mathbf{r}_\perp - \mathbf{b} \mid)$ for $b \gg \frac{1}{Z_I}$ similarly to Eq.(146). Since $b \gg \frac{1}{Z_I} > \frac{Z_A}{Z_I c}$ one can further expand the exponential function in (151) and obtain

$$a_{0n}^{eik}(\mathbf{b}) \approx \frac{2iZ_A}{cb} \sum A_j M_j K_1(M_j b) < \psi_n \mid (1-\alpha_z) \exp\left(i\frac{\omega_{n0} z}{c}\right) \mathbf{b} \cdot \mathbf{r}_\perp \mid \psi_0 > . \quad (152)$$

For the same region of impact parameters $b \gg \frac{1}{Z_I}$ the first order transition amplitude is approximately given by

$$a_{0n}^{p}(\mathbf{b}) \approx \frac{2iZ_A}{cb} \sum_j A_j B_j K_1(B_j b) < \psi_n \mid (1-\alpha_z) \exp\left(i\frac{\omega_{n0} z}{c}\right) \mathbf{b} \cdot \mathbf{r}_\perp \mid \psi_0 > . \quad (153)$$

As it follows from (152) and (153) the eikonal and first order amplitudes are approximately equal for $b \gg \frac{1}{Z_I}$ if $B_j \simeq M_j$. If the latter condition is not fulfilled the amplitudes (152) and (153) can still be approximately equal if there exists an overlap between $b \gg \frac{1}{Z_I}$ and $b \ll \frac{1}{M_j}$, and $b \gg \frac{1}{Z_I}$ and $b \ll \frac{1}{B_j}$. In the ranges $b \ll \frac{1}{M_j}$ and $b \ll \frac{1}{B_j}$ the amplitudes (152) and (153) can be further simplified using for small arguments $K_1(x) \approx \frac{1}{x}$. This yields

$$a_{0n}^{eik}(\mathbf{b}) \approx a_{0n}^{p}(\mathbf{b}) \approx \frac{2iZ_A}{cb^2} < \psi_n \mid (1-\alpha_z) \exp\left(i\frac{\omega_{n0} z}{c}\right) \mathbf{b} \cdot \mathbf{r}_\perp \mid \psi_0 > . \quad (154)$$

The inspection of the screening constants given in [33] shows that the strict conditions $\frac{1}{Z_I} \ll b \ll \frac{1}{M_j}$ and $\frac{1}{Z_I} \ll b \ll \frac{1}{B_j}$ are in general not fulfilled. However, the less restrictive conditions for the overlap $\frac{1}{Z_I} < b < \frac{1}{M_j}$ and $\frac{1}{Z_I} < b < \frac{1}{B_j}$ are fulfilled for very heavy projectile-ions where Z_I is considerably larger than $max\{M_j\}$.

In general the cross section (112) can be calculated according to the following simple rule. At any impact parameter the transition amplitude should be represented by the value obtained either from the eikonal or the first order transition amplitudes whichever gives the smallest transition probability.

References

[1] R. Anholt and H. Gould, Adv. At. and Mol. Phys. **22** 315 (1986)

[2] C.A. Bertulani and G. Baur, Physics Reports, **163**, 299 (1988)

[3] J. Eichler, Phys. Rep. **193** 165 (1990)

[4] J. Eichler and W.E. Meyerhof, *Relativistic Atomic Collisions* (Academic Press, 1995)

[5] E.C. Montenegro, W.E. Meyerhof and J.H. McGuire, Adv.At.Mol. and Opt. Phys. **34** 249 (1994)

[6] N. Stolterfoht, R.D. DuBois and R.D.Rivarola, *Electron Emission in Heavy Ion-Atom Collisions* (Springer 1997)

[7] J.H. McGuire *Electron Correlation Dynamics in Atomic Collisions* (Cambridge University Press, 1997)

[8] H.F. Krause, C.R. Vane, S. Datz, P. Grafström, H. Knudsen, S. Scheidenberger, and R.H. Schuch, Phys. Rev. Lett. **80**, 1190 (1998)

[9] H.F. Krause, C.R. Vane, S. Datz, P. Grafström, H. Knudsen, U. Mikkelsen, S. Scheidenberger, R.H. Schuch, and Z. Vilakazi, Phys. Rev. **A 63** 032711 (2001)

[10] C.R. Vane, U. Mikkelsen, H.F. Krause, S. Datz, P. Grafström, H. Knudsen, S. Møller, E. Uggerhøj, C. Scheidenberger, R.H. Schuch, and Z. Vilikazi, In Proceedings of XXI ICPEAC, p. 709 (2000)

[11] A.B. Voitkiv, N. Grün and W. Scheid, Phys.Rev. **A 61** 052704 (2000)

[12] A.B. Voitkiv, M. Gail and N. Grün J.Phys. **B 33** 1299 (2000)

[13] D.R. Bates and G. Griffing, Proc. Phys. Soc. London A **66** 961 (1953)

[14] D.R. Bates and G. Griffing, Proc. Phys. Soc. London A **67** 663 (1954)

[15] D.R. Bates and G. Griffing, Proc. Phys. Soc. London A **68** 90 (1955)

[16] J.H. McGuire, Adv. At. Mol., and Opt. Phys. **29** 217 (1991)

[17] E.C. Montenegro and T.J.M. Zouros, Phys.Rev. **A 50** 3186 (1994)

[18] E.C. Montenegro and W.E. Meyerhof, Phys.Rev. **A46** 5506 (1992)

[19] M.M. Sant'Anna, W.S. Melo, A.C.F. Santos, G.M. Sigaud, and E.C. Montenegro, Nucl. Instr. Methods **B 99** 46 (1995)

[20] P.L. Grande, G. Schiwietz, G. M. Sigaud, and E. C. Montenegro, Phys. Rev. **A 54** 2983 (1996)

[21] T. Kirchner, to be published in *Proceedings of the XXIII International Conference on Photonic, Electronic and Atomic Collisions*, Stockholm, Sweden, July 23-29, 2003

[22] A.B. Voitkiv, N. Gruen and W. Scheid, J.Phys. **B 33** 3431 (2000)

[23] W. Magnus, Commun.Pure Appl. Math., **7** 649 (1954)

[24] A.M. Dykhne and G.L. Yudin, Usp. Fiz. Nauk **125** 377 (1978) [Sov. Phys. Usp. **21** 549 (1978)]

[25] A.B. Voitkiv, G.M. Sigaud, and E.C.Montenegro, Phys.Rev. **A 59** 2794 (1999)

[26] R. Anholt, Phys.Rev. **A 31** 3579 (1985)

[27] D.M. Davidovic, B.L. Moiseiwitsch, P.H.Norrington, J.Phys. **B11** 847 (1978)

[28] R. Anholt, Phys.Rev. **A 19** 1004 (1979)

[29] R. Anholt and U. Becker, Phys.Rev. **A 36** 4628 (1987)

[30] A.H. Sørensen, Phys.Rev. **A 58** 2895 (1998)

[31] A.B. Voitkiv, N. Grün and W. Scheid, Phys. Lett. **A 260** 240 (1999)

[32] L.D. Landau and E.M. Lifshitz, *Quantum Mechanics*

[33] F. Salvat, J.D. Martinez, R. Mayol, and J. Parellada, Phys.Rev.**A 36** 467 (1987)

[34] J.D. Bjorken and S.D. Drell, *Relativistic Quantum Mechanics* (McGraw-Hill, 1964)

[35] J.D. Jackson, *Classical Electrodynamics* (John Wiley and Sons, 1975)

[36] A.S. Davydov, *Quantum Mechanics* Pergamon Press (1965)

[37] P.A. Amundsen and K.Aashamar, J.Phys. **B 14** 4047 (1981)

[38] B. Najjari, A.B. Voitkiv and J. Ullrich, J.Phys. **B 35** 533 (2002)

[39] G. Basbas, W. Brandt, and R. Laubert, Phys.Rev. **A 17** 1655 (1978)

[40] A.J. Baltz, Phys.Rev.Lett. **78**, 1231 (1997)

[41] A.B. Voitkiv, C. Müller and N. Grün, Phys.Rev. **A 62** 062701 (2000)

[42] R. Jackiw, D. Kabat and M. Ortiz, Phys. Lett. **B 277** 148 (1992)

[43] M. Abramowitz and I. Stegun, *Handbook of Mathematical Functions* (Dover Publications, Inc., New York, 1965)

[44] A.B. Voitkiv and A.V. Koval', Tech. Phys. **39**, 335 (1994)

[45] A.B. Voitkiv and A.V. Koval', J. Phys. **B 31**, 499 (1998)

[46] A.J. Baltz, Phys.Rev. **A 61**, 042701 (2000)

[47] Th.Stölker et al, Phys.Lett.**A 238** 43 (1998)

[48] Th.Stölker et al, Phys.Rev.**A 57** 845 (1998)

[49] C.A. Bertulani, Phys. Rev. **A 63** 062706 (2001)

[50] U. Becker, in *Physics of Strong Fields* ed. W.Greiner, NATO Advanced Study Institute series B: Physics, **153** 609 (Plenum, New York, 1987)

[51] G. Moliere, Naturforsch. **2A** 3 (1947)

[52] J.H. Hubbell, Wm.J. Veigele, E.A. Briggs, R.T. Brown, D.T. Cromer and R.J. Howerton, J. Phys. Chem. Ref. Data **4** 471 (1975)

[53] J.H. Hubbell and I. Øverbø, J. Phys. Chem. Ref. Data **8** 69 (1979)

[54] U. Fano, Annu. Rev. Nucl. Sci. **13** 1 (1963)

[55] R. Anholt, W.E. Meyerhof, X.-Y. Xu, H. Gould, B. Feinberg, R.J. McDonald, H.E. Wigner and P. Thieberger, Phys. Rev. **A 36** 1586 (1987)

[56] Th. Stölker et al, Nucl. Instr.Meth. **B 124** 160 (1997)

[57] C. Scheidenberger and H. Geissel, Nucl. Instr.Meth. **B 135** 25 (1998)

[58] C. Scheidenberger, Th. Stölker, W.E.Meyerhof, H. Geissel, P.H. Mokler and B. Blank, Nucl. Instr.Meth. **B 142** 441 (1998)

[59] N. Claytor, A. Belkacem, T. Dinneen, B. Feinberg, and H. Gould Phys.Rev. **A 55** R842 (1997)

[60] A.B. Voitkiv, N. Grün and W. Scheid J.Phys. **B 32** 3923 (1999)

[61] A.J. Baltz, Phys.Rev. **A 64**, 022718 (2001)

[62] T. Ludziejewsky et al, Phys. Rev. **A 61** 052706 (2000)

[63] D. Ionesku and Th. Stölker, Phys. Rev. **A 67** 022705 (2002)

[64] H. Bethe and E. Fermi, Z. Physik **77** 296 (1932)

[65] U. Fano, Phys. Rev. **102**, 385 (1956)

[66] Weick et al, GSI Preprint 2000-01 (2000)

[67] K.G. Dedrick, Rev. Mod. Phys. **34** 429 (1962)

[68] A.B. Voitkiv and N. Grün, J.Phys. **B 34** 267 (2001)

[69] C. Müller, A.B. Voitkiv and N. Grün, Phys. Rev. **A 66** 012716 (2002)

[70] A.B. Voitkiv, N. Grün and W. Scheid, Phys. Lett. **A 265** 111 (2000)

[71] A.B. Voitkiv, C. Müller and N. Grün, Nucl. Instr. Meth. **B 205** 504 (2003)

[72] A.B. Voitkiv, N. Grün and W. Scheid, Phys. Lett. **A 269** 325 (2000)

[73] A. Belkacem, N. Claytor, T. Dinneen, B. Feinberg, and H. Gould, Phys.Rev. **A 58**, 1253 (1998)

[74] J. Wu, J.H. Derrickson, T.A. Parnell and M.R. Strayer, Phys. Rev. **A 60**, 3722 (1999)

[75] L.I. Nemenov, Yad. Fiz., **41** 980 (1985)

[76] A.V. Tarasov and I.U. Christova, JINR P2-91-10, Dubna (1991)

[77] L. Afanasyev, A. Tarasov and O. Voskresenskaya, J.Phys. **G 25** B7 (1999)

[78] Z. Halabuka, T.A. Heim, K. Hencken, D. Trautmann, R.D. Viollier, Nucl. Phys. **B 554** 86 (1999)

[79] T.A. Heim, K. Hencken, D. Trautmann and G. Baur, J. Phys. **B 33** 3583 (2000)

[80] T.A. Heim, K. Hencken, D. Trautmann and G. Baur, J. Phys. **B 34** 3763 (2001)

[81] M. Schumann, T.A. Heim, K. Hencken, D. Trautmann and G. Baur, J. Phys. **B 35** 2683 (2002)

[82] H. Kollmus, R. Moshammer, R.E. Olson, S. Hagmann, M. Schultz and J. Ullrich, Phys. Rev. Lett. **88** 103202 (2002)

[83] R. Moshammer and J. Ullrich, private communications.